

UNIVERSITY
OF MICHIGANENGINEERING
LIBRARY

The Canadian Journal of Chemical Engineering

formerly

CANADIAN JOURNAL OF TECHNOLOGY

CONTENTS

Reduction of Oxides of Nitrogen in Vent Gases	<i>H. R. L. Streight</i>	3
Heat Transfer from Column Wall to Bed in Spouted, Fluidized and Packed Systems	<i>J. Klassen</i> <i>P. E. Gishler</i>	12
Relative Volatility and Enthalpy Data for the Systems C ₄ Hydrocarbons-Acetone-Water Developed from Vapor- Liquid Equilibria	<i>J. E. Ewanchyna</i> <i>C. Ambridge</i>	19
The Leaching of Manganese from Pyrolusite Ore by Pyrite	<i>G. Thomas</i> <i>B. J. P. Whalley</i>	37
Index of Authors and Articles—1957		45

Published by

THE CHEMICAL INSTITUTE OF CANADA
OTTAWA CANADA

The Canadian Journal of Chemical Engineering

formerly

Canadian Journal of Technology

VOLUME 36

FEBRUARY, 1958

NUMBER 1

EDITOR:

W. M. CAMPBELL

Chemistry and Metallurgy Division, Atomic Energy of Canada Limited,
Chalk River, Ont.

Managing Editor:

T. H. G. MICHAEL

Assistant Editor:

R. N. CALLAGHAN

Editorial Assistant:

R. G. WATSON

Circulation Manager:

M. M. HOLDEN

EDITORIAL BOARD:

Chairman

J. R. DONALD, Montreal, Que.

A. CHOLETTE, Quebec, Que.

W. H. GAUVIN, Montreal, Que.

GLEN GAY, Ottawa, Ont.

G. W. GOVIER, Edmonton, Alta.

A. I. JOHNSON, Toronto, Ont.

G. A. LEDINGHAM, Saskatoon, Sask.

E. B. LUSBY, Toronto, Ont.

LÉO MARION, Ottawa, Ont.

R. R. McLAUGHLIN, Toronto, Ont.

E. R. ROWZEE, Sarnia, Ont.

H. R. L. STREIGHT, Montreal, Que.

EX-OFFICIO:

O. J. WALKER, Edmonton, Alta.

L. PICHE, Montreal, Que.

H. P. GODARD, Kingston, Ont.

H. S. SUTHERLAND, Montreal, Que.

Authorized as second class mail, Post Office Department, Ottawa. Printed in Canada

Manuscripts for publication should be submitted to the Editor: Dr. W. M. Campbell, Chemistry and Metallurgy Division, Atomic Energy of Canada Limited, Chalk River, Ontario. (Instruction to authors are on inside back cover)

Proofs, correspondence concerning proofs, and orders for reprints should be sent to: The Chemical Institute of Canada, 18 Rideau Street, Ottawa 2, Ont.

Subscriptions, renewals, requests for single or back numbers and all remittances should be sent to: The Chemical Institute of Canada, 18 Rideau Street, Ottawa 2, Ont.

C.J.Ch.E. is published by The Chemical Institute of Canada every two months. Subscription rate is \$3.00 per year and .75c per single copy; U.S. and U.K.—\$4.00; and Foreign—\$4.50 per year.

Unless it is specifically stated to the contrary, the Institute assumes no responsibility for the statements and opinions expressed in *The Canadian Journal of Chemical Engineering*. Views expressed in the editorials do not necessarily represent the official position of the Institute.

Editorial Offices: Dr. W. M. Campbell, Chemistry and Metallurgy Division, Atomic Energy of Canada Limited, Chalk River, Ont.

Production and circulation offices: 18 Rideau Street, Ottawa 2, Ont.

Change of Address: Advise the Circulation Department, The Chemical Institute of Canada, 18 Rideau Street, Ottawa 2, Ont. in advance of any change of address, providing old as well as new address. Enclose address label if possible.

Reduction of Oxides of Nitrogen in Vent Gases¹

H. R. L. STREIGHT²

Oxides of nitrogen are present in the effluent gases from nitric acid and nylon intermediates plants and if released in sufficient quantity they could be objectionable owing to their intensive reddish-brown color and to their corrosive and poisonous nature. A paper study showed that the oxides of nitrogen could be reduced by absorption in an alkaline solution. Based on pilot plant tests, a large fume abatement unit was designed, installed, and operated in a satisfactory manner to reduce the concentration of the oxides of nitrogen. In 1956, the color of the combined effluent gases was practically eliminated when a more economic waste ammonia-caustic liquor replaced the dilute caustic scrubbing solution and finely dispersed ammonium salts were removed in a Venturi scrubber. The method may be used to eliminate the objectionable brownish-red color of effluent gases leaving a nitric acid plant.

Du Pont of Canada operates a complex organic chemical plant at Maitland, Ont., for the production of nylon intermediates, adipic acid and hexamethylenediamine, the raw materials which are combined and polymerized to make nylon filament and staple fibre at its Kingston plant. When it was decided to erect the Maitland plant which is located in a recreational and agricultural area, an extensive pollution abatement program was started and continued after the plant was in operation, to determine the amount of certain contaminants in the effluent gases and to learn if they could be reduced before release to the atmosphere.

The stack gases from a nitric acid plant, using the ammonia oxidation process, are released as brownish-red plumes as are reaction off-gases and vent gases from tanks and equipment in the nylon intermediates plant. The objectionable color is caused by a concentration of nitrogen dioxide (NO_2) above 50 p.p.m. On oxidation, nitric oxide (NO) forms objectionable NO_2 . Nitrogen dioxide can react with water vapor or rain to

form nitric acid. According to recent studies on pollution, the oxides of nitrogen can affect atmospheric pollution in an indirect way since they act as catalysts and oxidize organic materials in the presence of ultra-violet light or bright sunlight to objectionable compounds. The American Petroleum Institute and other scientific organizations in Los Angeles are investigating this problem. The other constituents of the stack gases are nitrous oxide (N_2O), carbon dioxide, oxygen and nitrogen. The N_2O does not cause any anxiety as it is a colourless gas occurring in such dilute concentration that its anaesthetic properties would be unnoticed. Oxides of nitrogen henceforth refer to NO and NO_2 .

The recovery of low concentrations of NO and NO_2 is not economic as the gases are too dilute for conversion into nitric acid. The problem accordingly was to remove a potential nuisance by reducing the emitted oxides of nitrogen to such a value that after dispersion from a stack, their maximum ground concentration would be less than the

safe threshold limits accepted for individuals and vegetation; then there would be no injury to the health of persons or damage to the apple trees in adjacent orchards and flowers in nearby gardens. Since the maximum safe ground concentration of each contaminant varies with the individual and the actual plant, the following values were accepted as the safe and maximum ground concentrations.

TABLE 1
THRESHOLD LIMITS FOR OXIDES OF NITROGEN

	Max. Ground Level Concentration	
	NO_2 , p.p.m.	Duration
Persons	5 (1) 10 (3)	continuous 8 hours/day, 5 days/week
Vegetation	<25 (2)	continuous

According to Table 1, the concentration of the NO and NO_2 released from a stack should be such that after dispersion in the atmosphere, the maximum ground concentration should not exceed 10 p.p.m. At this concentration, the effluent gas would be colorless as the reddish-brown color is clearly visible only above 50 p.p.m. NO_2 .

Literature search

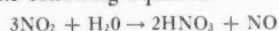
The technical literature was reviewed to provide information on the properties and reactions of NO and NO_2 , and methods for their reduction and removal.

Nitric oxide is a colorless and relatively stable gas which is only sparingly soluble in water. It slowly combines with oxygen to form the reddish-brown nitrogen dioxide

¹Manuscript received November 8, 1957.

²Principal Chemical Engineer, Engineering Department, Du Pont Company of Canada (1956) Limited. This article is based on a paper presented at the 40th Annual Conference of The Chemical Institute of Canada, Vancouver, B.C., June 3-5, 1957.

which reacts with water according to the following equation:



When NO and NO₂ occur together, they establish an equilibrium with the trioxide (N₂O₃); NO₂ is also in equilibrium with the tetraoxide (N₂O₄).

Equilibrium constants between the various oxides of nitrogen are shown in Table 2.

TABLE 2
EQUILIBRIUM CONSTANTS

Reaction	Equilibrium Constant K _p at 20°C.
$\text{NO} + \text{NO}_2 \rightleftharpoons \text{N}_2\text{O}_3$	0.83
$2\text{NO}_2 \rightleftharpoons \text{N}_2\text{O}_4$	10.1
$2\text{NO} + \text{O}_2 \rightleftharpoons 2\text{NO}_2$	4.2×10^{12}

The above equilibrium constants were applied to a gas containing 0.05% NO and 0.025 volume % NO₂. Quantitative calculations showed that the concentrations of tri- and tetraoxides would be exceedingly small and could be neglected. As the gas would contain approximately 4% oxygen, the third reaction would give substantially complete yields of NO₂ provided sufficient time was available; the effluent gas would require more than 30 minutes to reduce the initial NO content by 50% and more than 5 hours for 90%. Hence oxidation would be too slow for practical purposes, even with additional oxygen. A satisfactory catalyst for this reaction has not been found although long sought by nitric acid manufacturers who are always interested in improving the efficiency of their absorption units.

The following methods of reducing NO and NO₂ have been studied, although often not exhaustively.

1. Absorption (Absorbers, Distillation Columns and Venturi Scrubbers)
 - (a) water
 - (b) alkaline solution
 - (c) alkaline sulphite solution
 2. Absorption
 3. Combustion
 4. Chemical reaction, with one of following materials:
 - (a) sulphur dioxide
 - (b) chlorine
1. **Absorption.** For cheapness and availability, water was first considered as the absorbing medium in absorbers and Venturi scrubbers. The absorption of NO and NO₂ in water has the objection of removing only two-thirds of the NO₂. The

balance is converted to NO which, being insoluble in water, is released to the atmosphere where it oxidizes to NO₂, forming the objectionable reddish-brown color.

Alkaline absorption has been used to reduce the last traces of oxides of nitrogen leaving a Norwegian nitric acid plant, and to clean the fumes from an electroplating plant and recently from a Canadian chemical plant⁽⁴⁾; unfortunately information was not recorded for the design of another plant. The rates of absorption of NO and NO₂ in alkaline solutions have been determined in several laboratories but not in sufficient detail for design. The mechanism of absorption of low concentrations of NO₂ in caustic solutions was studied by Chambers and Sherwood⁽⁵⁾ and their results confirmed by Eagleton, Langer and Pigford⁽⁶⁾. The rate of absorption was found to be gas-film controlled and the absorption coefficients were considerably lower than expected. Various mechanisms were proposed to account for this discrepancy. The absorption rate in caustic soda was less than in water; the coefficients varied with the liquor rate, gas rate and water vapor content of the gas.

Further experiments using N₂O₃, instead of NO₂, showed that N₂O₃ reacts rapidly with NaOH probably according to the following reaction:



The formation of N₂O₃, from NO and NO₂, in a distillation column was shown by the increase of plate efficiency in proceeding up the column. Tests were not made with an NO and NO₂ feed stream⁽⁷⁾. If it is assumed that absorption proceeds through the formation of N₂O₃, the molal concentration of NO must not be greater than the molal concentration of NO₂ — otherwise excess NO will be released to the atmosphere.

After our test work was completed, other experimenters showed that removal was improved by supplying a maximum gas-liquid contact area applicable to absorbers, distillation columns and Venturi scrubbers (water is sprayed axially into the gas stream passing at a high velocity through a Venturi throat). For low concentrations of oxides of nitrogen (1% or less) spray towers and bubble cap columns were found to have low removal efficiencies when water was used as the scrubbing medium^(8,9).

Little information was found on scrubbing with an ammonium hydroxide solution although mention was made of the formation of am-

monium nitrate and ammonium nitrite in the scrubbing liquor and of preferential reaction of the liquor with NO₂ over NO. A strong alkaline solution of a common sulphite would not be satisfactory for scrubbing the Maitland gases as the oxygen would soon oxidize the sulphites to sulphates.

2. **Adsorption.** The adsorption of oxides of nitrogen by silica gel (or other adsorbents) is satisfactory for NO₂ concentrations higher than 0.1% and for NO concentrations higher than 1 to 1.5%^(10,11). Silica gel containing adsorbed NO₂ catalyzes the oxidation of NO and the formed NO₂ is removed by adsorption on the silica gel which on heating produces a higher concentration of NO₂ that can be used in a nitric acid plant. The equipment is expensive and operation costs would be high for low concentrations of the oxides of nitrogen.

3. **Combustion.** The effluent gases could be treated with a small amount of hydrogen over a suitable palladium catalyst. The presence of oxygen in the Maitland effluent gas obviates this method of removal since, in all likelihood, the hydrogen might react with the oxygen before the oxides of nitrogen^(12,13).

4. **Chemical Reaction.** The oxides of nitrogen can combine with sulphur dioxide or chlorine. Chemical reaction does not appear attractive as sulphur dioxide would have to be added to the effluent gases at a high temperature and the rate of reaction is very slow either for sulphur dioxide or chlorine^(14,15,16).

Proposed Method. Based on the literature search, the most promising method appeared to be absorption in a sodium carbonate or hydroxide solution. There was a potential objection owing to the presence and concentration of CO₂ in the combined effluent gases. Carbonate and bicarbonate would be formed in the solution until a steady state was reached when the carbonate/bicarbonate ratio and the total ionic strength would generate a back pressure of CO₂ comparable with the forward pressure in the transpired gas⁽¹⁷⁾. Accordingly a pilot plant absorber system was recommended as the next step in determining the potentially useful concentrations of alkaline scrubbing solutions and absorption efficiencies, for low concentrations of NO and NO₂. The test runs would use sodium carbonate solutions after establishing the method with water.

A Venturi scrubber might have a lower capital cost than an absorber for removing oxides of nitrogen. Accordingly pilot plant tests were scheduled on a Venturi scrubber to determine the number that would be required.

Pilot plant

An absorption column was constructed from 12-in diameter sections of glazed pipe containing a 5 or 10-ft. depth of random packed Raschig rings. The characteristics of the packing were as follows:

Free space	-77%
Ring dimensions	-1 x 1 x 0.1-in.
Liquid feed rate, for complete wetting	-1.0 cu. ft./min.

Each inlet gas line was equipped with a rotameter, manometer and facilities for gas sampling. Dilute air/ NO_2 mixtures were made to the correct concentrations. Liquid NO_2 was evaporated by an immersion heater operated at controlled wattage inside a Dewar container. This evaporator was calibrated empirically and evaporated NO_2 was measured before being mixed with the main air stream. A pump recirculated the liquor through the absorber, countercurrent to the gas stream. Special sampling and analytical techniques were required largely because of the low levels of concentration of these components in the waste gas. The collection of a large volume for sampling, coupled with a combination of photoelectric and chemical analytical methods, proved quite satisfactory. The analytical methods were revised and improved throughout the experimental work.

The initial experimental work was conducted in the period April-September 1952, and involved the preparation of a "synthetic" waste gas containing 0.05 volume % NO_2 which was absorbed by water in the pilot plant absorber. The results of this first group of runs showed that the absorption of NO_2 was limited by the gas-film coefficient and the "Height of a Transfer Unit" (H.T.U.) for absorption of NO_2 in water was much higher than predicted on the basis of the two-film diffusion mechanism, by a ratio approximately 33:1. Several runs were conducted with NH_3 and Cl_2 present as contaminants in the waste gas, in concentrations of 0.05-0.10 volume %. The H.T.U. values obtained with NH_3 were comparable to those with uncontaminated waste gas, while those obtained with Cl_2 were even higher.

Subsequent runs centered around the absorption of NO_2 in a solution of sodium carbonate. Complications were expected with the use of this solution as the waste gas contained approximately 2.4 volume % of CO_2 . Recirculation of the absorbing liquor resulted in a continuously increasing bicarbonate/carbonate ratio in the liquor (up to the point of equilibrium), with an attendant decrease in the absorpition efficiency of the absorber. The absorption efficiency of NO_2 in a gas containing 2.4 volume % CO_2 dropped from 40-50% for a bicarbonate/carbonate ratio of 0-0.3, to 20-25% for a bicarbonate/carbonate ratio of 4. The possibility of ventilating the recirculated liquor in order to reduce the bicarbonate/carbonate ratio was investigated in a series of runs. Although the bicarbonate/carbonate ratio did decrease, the efficiency of

oxide absorption failed to show the expected recovery. Thus regeneration of the recirculating liquor in terms of CO_2 content, was ruled out. One important aspect in the utilization of the alkaline absorbent is the extent to which the absorbent can be exhausted, in terms of sodium ion content, before it becomes useless. Exhaustion is defined as the percent of sodium ions originally present in the solution which have been converted to nitrate and nitrite salts. Initial work was conducted with 50% exhausted liquor containing equilibrium amounts of bicarbonate and carbonate, as well as 50% exhausted liquor containing higher than equilibrium bicarbonate/carbonate ratios.

A comparison of water and Na_2CO_3 solutions as absorbing media is shown in Table 3.

TABLE 3
COMPARISON OF WATER AND Na_2CO_3 SOLUTIONS AS NO_2 ABSORBING MEDIA

Gas Rate 60 cu.ft./min.*	Packed Depth = 5-ft.	Liquor Rate 1 cu.ft./min.
	Water	5% Na_2CO_3 Solution
P_{CO_2}	0 atm.	0.024 atm.
P_{NO_2}	0.0005 atm.	0.0005 atm.
Absorption efficiency.....	21%	at zero exhaustion = 50% at 50% exhaustion = 22%

*Tests were made on gas rates ranging from 40 to 100 cu.ft./min., 118 cu.ft./min. being the calculated carry-over rate.

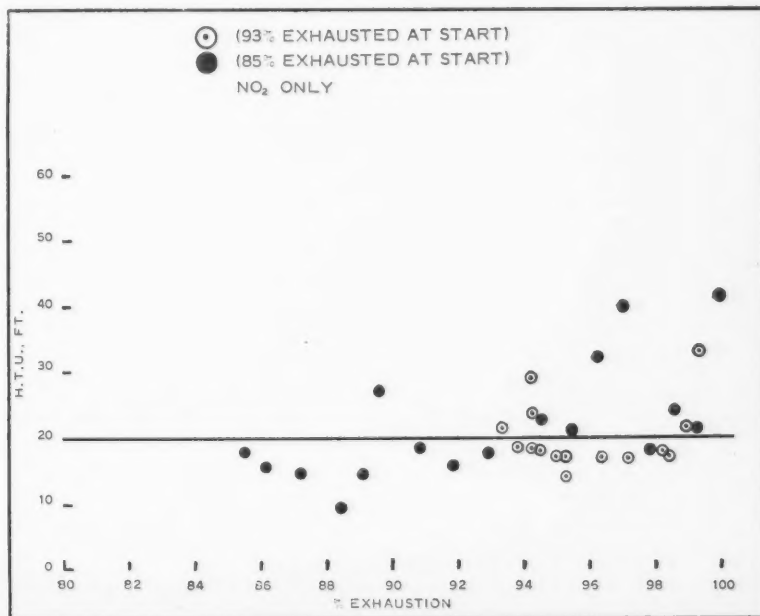


Figure 1—Effect of exhaustion on H.T.U.

The tests showed that a 50% exhausted alkaline solution offered only slightly better absorption efficiency than water. The disadvantage of water was the very slight solubility of NO and its release to the atmosphere. Thus as the waste fumes contained NO and the absorption of NO₂ in water would liberate one-third of its volume as NO, sodium carbonate solutions were selected as the absorbing medium.

During the period December 1952-February 1953, the experimental data on carbonate solutions were extended to higher exhaustion levels, using synthetic waste gases containing NO₂. The absorption coefficients for liquor exhaustion levels of 78-100% were somewhat scattered, possibly because of impurities in the prepared "waste" gas. As Figure 1 will illustrate, the absorption efficiency remains relatively constant up to about 90-95% liquor exhaustion. The H.T.U. values were calculated assuming zero back-pressure for the dissolved NO₂.

Table 4 arbitrarily divides the tests of Figure 1 and shows the observable trend.

TABLE 4
THE EFFECT OF EXHAUSTION ON
H.T.U. FOR NO₂

Exhaustion	H.T.U.	Deviation	No. of Results
78-88%	16.5 ft.	±4.8 ft.	9
88-92%	17.4	2.5	8
92-96%	20.8	5.0	12
96-100%	25.4	9.4	10

Before designing a large absorber, it was important to learn if H.T.U. was enhanced in an absorber with a short depth of packing, 5-ft., by absorption at the top and bottom ends. The effect of packed depth on the absorption efficiency of alkaline solutions was examined by performing a number of runs with a 10-ft. depth. The observed efficiencies were twice those obtained with 5-ft. of packing.

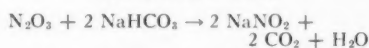
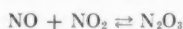
The effect of pH on absorption efficiency was studied by using a dilute caustic solution as the absorbing liquor. The CO₂ in the waste gas rapidly converted the solution to one of sodium carbonate. The pH of the solution, initially 12.8, decreased to a value slightly higher than 7, providing an opportunity for continuously testing absorption efficiencies in this pH range. No marked variation of efficiency was noted.

At this stage of the experimental work, additional process information indicated that the concentration of NO in the combined effluent gases

TABLE 5
THE EFFECT OF NO ON THE ABSORPTION OF NO₂

Run No.	Exhaustion	P _{NO₂}	P _{NO}	H.T.U.	Standard Deviation	No. of Results
52	50%	0.001 atm.	—	14.1 ft.	±1.6	3
53	50%	0.001	0.001	9.3	0.9	6
59	55%	0.001	—	7.8	0.1	2
60	55%	0.001	0.001	7.7	1.8	4
57	91%	0.001	—	16.9	2.7	4
58	91%	0.001	0.001	20.6	3.1	7

from the plant, previously assumed to be of a molal ratio of 2NO/1 NO₂, would more likely be 1/1 or even slightly lower in NO. This is a more favourable ratio for absorption in sodium carbonate/bicarbonate solutions which may take place according to the following reactions:



Initial work with mixed oxides of nitrogen in the ratio of 1 NO/1.1 NO₂ showed an improvement in overall oxide absorption efficiency, in agreement with the findings of earlier workers^(18, 19). Additional absorption runs were made on synthetic "waste" gas containing mixtures of NO and NO₂ in a 1/1 ratio, with absorbing liquor exhausted to 50% and 90%. The H.T.U. values are based on total oxides of nitrogen, assuming no back pressure of dissolved oxides. The H.T.U.'s were somewhat erratic as shown in Table 5.

The only reason which can be advanced for this inconsistency is the possibility that the oxides of nitrogen, produced in the laboratory for runs 57, 58, 59 and 60, contained impurities.

For plant design a number of solubility determinations were conducted on the system NaHCO₃ - Na₂CO₃ - NaNO₃ - NaNO₂ - H₂O, the liquor samples being saturated with a gas comparable to the combined Maitland effluent. Experiments showed that at liquor exhaustions of over 30%, precipitation would not occur. In the range 0-30% exhaustion, NaHCO₃ precipitated at a temperature below 8.5 and 5°C. for 0 and 20% exhausted solutions. The solutions easily became super-saturated and even after seeding with NaHCO₃, there was a protracted time before crystal growth gave a visible precipitate.

An investigation was made between December, 1952, and Febru-

ary, 1953, on using a Venturi scrubber for absorbing the oxides of nitrogen in a 5% sodium carbonate solution. Liquor was introduced into the throat of a Venturi tube by radial and axial injection methods. Nitrogen dioxide alone, and a 1/1 ratio of NO and NO₂, were passed through this scrubber at absorption efficiencies of less than 40%. As a consequence Venturi scrubbers were not considered practical for a plant installation.

From the preceding description of experimental work, it was concluded that the absorption of the oxides of nitrogen could be most effectively performed in an alkaline solution of sodium carbonate or hydroxide. An absorption column designed for the removal of NO₂ will be equally capable of dealing with NO/NO₂ mixtures up to a 1/1 mole ratio although the tests did not consistently reproduce the well-documented claim that N₂O₃ is more easily absorbed than NO₂ in alkaline media. For design, the H.T.U. can be safely taken as equal to 20-ft. for random 1-in. rings, up to 90-95% exhaustion of alkalinity; the absorption efficiency will decrease if the liquor is exhausted more than 90-95%.

Fume absorption installation

Basis of Design. In 1953 a fume absorption system was designed, on the basis of the pilot plant runs, to reduce the oxides of nitrogen in the effluent gases of the nitric acid and nylon intermediates plants in a satisfactory manner for the forecasted and maximum loads. The forecasted load represented normal operation after plant start-up and the maximum rate corresponding to an increased production of nitric acid.

Vent gases containing NO and NO₂ come from three sources:

1. Off-gases from the nitric acid plant.
2. Reaction off-gases.
3. Vent gases from tanks and process equipment.

Several schemes were investigated to determine whether all or part of the above effluent gases should be passed through one or more fume absorbers. Dilution by the addition of air to the vent fumes having the highest concentrations of NO and NO₂ was considered and rejected as pollution would be too high in the immediate vicinity under adverse meteorological conditions. In the adopted scheme, all effluent gases containing NO and NO₂ were passed through a single absorber.

The concentrations of NO and NO₂ were calculated on the best available information, attention being given to the increase of NO and NO₂ content of the off-gas with increased production and higher cooling water temperature. As the estimates made on the vent gases from tanks and other equipment vary widely with changes in operation, an allowance was made for surges. Since start-up, the flow and composition of the majority of the off-gases have altered, owing to the development of economic process changes. The present flows differ from the values used for design.

The NO and NO₂ contents of the off-gases were calculated for various depths of packing in the fume absorber. The proposed absorber with a 40-ft. depth of wetted packing, equivalent approximately to 1.2 H.T.U., should give conservative exit concentrations of NO and NO₂, particularly since calculations showed that diffusion would keep the maximum ground concentration below the threshold limit. The results are incorporated in Table 6 and should be compared with the threshold limit of 10 p.p.m.

The design flows and compositions of the inlet and off-gases are given in Table 7.

The liquor system was designed for batch operation, starting with 3.5-4.0% caustic solution which would be essentially exhausted before the spent liquor was sent to sewer and replaced with fresh liquor.

Equipment. The fume absorption system was designed in 1953 to provide the greatest possible reduction of the oxides of nitrogen in a single absorber with ancillary equipment. This system is shown in Figure 2.

The low pressure off-gases are collected in appropriate process buildings and passed through a blower to the fume absorber. High pressure reaction off-gases, from a nylon intermediates process building and the nitric acid plant, pass directly to the

TABLE 6
NO AND NO₂ CONCENTRATIONS

	Forecast Load p.p.m.	Maximum Load p.p.m.
Gas to absorber.....	5,200	19,400
Gas from absorber.....	1,850	6,100
Max. ground concentration,* based on design of absorber and after diffusion in a 2 to 3 mi./hr. wind.....	0.49 (av.) 1.2 (max.)	1.9 (av.) 4.7 (max.)

*The maximum ground concentrations have been found to be 50 to 67% of the calculated values (20).

TABLE 7
FLOWS AND COMPOSITIONS FOR FUME ABATEMENT SYSTEM

	Design Conditions			
	Total Inlet Gas		Off-Gas	
	Forecast Load	Maximum Load	Forecast Load	Maximum Load
Flow, lb./hr.....	19,417	31,931	19,572	31,893
Flow, cu.ft./hr.*.....	247,600	410,700	250,000	412,000
Temperature, °C.....	43	43	25	25
Pressure, lb./sq.in.ga.....	2	2	1.3	1.3
Density, lb./cu.ft.....	0.078	0.078	0.078	0.078
Composition, lb./hr.....				
Nitrogen.....	17,074	28,268	17,074	28,268
Oxygen.....	658	1,054	658	1,054
Water.....	117	156	339	557
Carbon dioxide.....	696	870	694	856
N ₂ O.....	771	964	771	964
NO**.....	23	139	8	57
NO ₂ ***.....	78	480	28	137

* Measured at operating conditions.

** Variation per inlet effluent stream, 0.05 to 33 wt. %.

***Variation per inlet effluent stream, 0.07 to 49 wt. %.

TABLE 8
LIQUOR SYSTEM

Batch size, U.S. gal.....	2,570
Circulation rate, U.S. gal./min.....	250
Fresh batch composition, wt. % NaOH.....	3.8
Time/batch, hr.....	
Forecast load.....	12.5
Maximum load.....	2.2
NaOH exhaustion, %.....	95
Composition of purge liquor	
NaNO ₂ wt. %.....	5.4
NaNO ₃ wt. %.....	1.5

absorber in which the combined gases are scrubbed by a caustic soda solution before being vented to the atmosphere. The knockout drum for recovery of condensed nitric acid and the separator for removing vapor from the circulating liquor are positioned in the circulating system as shown in Figure 2; later equipment changes for use of the system with a waste ammonia-caustic soda solution are marked separately.

In designing the absorber, the following points were considered:

- A suitable packing.
- A high gas velocity to improve absorption efficiency.
- A liquor rate to wet all of the packing.
- H.T.U. based on the results of the pilot plant tests corrected for changes in the packing and gas velocity.

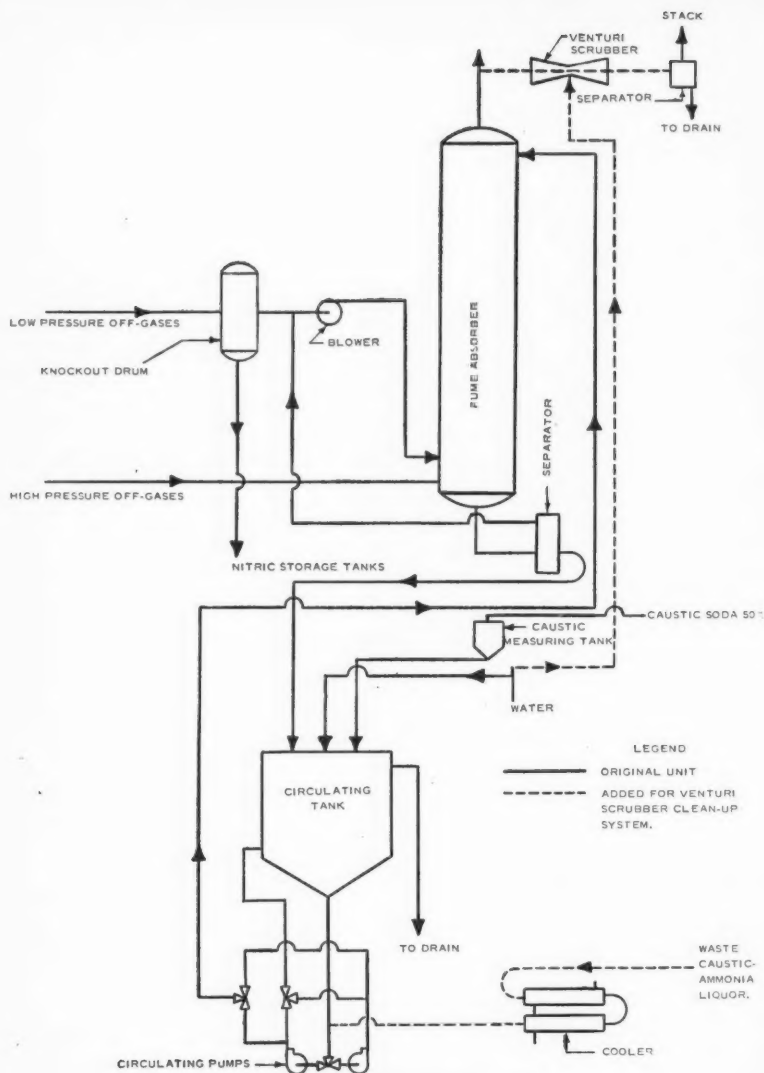


Figure 2—Fume abatement system.

(c) A packed tower height commensurate with optimum incremental removal of NO and NO₂.

The 8-ft. diameter absorber contains a 41.5-ft. depth of 2-in. random packed Raschig porcelain rings, 18-in. acting as an entrainment separator around the 26 liquor dip-pipes. The top of each dip-pipe contains a sloping orifice disc designed for a head of 9-in. of liquor and the bottom is flared and placed over a splash block located in the rings. The inlet liquor pipe divides inside the absorber and feeds a single central liquor feed trough which passes the liquor through notches into five liquor distributors, with attached dip pipes, supported across the absorber.

The absorber was constructed of rubber lined mild steel. Transfer lines and all other equipment which

come in contact with the waste gas were constructed of stainless steel (type 304). The equipment and lines handling the alkaline solution were constructed of mild steel.

The packing was dumped into a water filled section of the absorber and can be removed through a manhole above the supporting grid holding the packing. The distribution of liquor, with no gas flowing through the absorber, can be seen through an open manhole under the grid. The fumes enter near the base and leave at a high velocity through a 15-in. diameter stack attached to the top centre of the absorber.

A number of safety precautions are incorporated in the design. For instance, all headers leading from the tanks to the waste gas blower, are supplied with vents which are open to the atmosphere. These vents have

the dual function of allowing the escape of the waste gas to the atmosphere, in the event of a blower stoppage, and preventing the blower from pulling a vacuum on the tanks by admitting atmospheric air to the headers in the event of a waste gas flow decrease. Broken rings are retained by wire mesh strainers on the pump suction lines and stopped by an internal wire covered perforated pipe through which the liquor passed before leaving the circulating tank. No pump trouble has been experienced although many finely-broken rings were removed in the first few weeks of operation. On failure of a circulating pump or during a dump, a mercoird switch stops the blower and opens an automatic valve, venting the high pressure reaction off-gases to a stack and preventing the fumes from entering the absorber. At the same time an alarm on the blower sounds and the operator vents the waste gases from the nitric acid plant through another stack to prevent acidic conditions in the absorber.

Plant Tests. Although a caustic soda liquor proved satisfactory in reducing NO and NO₂ in the vent gases, the operating costs could be reduced substantially by using an available waste ammonia-caustic soda solution (0.5% free NaOH, 0.45% Na₂CO₃ and 0.03-0.5% NH₃) which was tested during 1955 in the fume abatement system as an alternative scrubbing medium. The waste stream was cooled to 35°C. to avoid damaging the rubber lining of the absorber and passed through additional piping to the fume abatement system. Several plant tests of a semi-continuous nature were made to determine the percentage exhaustion, and the color and appearance of the plume leaving the absorber. The utility of the ammonia-caustic liquor was better than 80%. An analysis of the solution showed a straight line relationship between pH and the degree of exhaustion of the spent liquor between 40 and 100% exhaustion. On 100% exhaustion, equivalent to a pH of 7.5, the liquor released CO₂ gas. This gave a ready method of control since a pH meter, with recorder and alarm, could replace an operator who formerly spent considerable time on control analysis. Based on preliminary analytical tests, the removal efficiency of NO and NO₂ with the waste liquor was as good as that obtained with a caustic soda solution. This comparison is not out of line with the early pilot plant tests conducted with NH₃ present in the

gas phase. The plume from the stack of the fume absorber changed from a light reddish-brown to an intense white color; it is quite possible that the whiteness of the plume obscured any brown coloration of the gas. The appearance of the white color was attributed to the presence of ammonium nitrate and nitrite released in a finely divided state; the nuisance that can be caused by these white solids has been reviewed in a recent article⁽²¹⁾. This objection had to be overcome before the waste liquor could be used for continuous operation.

The addition of NH_3 to the base of the absorber and subsequent installation of water sprays above the packing failed to reduce the white plume which under certain meteorological conditions tended to settle on the ground downwind from the stacks.

A microscopic examination of the solids showed that they were very small, 0.1 to 10 microns in size. As wet scrubbers are satisfactory for removing such small particles, tests were made in a pilot plant Venturi scrubber which was reported to give satisfactory removal for sub-micron sized particles. Information on the design and applications of the Venturi scrubber is given by Johnston and Roberts⁽²²⁾. As the inlet water enters the throat of the Venturi and is dispersed into small particles by the high velocity of the gas, intimate mixing is maintained between the liquid and the gaseous phases. When water was added to the test Venturi scrubber, 60 to 90% of the white fumes was removed, higher values being obtained when steam was added to coalesce the particles prior to the scrubber.

System improvements. Following the test work conducted with a Venturi scrubber for the removal of fine solids, the findings were reviewed with Sheldons Engineering Limited, Canadian suppliers of Venturi scrubbers. Their proposal for a Venturi scrubber and separator was accepted. Figure 3 illustrates the Venturi scrubber and separator installed in the fume abatement system. A simple separator follows the scrubber to remove large liquid droplets, 50 to 150 microns in diameter.

The Venturi scrubber and separator were designed for a gas flow of 7,000 cu. ft./min. and a liquid flow of 42 U.S. gal./min. with a total pressure drop of 22 in. W.G. and recovery efficiency of 99.0% plus. The dimensions of the Venturi scrubber are 9-1/4 and 18-in. for

throat and end diameters and 10-ft. 6-in. for length and of the separator, 4-ft. for diameter and 9-ft. for length.

Performance

The fume absorber was first checked for liquor distribution under varying rates of flow. Water was found to leave the packing in a uniform manner across the tower, without any sign of cascading down the wall. Good distribution was again noted after a year's operation although an additional 6-in. of packing had to be added to retain its initial depth.

After the start-up of the plant, a feed liquor containing 3.5-5% caustic was circulated in the absorber until near exhaustion when it was replaced with a fresh batch. Because of analytical difficulties no reliable absorption data are available for this period of operation, although the color of the off-gas stream indicated

substantial reduction of the NO_2 content.

Adequate material balances have been developed around the absorber with the waste ammonia-caustic soda solution as the scrubbing liquor. These studies were conducted at a time when the plant was operating at a capacity halfway between the forecast and maximum loads. The quantities of NO and NO_2 present in the waste gases were considerably reduced by improvements and changes in plant operation. In Table 9 the plant results are compared with design figures derived from Table 7.

Owing to surges, the quantity of oxides of nitrogen in the waste gas varies considerably.

The caustic scrubbing solution was circulated on a batch basis with periodic titrations and dumped when it had attained a 95% exhaustion. Since employment of the waste am-

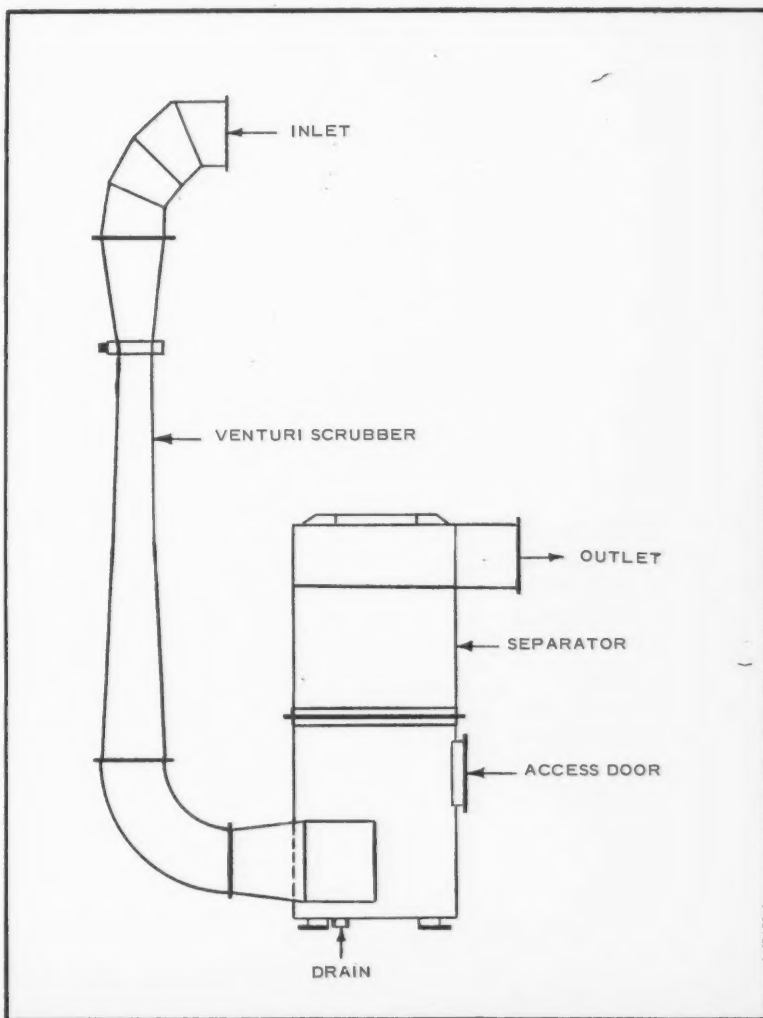


Figure 3—Venturi scrubber and separator.

TABLE 9
DESIGN AND PLANT PERFORMANCE ABSORPTION EFFICIENCIES

	In, lb./hr.		Out, lb./hr.		Absorption Eff. %
	NO	NO ₂	NO	NO ₂	NO and NO ₂
DESIGN DATA					
Forecast Load.....	23	78	8	28	65
Maximum Load.....	139	480	57	137	65
PERFORMANCE DATA (NO expressed as NO ₂)					
Nov. 1956.....	91		24		74
Dec. 1956.....	47		11		75
Jan. 1957.....	76		12		84

TABLE 10
PLANT PERFORMANCE DATA

		Aug. 1957	Sept. 1957	Oct. 1957
Gas Rate,	cu.ft./hr.....	340,000	340,000	300,000
NO ₂ into absorber,	lb./hr.....	105	60	75
NO into absorber,	lb./hr.....	25	14	18.4
NO ₂ in absorber off-gas, lb./hr.....		18.5	3.7	12.5
NO in absorber off-gas, lb./hr.....		1.7	1.6	4.4
NO ₂ in Venturi off-gas, lb./hr.....		2.5	2.0	2.2
NO in Venturi off-gas, lb./hr.....		0.3	0.7	0.5
Final concentration of outlet gas, p.p.m. oxides of nitrogen.....		105	102	115

TABLE 11
COMPARISON OF PILOT PLANT, DESIGN, AND PERFORMANCE H.T.U. VALUES

	Pilot Plant	Design	Experimental				
			Calculated		Observed		
			Case 1 & 2*	Case 3*	Case 1*	Case 2*	Case 3*
Column Diam., ft.....	1	8	8	8			
Flow Area, sq. ft.....	0.785	50.2	50.2	50.2			
Size of Rings, in.....	1	2	2	2			
Voidage.....	0.80 **	0.74**	0.74**	0.74**			
Area of Packing, sq.ft./cu.ft....	46.7 **	25.7 **	25.7 **	25.7 **			
Gas Rate, cu.ft./min.....	60	6,850	5,670	5,000			
Gas Velocity through Packing, ft./sec.....	1.6	3.1	2.55	2.25			
Gas Packing Factor.....	2.7 ***	3.25***	3.25***	3.25***			
Liquid Rate, U.S.gal./min....	7.5	250	250	250			
H.T.U., ft.....	20	34.3	32.2	31.4	21	15	24

* Cases 1, 2, and 3 refer to Aug., Sept., and Oct. 1957 respectively.

** Packing physical properties furnished by supplier.

***Gas packing factors obtained from reference (23) and corrected by an experience factor of 20% for the 2 in. packing.

monia-caustic solution, the scrubbing medium has been used on a continuous bleed-off and make-up basis. The average exhaustion of the liquor to the sewer is 63%, with exhaustion values ranging from 40 to 100%, the actual value depending on the availability of the waste liquor which was completely passed through the absorber. Vaporized ammonia is added automatically to control the pH.

More recent data have become available. These have resulted from the employment of better analytical methods and are recorded in Table 10.

It is of some interest to compare the calculated values of H.T.U. with those actually obtained, based on total NO and NO₂ absorption. Table 11 provides this comparison. The "Design" and "Experimental-Calculated" values were computed according to reference (23), for a gas-film controlled absorption process (5 and 6). A satisfactory explanation cannot be offered for the lower H.T.U. values and improved performances obtained by the experimental tests.

The Venturi scrubber has proved to be satisfactory in reducing the heavy white plume of ammonium nitrate and nitrite. A demonstration of its effectiveness can readily be observed by noting the change in the appearance of the stack gases after

water is added to the scrubber. The reddish-brown color of the plume nearly disappears and the white discharge is reduced in volume and density. According to Table 10, the removal of ammonium nitrate and nitrite solids, and gaseous NO and NO₂ ranges from 50 to 85%. The removal of solids, based on nitrate only ranges from 92 to 97%.

Hazard

In the removal of NO and NO₂ by ammonia liquor, the deposition and detonation of solid ammonium nitrite are a potential danger as this is an unstable compound and will detonate especially with increase of temperature. Aqueous solutions of ammonium nitrite decompose very slowly and there should be no likelihood of decomposition of the weak liquor in the fume absorption system. To maintain a high level of safety, every precaution is taken during operation to prevent the formation and deposition of solid ammonium nitrite. The surface of the scrubbing and exhaust systems are kept wet, when fume is not passing through the absorption unit.

The equipment was thoroughly inspected after the waste ammoniacal liquor had been added for over a year. No visible deposits of

ammonium nitrite or nitrate were found in the equipment including absorber, Venturi scrubber, separator and associated piping. The removal of the top of the absorber disclosed a yellowish-green colored droplet formation which on analysis showed no ammonia although 4% nitrite and 0.5% nitrate. Washings from the base of the Venturi scrubber and the separator showed traces of nitrite, 5-10 p.p.m.

Inspection will continue on a periodic basis.

Conclusions

In keeping with the policy of the Company, considerable time and expense were directed towards the problem of eliminating a potential nuisance, the release to atmosphere of oxides of nitrogen which are corrosive in nature and unsightly with their intense reddish-brown color. A satisfactory method has been developed through a literature search, a pilot plant study and the design and operation of a fume absorption system whose efficiency has been improved by plant investigations. By adopting the methods presented in this paper it is now possible to remove the oxides of nitrogen from the effluent gases leaving a nitric acid plant.

References

- (1) Arch. Ind. Hyg. and Occ. Med., 9, 6 (1954).
- (2) Magill, P. L., Holden, F. R. and Ackley, C., "Air Pollution Handbook", McGraw-Hill Book Co. Inc., (1956).
- (3) "Nitrous Fumes", Leaflet No. 5, Dept. of Scientific and Industrial Research of Great Britain, H.M. Stationery Office, London (1939).
- (4) Hogg, W. J., Chem. Can., 4, 11, 32 (1952).
- (5) Chambers, F. S. and Sherwood, T. K., Ind. Eng. Chem., 29, 1415 (1937).
- (6) Eagleton, L. C., Langer, R. M. and Pigford, R. L., page 380 of "Absorption and Extraction" by Sherwood, T. K., and Pigford, R. L., McGraw-Hill Book Co. Inc., (1952).
- (7) Private communication from M. S. Peters, University of Illinois.
- (8) Peters, M. S., Ross, C. P. and Anderson, L. B., A.E.C. Technical Report No. 10 (COO-1011), (1953).
- (9) Peters, M. S., Chem. Eng., 5, 197 (1955).
- (10) Daniels, F., Ind. Eng. Chem., 40, 1719 (1948).
- (11) Foster, E. G. and Daniels, F., Ind. Eng. Chem., 43, 986 (1951).
- (12) Adadurov, I. E., Atroschenko, V. I., and Reshetnikowa, M. P., J. Applied Chem. (U.S.S.R.) 10, 1541 (1937).
- (13) Andrussov, L., Ber., 60, 536 (1927).
- (14) Terres, E., and Constantinescu, M., Angew. Chem., 47, 468 (1934).
- (15) Coates, J. E., and Finney, A., J. Chem. Soc., 105, 2444 (1914).
- (16) Kassel, L. S., "Kinetics of Homogeneous Gas Reactions", Chemical Catalogue Co. (1932).
- (17) Walker, A. C., Bray, U.B., and Johnston, J., J. Am. Chem. Soc., 49, 1235 (1927).
- (18) Australian Patent, 106,944 (1939).
- (19) Perelman, S. S., and Kantorovich, L., J. Chem. Inc. (U.S.S.R.) 17, 3 (1940).
- (20) Streight, H. R. L., Eng. J. (Can.) 41, 1, 69 (1958).
- (21) Dorn, H. W., Ann. N.Y. Acad. Sci., 58, 2, 30 (1954).
- (22) Johnston, H. F. and Roberts, M. H., Ind. Eng. Chem., 41, 2417 (1949).
- (23) Morris, G. A. and Jackson J., "Absorption Towers", Butterworth Scientific Publications (1953).

★ ★ ★

Heat Transfer from Column Wall to Bed in Spouted, Fluidized and Packed Systems¹

J. KLASSEN² and P. E. GISHLER³

Heat transfer data have been obtained for heat flowing from a steam jacketed column to a packed, fluidized and spouted bed. The data for packed and fluidized beds are compared with generalized correlations previously proposed. In the case of spouted beds, the heat transfer coefficient increases sharply at the onset of spouting and passes through a maximum as the gas velocity is increased. The maximum heat transfer coefficient is from 25-75% lower for a spouted bed than for a fluidized bed under similar flow conditions. Rice, wheat and Ottawa sand were used as bed materials.

THE spouted bed method of fluid solid contacting has recently been described in detail by Mathur and Gishler⁽¹⁾. Briefly, a spouted bed is obtained by introducing the fluid as a jet at the bottom of a coarse granular bed so as to produce a core of dispersed particles which rises up the centre of the bed and culminates in a fountain at the top. The particles fall out of the fountain or spout and form a dense phase annulus which slowly travels down towards the bottom of the column where the cycle is repeated. The annulus behaves like a moving packed bed since there is little relative sideways motion of the individual particles.

The spouted bed technique has been successfully applied to the drying of wheat⁽²⁾ and shows promise of being suitable for other fluid-solid contacting operations. Essential prerequisites for an evaluation of this technique in connection with any particular possible application include a knowledge of the flow characteristics, heat transfer rates and mass transfer properties of spouted systems. Much work has already been done

on the first phase⁽¹⁾, and it is the aim of the present paper to present the results of heat transfer measurements in spouted systems as a contribution to the second field of spouted bed behaviour. In particular our concern is with heat flow from the column wall to the bed. In order to compare the spouted bed with other fluid-solid contacting operations, corresponding data were taken for packed and fluidized systems.

Apparatus

In almost every case the spouted, packed and fluidized beds were contained in a 1 ft. diameter column 8 ft. high. A few runs on a 6 in. diameter unit are reported; this apparatus will be described later.

Most of the larger column consisted of bell-and-spigot type sections of "Pyrex" piping mounted on a 60° steel cone. The air inlet at the bottom of the cone was 3 in. in diameter, the same size as the air line leading to the unit. The inlet diameter was varied by inserting screened orifices of different sizes between the two halves of the connecting flange. A straightening

section of $\frac{1}{2}$ in. copper tubes 10 in. long preceded the air inlet to the column. Air flow rates above 60 CFM were measured with an orifice meter while a rotameter was used for the lower flows.

Heat was transferred from a steam jacket through the wall of the column into the bed. The heat transfer surface consisted of an 18 in. long steel section, held between two of the "Pyrex" sections, 18 in. above the top of the cone or 26 in. above the air inlet. The adjacent "Pyrex" sections minimized longitudinal conduction and ensured that the heat reached the bed via the steel wall. The heat transfer section is depicted in Figure 1. It

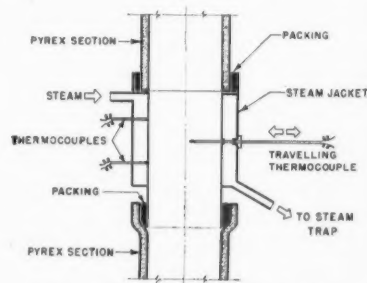


Figure 1—Heat transfer section.

consisted of a 12 in. diameter cylinder of $\frac{1}{8}$ in. thick steel surrounded by a $13\frac{1}{2}$ in. diameter steam jacket. The jacket was terminated 6 in. from the bottom of the section in order to leave room for the bell-and-spigot connection with the "Pyrex" section. A steel bell at the top of the section facilitated connection with the upper "Pyrex" portion of the column. The outside of this heat transfer section was insulated with $4\frac{1}{2}$ in. of asbestos sheet insulation.

¹Manuscript received December 2, 1957.

²Supervisor, Chemical Engineering, Research and Development Laboratories, Du Pont of Canada (1956) Limited, Kingston, Ont.

³Manager, Research and Development, Canadian Chemical Co. Limited, Edmonton, Alberta.

Contribution from the Division of Applied Chemistry, National Research Council of Canada. This article is based on a paper presented at the 38th Annual Conference of The Chemical Institute of Canada, Quebec, Que., June, 1955.

The 6 in. diameter unit was similar to the 12 in. unit except that it was only 3½ ft. high with the heat transfer section 6 in. above the air inlet. Flanged connections were used with the steam jacket extending over the whole 6 in. length of the heat transfer section.

Temperature measurements were made with copper-constantan thermocouples. Two were embedded 6 in. apart, one below the other, in the wall of the heat transfer section to read the wall temperature. A third thermocouple was installed on a level between the first two in such a way that it could be moved horizontally across a column diameter to read radial temperature profiles. The thermocouple leads passed out through the steam jacket and then to a Rubicon potentiometer and ice-water system where the thermal emf's were measured.

The heat transfer rate was calculated from the enthalpy of the incoming and outgoing steam and the steam flow rate. The initial enthalpy was determined from the temperature and pressure of the incoming steam, which had been superheated 5 to 10°F. with a 100 watt electric heater inserted in the steam line. After leaving the steam jacket and passing through a float-type steam trap, the condensate was led to a calorimeter for determination of the final enthalpy and flow rate.

Experimental and Calculations

A. Physical Properties of the Solids

Before any heat transfer runs were conducted some of the physical properties of the various materials used were measured. These properties included bulk densities, absolute particle densities and particle size. Table 1 lists these properties for each of the materials.

The bulk densities were determined by weighing the quantity of material needed to fill a 2 litre cylinder. The absolute densities were determined by several methods. For the Ottawa sand a water displacement pycnometer was used. The values for rice and wheat were measured with an absolute alcohol displacement pycnometer. In the case of the alundum spheres 25 particles were each weighed and the diameter measured with a micrometer.

The particle size of the Ottawa sand (20-30 mesh) was taken as the average of the openings of the two screen sizes. In the case of the wheat and rice two of the dimensions of each of 25 particles were measured with a travelling microscope. The third and smallest dimension was de-

TABLE 1
PHYSICAL PROPERTIES OF THE VARIOUS MATERIALS

Material	Bulk Densities lb./cu.ft.	Absolute Densities lb./cu.ft.	Particle Sizes in.
Ottawa sand (20-30 mesh).....	98.1	165	0.0232
Alundum spheres.....	125	216	0.137
Rice.....	56.3	92.5	0.187 x 0.093 x 0.066
Wheat.....	46.4	86.6	0.206 x 0.117 x 0.105

termined with a micrometer. An average based on the 25 particles is reported for each dimension. The diameters of the spherical alundum particles were read from a micrometer. Again 25 particles were taken as the sample.

B. Heat Transfer Coefficient

The heat transfer coefficient was calculated from the observations by means of the equation:

$$h = \frac{q}{A\Delta t} \dots \dots \dots (1)$$

Heat transfer rate and temperature difference were obtained as follows:

C. Heat Transfer Rate

The heat transfer rate, q , was taken as the difference between the heat given up by the condensing steam and the heat losses through the insulation and steam trap. The former quantity was based on the enthalpy change of the steam in passing

through the unit and the steam flow rate. The pressure and temperature of the incoming steam, which was superheated 5 to 10°F., together with the data of the steam tables, permitted a determination of the initial steam enthalpy.

A calorimeter sitting on a balance pan and equipped with a Beckmann differential thermometer was used to measure the enthalpy of the steam condensate as well as the steam flow rate. The weight of water in the calorimeter was about 40 lb., while the amount of condensate collected per determination was about 2 lb. Weighings were accurate to within 0.1 oz. The calorimeter determination was timed with a stop-watch; the time varied from a few minutes to over an hour. A weight calibration of the calorimeter showed that the buoyant effects on the thermometer, agitator, etc. were negligible while a thermal calibration showed that the heat capacity of the unit, based on the weight

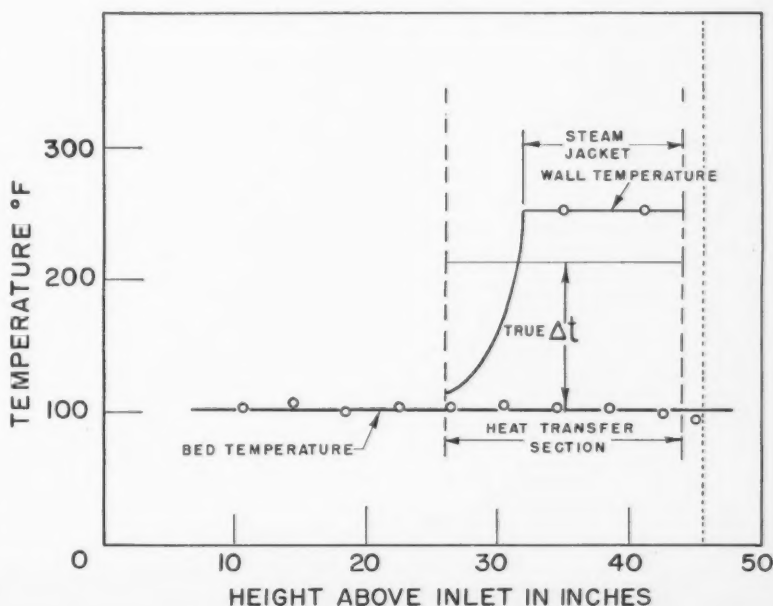


Figure 2—Vertical temperature profiles.

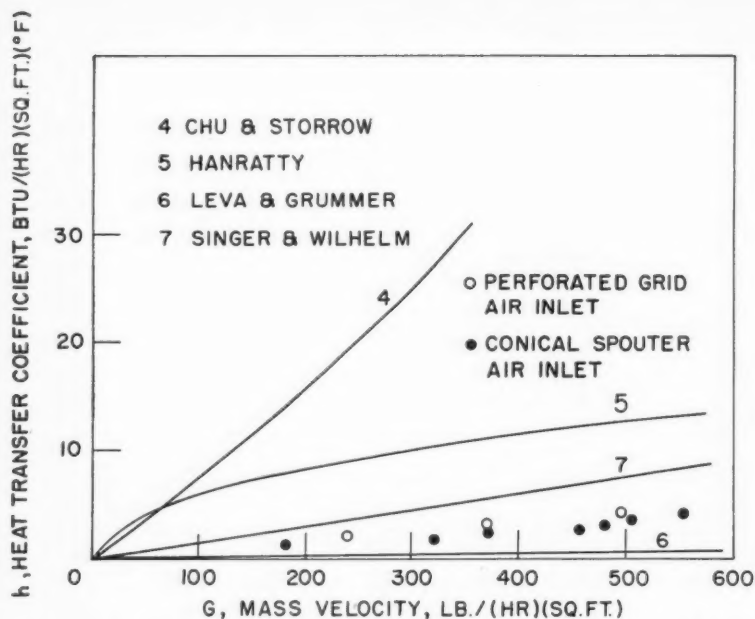


Figure 3—Calculated and observed values of h for a packed bed of rice.

TABLE 2
HEAT TRANSFER IN PACKED BEDS*

	Inlet Diam. in.	Air Flow Rate G , lb./hr. (sq.ft.)	t_a °F.	t_b °F.	Δt °F.	q BTU/hr.	h BTU/(hr.) (sq.ft.)(°F.)
perforated grid air inlet		239	252	74	156	1530	2.2
		371	252	75	151	2210	3.3
		496	252	77	146	2870	4.4
conical air inlet	1	456	251	79	147	1820	2.8
	2	182	254	80	159	960	1.4
	2	371	253	80	150	1870	2.8
	2	480	255	81	148	2210	3.4
	2	554	253	81	143	2800	4.4
	3	322	254	83	152	1320	1.9
	3	505	253	76	150	2470	3.9

* Material: rice, D_c : 1 ft.
bed depth: 4 ft., fluid: air.

of water, varied with the time of operation. This variation was described by

$$\text{heat capacity} = 1 + 0.00782 (\text{time in minutes})^{0.75}$$

The heat losses, i.e. the heat given up by the steam which did not reach the bed via the heat transfer surface, were determined from runs with free convection in the empty column. A correlation for free convection at

vertical surfaces, recommended by McAdams⁽³⁾ was used.

$$\frac{h_c L}{k_f} = 0.13 \left[\left(\frac{L^3 \rho^2 g \beta \Delta t}{\mu^2} \right) \left(\frac{C_p \mu_i}{k_f} \right) \right]^{1/4}$$

For the conditions existing in the 12 in. diameter column

$$\begin{aligned} \text{i.e. fluid is air} \\ \Delta t = 89^\circ \text{F.} \\ A = 4.48 \text{ sq. ft.} \end{aligned}$$

the above equation gives $h_c = 0.87$ BTU/hr. sq. ft.°F.

Heat lost by convection

$$\begin{aligned} q_c &= h_c A \Delta t \\ &= 350 \text{ BTU/hr.} \end{aligned}$$

Heat is also lost from the heat transfer section by radiation. The coefficient of heat transfer by radiation is given by the following equation:

$$h_r = 0.173 \times \epsilon \times \left[\left(\frac{t_a + 460}{100} \right)^4 + \left(\frac{t_b + 460}{100} \right)^4 \right] \frac{t_a - t_b}{t_a - t_b}$$

It is assumed that the heat lost by radiation is equivalent to that lost by two discs equal in area to the cross-section of the column and having the same temperature (252°F.) and emissivity (0.66) as the heat transfer surface. Heat from the top disc is then lost to that part of the column which is at the bed or warm air temperature. That from the lower disc is lost to the column which is at ambient temperature. Substituting these conditions i.e. bed temperature 150° and ambient temperature 80°F., the coefficients of heat transfer are 1.32 and 1.14 BTU/hr.sq.ft.°F. for the top and lower ends respectively.

Cross-sectional area of column = 0.785 sq. ft.

Heat lost from top end,

$$\begin{aligned} q &= h_r A \Delta t \\ &= 1.32 \times 0.785 \times (252 - 150) \\ &= 106 \text{ BTU/hr.} \end{aligned}$$

Heat lost from lower end

$$\begin{aligned} &= 1.14 \times 0.785 \times (252 - 80) \\ &= 154 \text{ BTU/hr.} \end{aligned}$$

Hence total heat passing through heat transfer section and into the column, $q_t = 350 + 106 + 154 = 610$ BTU/hr.

Total heat given up by steam = 1440 BTU/hr. Heat losses in steam pipes, jacket, insulation, etc. are, 1440 - 610 = 830 BTU/hr.

Variation of steam jacket temperature had little effect on the heat transfer coefficient. Most runs were therefore carried out at the same temperature and the heat loss for all runs was constant. A correction of 830 BTU/hr. has been applied in each case.

D. Temperature Difference

The temperature difference, Δt , was calculated from the surface temperatures measured by the two thermocouples embedded in the column wall and the average bed temperature as measured by the travelling thermocouple. Measurements of the vertical temperature profile were made to see if a bed temperature reading at one level (i.e., that of the radially-travelling thermocouple) would be sufficient for calculating Δt . This profile together with the cor-

responding wall temperatures to be discussed subsequently, is given in Figure 2. The uniformity of the bed temperature justifies the use of the bed temperatures read on the one level.

The wall temperature profile is complicated by the fact that the steam jacket extends only a part of the way down the heat transfer section. As would be expected and as was born out by the readings of the two embedded thermocouples the wall temperature is constant over that portion of the surface backed by the steam jacket. A temperature gradient is to be expected, however, over the rest of the surface. This gradient can be formulated mathematically by solving the differential equation for steady state conduction in rods and other projections with the aid of appropriate boundary conditions. This has been done in the appendix. The resulting wall temperature profile has been included in Figure 2 together with the true Δt which, according to the appendix, can be calculated as

$$\Delta t = \left(\frac{A_s + \frac{P}{m} \tanh ml}{A} \right) (t_s - t_b) \dots (5a)$$

$$= \phi (t_s - t_b) \dots (5b)$$

The introduction of equation (5b) into equation (1) gives

$$q = (h\phi) A (t_s - t_b) \dots (3)$$

Equations (5a) and (5b) show that ϕ is a function of h . By choosing values of h and calculating values of ϕ a graph of ϕ vs h or, as is more convenient, a graph of $h\phi$ vs ϕ can be plotted. For each run a value of $h\phi$ can be calculated from equation (3). The graph referred to above gives a corresponding value of ϕ which allows a calculation of the heat transfer coefficient to be made $h = (h\phi)/\phi$.

Results

A. Packed Beds

The majority of the packed bed heat transfer data were taken for beds of rice. Table 2 and Figure 3 show the results. The fact that the data obtained with a perforated grid coincide with the data obtained with a spouting-type air inlet indicates that the air distribution must have been similar in both cases.

Extrapolations of correlations of several workers in the field of wall to packed bed heat transfer have been included in Figure 3 (4,5,6,7). The wide differences are most striking. This seems to be due to the extrapolation of the correlations, which were developed from data in columns under 6 in. in diameter, to a column diameter of 12 in. There is an indica-

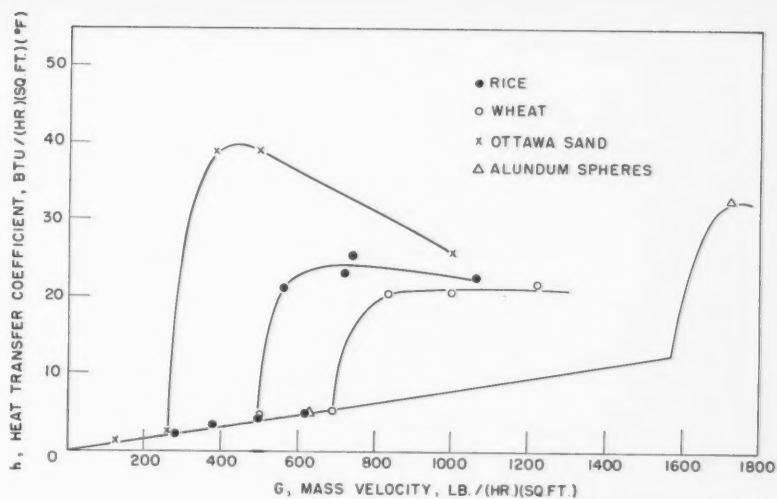


Figure 4— h vs G curves for fluidized beds of rice, wheat, sand, and alundum spheres.

TABLE 3
HEAT TRANSFER IN FLUIDIZED BEDS*

Material	Air Flow Rate G, lb./ (hr.) (sq. ft.)	t_s °F.	t_b °F.	Δt °F.	q BTU/hr.	h BTU/(hr.) (sq. ft)(°F.)
Ottawa sand	126	252	77	159	970	1.4
	228	251	75	153	1800	2.6
	372	250	185	46.7	8220	39.3
	486	249	178	51.6	9010	39.2
	991	249	134	84.7	10050	25.6
Alundum spheres	628	251	77	143	3300	5.2
	1724	248	113	97.8	14040	32.0
Rice	239	252	74	156	1530	2.2
	371	252	75	151	2210	3.3
	496	252	77	145	2870	4.4
	557	250	150	74.3	6960	20.9
	609	251	143	89.2	2740	4.7
Wheat	708	249	138	82.2	8370	22.9
	736	251	135	85.7	9670	25.2
	1060	250	123	94.3	10310	22.3
	492	252	74	147	2960	4.5
	683	252	75	144	3440	5.2
	819	250	128	90.5	8220	20.3
	991	250	121	95.7	8750	20.4
	1219	250	117	99.2	9450	21.3

* D_c : 1 ft., bed depth: 4 ft.

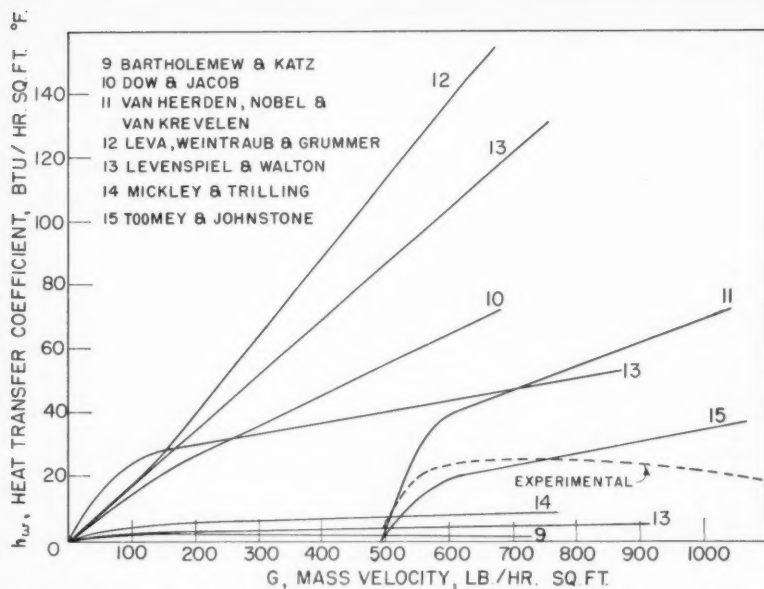


Figure 5—Calculated and observed values of h for fluidized bed of rice.

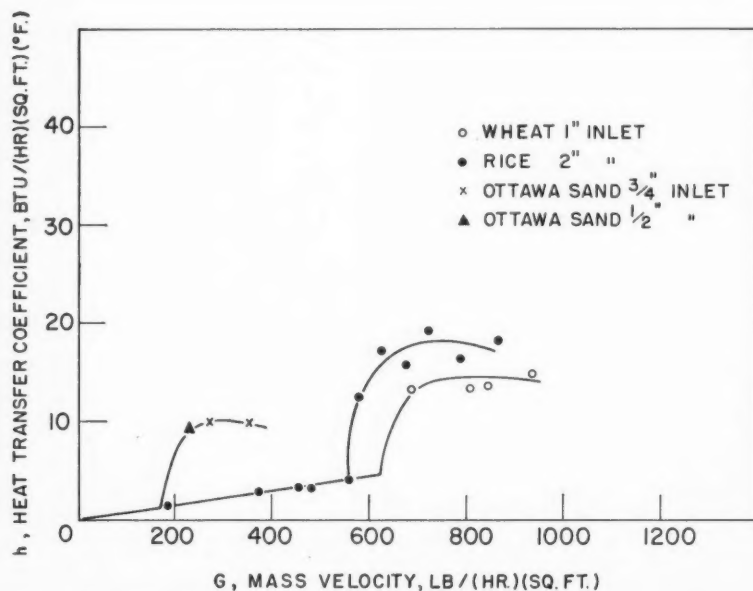


Figure 6— h vs G curves for spouted beds of sand, rice and wheat.

tion that generally the column diameter has only a minor effect on the heat transfer because if the correlations are modified by ignoring the factors involving the diameter they tend to coincide more closely.

B. Fluidized Beds

Fluidized bed heat transfer data were obtained with sand, aluminum spheres, rice, and wheat as bed materials. These materials, particularly the latter three, fluidized poorly because of severe bumping. The data are contained in Table 3 and plotted

in Figure 4. The general shape of the curves with a maximum value of the heat transfer coefficient is in agreement with previous work⁽⁸⁾ as is the trend of heat transfer with particle size, i.e., the larger the particle the lower the maximum heat transfer coefficient. The maximum is the resultant effect of two opposing mechanisms. With increasing air flow rate the turbulence in the bed increases tending to increase h . The increasing flow rate also causes an expansion of the bed with a corresponding decrease in interstitial air velocity. At low air

flows the first effect predominates while at high flows the latter effect governs the behaviour. Somewhere in the intermediate region the two opposing effects must produce a maximum.

The experimental curve for rice is shown in Figure 5 along with curves computed from various proposed formulas^(9,10,11,12,13,14,15). It is evident that only a few of these formulas came close to predicting the heat transfer coefficients actually obtained in the twelve inch unit. Only correlating formulas by Van Heerden et al⁽¹¹⁾ and Toomey, R. D. I. and Johnstone, H. F.⁽¹⁵⁾ take into account the fact that the heat transfer rises suddenly at incipient fluidization, but even these do not predict the shape of the heat transfer curve over a velocity range. Clearly, a generalized heat transfer correlation is not yet available (as already noted by Van Heerden⁽¹⁶⁾) for predicting fluidized bed heat transfer coefficients over a gas velocity range.

C. Air Spouted Beds

The data on heat transfer in spouted beds are given in Tables 4 and 5. Some of the results of Table 4 have been plotted in Figure 6. The general shape of the heat transfer coefficient vs. mass velocity curve is very similar to the curve for a fluidized bed. In both cases there is a sharp increase at the point of transition from a packed to a moving bed. The heat transfer coefficient rises to a maximum after which it falls off with increasing velocity. The coefficient for a spouted bed is invariably lower than for the corresponding fluidized bed. This is to be expected as there is greater turbulence of the particles in the latter compared with the smooth, orderly, laminar-like motion of the particles at the wall in the former.

Apparently the smaller the particles the lower the heat transfer coefficient for the spouted system and the greater the difference in heat transfer rates between the spouted and fluidized state. This is evident when the data for sand (particle diameter of about 0.02 inches) is compared with that for wheat and rice (particle diameter of about 0.15 in.). The larger bed turnover rates associated with the spouting of larger particles may give rise to the larger heat transfer coefficients. This shows that the effect of particle diameter on heat transfer coefficient in a spouted bed is the reverse of the trend for a fluidized bed. Too few materials were available to make a more reliable study of this variation.

TABLE 4
HEAT TRANSFER IN SPOUTED BEDS

Material	Column Diam. in.	Inlet Diam. in.	Bed Height in.	Air Flow Rate G,lb./.(hr.)(sq.ft.)	t_a °F.	t_b °F.	Δt °F.	q BTU/hr.	h BTU/(hr.)(sq.ft.)(°F.)
Ottawa sand	12	0.5	4	229	251	101	118	4920	9.4
	12	0.75	4	272	250	97	119	5250	9.9
	12	0.75	4	352	251	104	115	5040	9.8
Rice	12	1	4	456	251	79	148	1820	2.8
	12	1	4	556	248	86	124	7530	13.6
	12	1	4	616	249	93	120	6840	12.8
	12	1	4	652	248	90	121	6480	11.8
	12	1	4	681	250	96	112	6910	13.1
	12	2	4	182	254	80	159	960	1.3
	12	2	4	371	254	80	150	1870	2.8
	12	2	4	480	255	81	148	2210	3.4
	12	2	4	554	253	81	143	2800	4.3
	12	2	4	572	251	88	125	7030	12.5
	12	2	4	628	253	96	117	9760	17.1
	12	2	4	677	251	91	121	8570	15.9
	12	2	4	720	252	90	121	10250	19.2
	12	2	4	794	252	91	121	8750	16.1
	12	2	4	862	251	90	121	9750	18.1
	12	3	4	322	254	83	152	1310	3.5
	12	3	4	505	253	76	149	2590	3.9
	12	3	4	572	251	97	119	7010	13.2
	12	3	4	733	251	91	122	8040	14.7
	12	3	4	886	251	91	121	8600	15.9
Wheat	6	1	2	543	248	80	167	140	1.1
	6	1	2	606	249	136	112	1510	17.2
	6	1	2	650	248	127	120	1890	20.0
	12	1	4	681	247	100	113	6460	13.2
	12	1	4	804	248	96	116	7030	13.5
	12	1	4	348	248	93	118	8260	13.7
	12	1	4	939	248	93	117	7900	15.0
	12	3	4	322	252	76	150	2190	3.3
	12	3	4	677	249	96	131	7490	14.2
	12	3	4	751	251	81	140	3040	4.9
	12	3	4	819	249	91	119	8360	15.6

The maximum heat transfer coefficients at different inlet diameters are given in Table 5, for the various materials of this study. It can be concluded that the inlet diameter had no effect, or that the particle break-up, which was much more pronounced for the smaller inlet sizes, changed the effective particle diameter so as to counteract any effect of the inlet diameter alone. The particle break-up was a serious problem in this work. Each run required a period of one or more hours for the attainment of steady-state conditions. Even a small rate of particle break-up could have produced major changes in the system after such long periods. The materials included in this project were chosen after numerous solids had been examined. Many were quickly ruled out after their excessively high attrition rates were observed. The materials which were studied were therefore chosen primarily because of their attrition resistance.

It should be noted that column diameter had no apparent effect on the observed heat transfer coefficient. Pertinent data obtained with rice using the 6 in. and 12 in. column are listed in Table 4.

TABLE 5
MAXIMUM HEAT TRANSFER COEFFICIENT IN A SPOUTED BED USING VARIOUS AIR INLET DIAMETERS*

Material	Inlet Diameter in.	Maximum heat transfer coefficient BTU/(hr.)(sq.ft.)(°F.)
Ottawa sand.....	½	9.4
	¾	9.9
Rice.....	1	13.6
	2	19.2
	3	15.9
Wheat.....	1	15.0
	3	15.6

* $D_c = 12$ in., bed height: 4 ft.

Summary of Results

1. In fluidized beds, heat transfer coefficients increase suddenly on the onset of fluidization, and pass through a maximum value as mass velocity is increased, confirming previous data obtained in a smaller unit.

2. In spouted beds, heat transfer coefficients follow a similar relationship with increasing mass velocity,

but the maximum values are smaller—about 25 to 75% lower than for a fluidized bed under similar conditions.

3. The maximum heat transfer coefficient in a spouted bed is independent of inlet orifice diameter, and of column diameter. There are indications that h_{max} increases with bed particle diameter rather than decreases as normally observed with fluidized beds.

Appendix

A. Calculation of Wall Temperature Profile and an Effective Δt for Heat Transfer

The wall of the heat transfer section backed by the steam jacket (see Figure 1) will be at the condensing steam temperature. The portion of the wall below the level of the steam jacket will contain temperature gradients. A heat balance around an element of this part of the wall results in the differential equation:

$$\frac{d^2T}{dx^2} - m^2T = 0 \dots \dots \dots (4)$$

The section on nomenclature defines all the letters and symbols.

Equation (4) can be solved with the boundary conditions:

$$T = T_s \text{ at } x = 0 \\ (dT/dx) = 0 \text{ at } x = l$$

to give

$$\frac{T}{T_s} = \cosh mx - \tanh ml \sinh mx$$

The effective temperature difference can be calculated from

$$q = hA \Delta t = hA_s T_s + Ph \int_0^l T dx$$

or

$$\Delta t = \left(\frac{A_s + \frac{P}{m} \tanh ml}{A} \right) (t_s - t_b) \dots (5a)$$

$$= \phi (t_s - t_b) \dots \dots \dots (5b)$$

For the 12 in. diameter column

$$A = 4.48 \text{ sq. ft., } a = 0.0315 \text{ sq. ft.,} \\ l = 0.5 \text{ ft.}$$

$$k = 26 \text{ BTU/hr. ft. } ^\circ\text{F. for steel, ref (17)}$$

$$m^2 = \frac{hP}{ka} = \frac{h \times \pi \times 11.5}{12 \times 26 \times 0.0315} = 3.67 \text{ h ft.}^{-2}$$

$$m = 1.917 \text{ h}^{1/2} \text{ ft.}^{-1}$$

$$ml = 0.958 \text{ h}^{1/2}$$

$$\frac{P}{m} = \frac{\pi \times 11.5}{12 \times 1.917 \times \text{h}^{1/2}} = 1.57 \text{ h}^{-1/2} \text{ ft.}^2$$

Substituting in equations (5a) and (5b)

$$\phi = \frac{2.99 + 1.57 \text{h}^{-1/2} \tanh 0.958 \text{ h}^{1/2}}{4.48}$$

Nomenclature

- A = area through which heat flows, sq. ft.
- A_s = heat transfer area backed by steam jacket, sq. ft.
- a = cross sectional area through which heat is being conducted = $\pi D_c x$ (thickness of metal), sq. ft.
- C_p = heat capacity, BTU/(lb.) (°F.).
- D_c = column diameter, ft.
- G = mass velocity, lb./ (hr.) (sq. ft.)
- g = gravitational acceleration = 4.2 x 10⁸ ft./ (hr.) (hr.)
- h = heat transfer coefficient for heat flow from the column wall to the bed, BTU/(hr.) (sq. ft.) (°F.)
- h_c = heat transfer coefficient for free convection, BTU/(hr.) (sq. ft.) (°F.)
- h_{max} = maximum heat transfer coefficient, BTU/(hr.) (sq. ft.) (°F.)
- h_r = heat transfer coefficient for radiation BTU/(hr.) (sq. ft.) (°F.)
- k = thermal conductivity of a solid, BTU/(hr.) (ft.) (°F.)
- k_f = thermal conductivity of a fluid, BTU/(hr.) (ft.) (°F.)
- L = height of heat transfer section, ft.
- l = vertical distance between the bottom of the steam jacket and the bottom of the heat transfer section, ft.
- m = $h P/ka$, ft.⁻¹
- P = circumferential perimeter of heat transfer section = πD_c , ft.
- q = heat flow rate from column wall to the bed, BTU/hr.

- T = $t_w - t_b$, °F.
- T_s = $t_s - t_b$, °F.
- Δt = temperature difference between column wall and bed, °F.
- t_b = bed temperature, °F.
- t_s = temperature of condensing steam, °F.
- t_w = wall temperature, °F.
- x = vertical distance below the bottom of the steam jacket, ft
- β_f = fluid coefficient of thermal expansion, (°F.)⁻¹
- μ_f = fluid viscosity, lb./ (ft.) (hr.)
- π = 3.14159
- ρ_f = fluid density, lb./cu. ft.
- ϕ = $(A_s + P/m \tanh ml/A)$
- ϵ = emissivity of heat transfer section.

References

- (1) Mathur, K. B., and Gishler, P. E., A. I. Ch. E. Journal, 1, 157 (1955).
- (2) Mathur, K. B., and Gishler, P. E., J. Appl. Chem. 5, 624 (1955).
- (3) McAdams, W. H., "Heat Transmission", 3rd ed., p. 172, McGraw-Hill Book Co., Inc., New York.
- (4) Chu, Y. C., and Storrow, J. A., Chem. Eng. Sci., 1, 230 (1952).
- (5) Hanratty, T. J., Chem. Eng. Sci., 3, 209 (1954).
- (6) Leva, M., and Grummer, M., Ind. Eng. Chem., 40, 415 (1948).
- (7) Singer, E., and Wilhelm, R. H., Chem. Eng. Prog., 46, 343 (1950).
- (8) Baerg, A., Klassen, J., and Gishler, P. E., Can. J. Res., F28, 287 (1950).
- (9) Bartholomew, R. N., and Katz, D. L., Symposium Series No. 4, p. 3, A. I. Ch. E., New York, 1952.
- (10) Dow, W. M., and Jacob, M., Chem. Eng. Prog., 47, 637 (1951).
- (11) Van Heerden, C. Nobel, P., and van Krevelen, D. W., Chem. Eng. Sci., 1, 51 (1951).
- (12) Leva, M., Weintraub, M., and Grummer, M., Chem. Eng. Prog., 45, 563 (1949).
- (13) Levenspiel, O., and Walton, J. S., Symposium Series No. 9, 1, A. I. Ch. E., New York, 1954.
- (14) Mickle, H. S., and Trilling, C. A., Ind. Eng. Chem., 41, 1135 (1949).
- (15) Toomey, R. D., and Johnstone, H. F., Symposium Series No. 5, p. 51, A. I. Ch. E., New York, 1953.
- (16) Van Heerden, C., J. Applied Chemistry, 2, S No. 1, 7 (1952).
- (17) Perry, J. H., editor, "Chemical Engineers' Handbook", 3rd ed., p. 456, McGraw-Hill Book Co., Inc., New York, 1950.

★ ★ ★

Relative Volatility and Enthalpy Data for the Systems C_4 Hydrocarbons-Acetone-Water Developed from Vapor-Liquid Equilibria¹

J. E. EWANCHYNA² and C. AMBRIDGE³

Extractive distillation is widely used in separating C_4 hydrocarbons. A typical extractive solvent for such a separation is an acetone-water mixture. Correct design and selection of optimum operating conditions for extractive distillation towers are ensured by a knowledge of the vapor-liquid equilibria involved.

Pseudo-binary systems of each of the C_4 hydrocarbons, *n*-butane, isobutane, butene-1, and *cis*-butene-2, and acetone-water solvent were investigated at temperatures of 100°, 150°, and 200°F., at water concentrations of 5, 11, and 17 wt. %, (C_4 hydrocarbon-free) and at hydrocarbon concentrations up to 28 mole %. The results were interpreted as activity coefficients, and showed good consistency. The binary Margules three-suffix and van Laar two-suffix equations correlate the measured activity coefficients adequately as a function of concentration.

Dependence of activity coefficients on temperature was used to evaluate the differential heats of solution of the hydrocarbons in the acetone-water solvent. The results were also used to derive partial liquid enthalpy-concentration curves.

Ternary Margules three-suffix and van Laar two-suffix equations gave a satisfactory correlation of activity coefficients for pseudo-ternary systems. The ternary Margules equations were used to calculate relative volatilities, which are presented graphically as functions of temperature and composition.

To ensure correct design and economic operation of extractive distillation towers used in separations of C_4 hydrocarbons, knowledge is required of the vapor-liquid equilibria that are involved. Such information is needed particularly for multicomponent systems which deviate considerably from ideality, because the relative volatilities of the hydrocarbons in the extractive solvent depend on the total concentration of hydrocarbon in the solvent and the relative concentrations with respect to each other. Two widely used extracting solvents are acetone-water mixtures and furfural-water mixtures.

Accurate determinations have been reported of vapor-liquid equilibrium data on C_4 hydrocarbons with dry furfural^(1,2) and with furfural-water

mixtures^(3,4). These binary, ternary and quaternary mixtures of non-ideal components were successfully treated with the Margules three-suffix and van Laar two-suffix equations which were derived by Carlson and Colburn⁽⁵⁾ and Wohl⁽⁶⁾. It was shown^(3,4) that ternary mixtures of hydrocarbon with furfural and water, and quaternary mixtures of two hydrocarbons with furfural and water, could be simplified to pseudo-binary and pseudo-ternary mixtures respectively. This could be done by treating the solvent, furfural-water, as one pseudo-component as long as the water content of the solvent remained constant. Such treatment of data greatly simplified expressions for calculating relative volatility, reduced the number of systems that needed to be studied,

and enabled easier graphical representation of data.

The object of this investigation was to measure vapor-liquid equilibrium data for C_4 hydrocarbon-acetone-water systems for derivation of relative volatility and enthalpy data. Pseudo-binary systems of each of the hydrocarbons, *n*-butane, isobutane, butene-1, and *cis*-butene-2, and the solvent, acetone-water, were investigated at temperatures of 100°, 150°, and 200°F., at water concentrations of 5, 11, and 17 wt. %, (C_4 hydrocarbon-free) and at hydrocarbon concentrations up to 28 mole %. The studies were confined to a range of approximately 0 to 28 mole % hydrocarbon to avoid phase separation. For all calculations the acetone-water solvent was treated as a single pseudo-component. A pseudo-ternary system of *n*-butane-butene-1-acetone-water was investigated at 100° and 150°F., with a water concentration of 11 wt. % (C_4 hydrocarbon-free).

Materials

Pure grade acetone containing up to 0.4 wt. % water was used. The solvent mixtures were made up by adding the calculated weight of water, followed by readjustment with water or acetone to give the required water content as determined by analysis.

The hydrocarbons were obtained from Phillips Petroleum Company and were the pure grade, specified over 99% pure.

Description of apparatus

A flow-type of apparatus was used in which a vapor stream flowed through a liquid mixture at constant temperature and pressure until equilibrium was attained. A schematic flow diagram is shown in Figure 1. This apparatus is a slightly modified

¹Manuscript received November 18, 1957.

²Chemical Engineer, Chemical Engineering Department, Polymer Corporation Limited, Sarnia, Ont.

³Chemist, Research and Development Division, Polymer Corporation Limited, Sarnia, Ont.

Contribution from Polymer Corporation Limited, Sarnia, Ont.

This article is based on a paper presented at the 7th Annual Conference of the Chemical Engineering Subject Division, The Chemical Institute of Canada, Kingston, Ont., March 12, 1957.

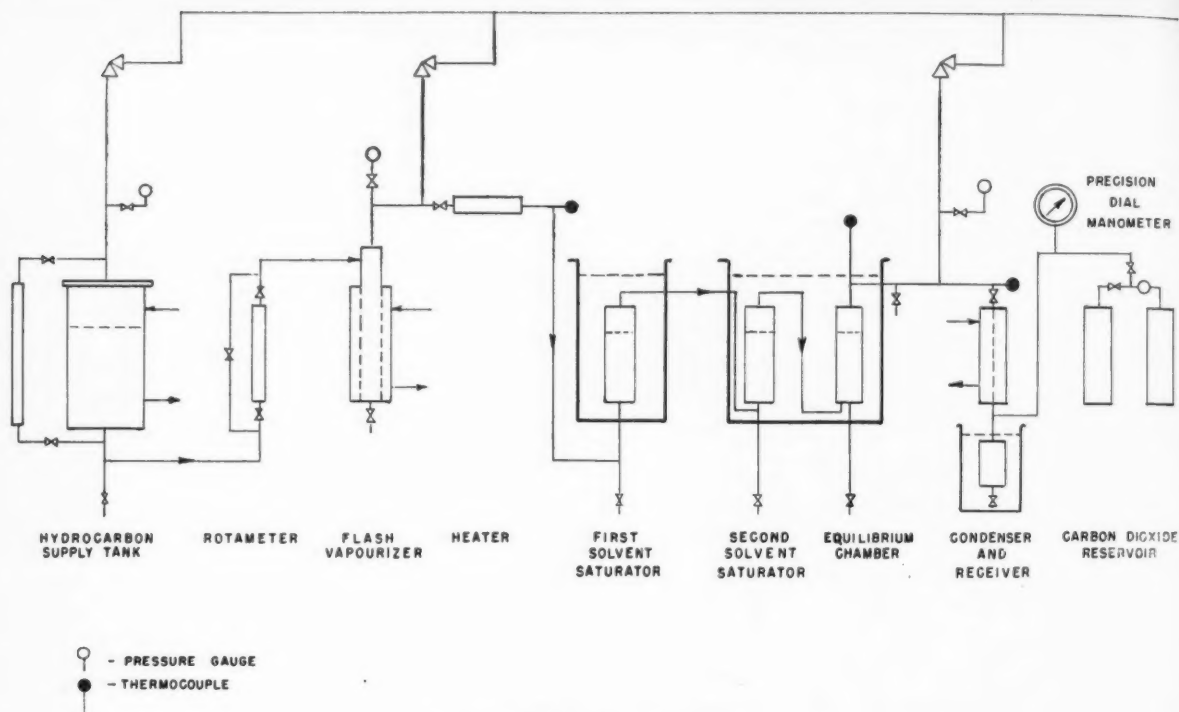


Figure 1—Equilibrium apparatus.

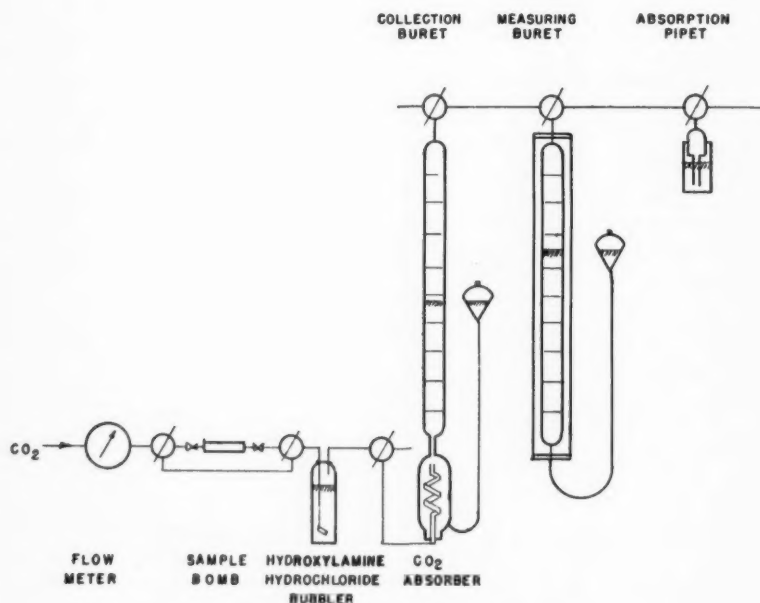


Figure 2—Stripping apparatus.

version of that used at the University of Delaware ⁽¹⁾.

Liquid hydrocarbon stored in the supply tank was heated to keep its vapor pressure at a level sufficient to maintain a flow through the apparatus. Liquid hydrocarbon was metered through a rotameter and vaporized in the flash vaporizer. The hydrocarbon

vapor passed into the first saturator chamber through a heater, which maintained the temperature of the vapor a few degrees above that of the saturator. The vapor next passed through a second saturator into the equilibrium chamber, both vessels being maintained at the same temperature by thermostatic control. The

temperature of the first saturator was adjusted independently of that of the second saturator and equilibrium chamber, and was normally maintained a few degrees higher.

Both saturators contained solvent to ensure that the vapor stream entering the equilibrium chamber was saturated with solvent vapor and would not change in composition as it passed through the solvent in the equilibrium chamber. Use of a second saturator was the major modification of the apparatus from that used at the University of Delaware. The composition of the liquid in the first saturator alters slightly due to the fact that the acetone/water ratio in the vapor differs from that in the liquid; without the second saturator this would affect the composition of the vapor entering the equilibrium chamber. In practice the effect was negligible at 100° and 150°F., but was appreciable at 200°F. With the second saturator the composition of the vapor entering the equilibrium chamber was constant at all three temperatures.

The vapor stream leaving the equilibrium chamber was condensed and collected in a receiver. Constant pressure in the equilibrium chamber was maintained by carbon dioxide back pressure. Diffusion of carbon dioxide to the equilibrium chamber was prevented by the flow of hydrocarbon through the condenser.

Sampling procedure

Sample bombs were made of brass or aluminum, and were fitted at each end with a $\frac{1}{8}$ in. Hoke valve. The size of bomb ranged from 2 ml. to 50 ml., so that samples of any required volume could be taken, depending on the composition of the sample and the analysis required.

In taking liquid samples, a weighed evacuated bomb was securely connected to the sample line at the bottom of the equilibrium chamber. The valves were opened to allow liquid to fill the bomb, then the bomb outlet valve was cracked open and the bomb was slowly flushed with at least four times its volume of liquid. The valves were closed, and the bomb was disconnected, dried and weighed to determine the weight of sample.

In taking vapor samples, it was necessary to condense a sample of vapor into a bomb in order to obtain sufficient sample for analysis. It was important to prevent condensation occurring in the line before the sample point, and to ensure that complete condensation took place as the sample entered the bomb. The sample point was located as close as possible to the equilibrium chamber, and the temperature of the vapor was maintained 5°F. above that of the chamber by means of a heating tape wrapped around the line. A weighed evacuated bomb was connected to the sample point, the space in the union connection was evacuated, and the bomb and connection were carefully tested for leaks. The lower end of the bomb was cooled with liquid nitrogen, while the line up to the

TABLE 1
EXPERIMENTAL COMPRESSIBILITY FACTORS AT APPROXIMATELY 75°F. AND 1.0 ATMOSPHERE

Hydrocarbon	Mean Experimental Determination C	Number of Determinations	Standard Deviation	Literature Value	Reference
n-Butane	0.9732	7	0.0025	0.9728	1
Butene-1	0.9711	9	0.0046	0.9703	1
Isobutane				0.9754	1
cis-Butene-2				0.9741	4

valve was maintained at a high temperature. The valve was cracked open, and a sample slowly condensed into the bomb. The sample was taken slowly in order to maintain a flow of vapor through the condenser to prevent carbon dioxide from leaking back to the sample point.

A run was usually completed in less than 8 hours. The level of liquid in the equilibrium chamber was observed to rise as hydrocarbon was dissolved, and equilibrium was indicated when this level remained steady. This usually occurred about two hours from the start of the run, and sampling was then started. Three sets of samples were taken for each run. Each set consisted of two liquid and two vapor samples, because in each phase one sample was required for hydrocarbon and acetone analysis, and one for water analysis. Normally two sets of samples were analyzed, and if the agreement was good the third set was discarded. For some

runs only one set of results has been recorded; in these cases one or more samples were accidentally spoiled and the complete analysis was not available, but in no case was a result accepted unless the hydrocarbon analyses on two successive liquid samples showed that equilibrium had been attained.

Analytical procedure

The scheme of analysis for hydrocarbon and acetone was to flush the sample from the bomb with carbon dioxide, remove acetone by passing the stream through an aqueous solution of hydroxylamine hydrochloride, and measure the volume of hydrocarbon in a gas buret after removing the carbon dioxide by absorption in a concentrated caustic solution. Figure 2 is a schematic diagram of the apparatus. Acetone was determined by titrating the hydroxylamine hydrochloride solution with standard alkali solution. Water was determined on a separate sample by titration with

TABLE 2
PSEUDO-BINARY VAPOR-LIQUID EQUILIBRIUM DATA FOR n-BUTANE AND BUTENE-1 IN ACETONE-WATER SOLVENT CONTAINING 5.4 WT. % WATER (C₄ HYDROCARBON-FREE)

Run No.	Total Pressure Mm. Hg.	Vapor Analysis (Mole %)			Liquid Analysis (Mole %)			Correction Factor z	Activity Coefficient of Hydrocarbon
		Acetone	Water	Hydrocarbon	Acetone	Water	Hydrocarbon		
		n-Butane, Temperature 150.3°F.							
100	1773	47.5	5.7	46.8	82.3	14.5	3.20	1.128	5.35
	1769	47.0	5.7	47.3	81.9	14.8	3.28	1.128	5.25
99	2787	27.3	4.0	68.7	76.6	14.4	9.00	1.092	4.24
	2784	27.6	3.6	68.8	76.5	14.6	8.94	1.092	4.27
116	3534	20.1	3.1	76.8	71.4	13.4	15.21	1.065	3.47
105	4303	16.9	2.2	80.9	62.7	11.6	25.73	1.039	2.56
	4303	16.2	2.0	81.8	62.0	12.1	25.92	1.039	2.58
		Butene-1, Temperature 150.4°F.							
113	1764	48.3	5.3	46.4	81.8	14.0	4.20	1.151	3.45
	1764	47.9	5.5	46.6	81.6	14.2	4.17	1.151	3.49
114	2788	26.3	4.0	69.7	74.6	14.0	11.42	1.117	2.92
	2788	26.1	4.3	69.6	74.9	13.8	11.34	1.117	2.94
111	3535	20.7	3.5	75.8	68.7	13.4	17.92	1.092	2.51
	3535	18.7	3.5	77.8	68.8	12.9	18.34	1.092	2.52
108	4303	15.2	2.7	82.1	60.4	11.7	27.92	1.068	2.07
	4303	15.9	2.3	81.7	60.6	11.3	28.09	1.068	2.05

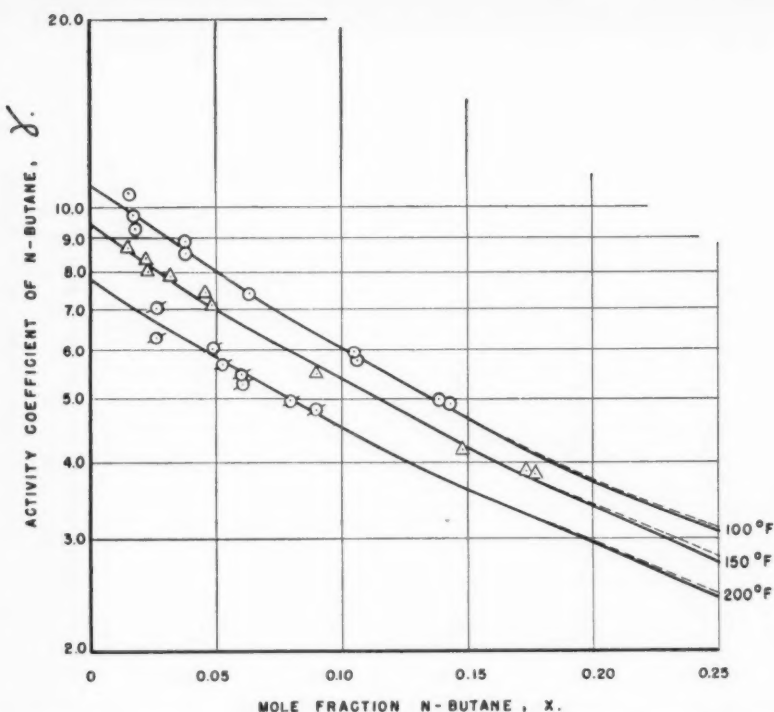


Figure 3—Activity coefficient values for n-butane in acetone-water solvent containing 11.0 Wt. % water (C. Hydrocarbon-Free) showing effect of varying temperature. Solid curves are predicted by binary Margules equation. Dotted curves are predicted by van Laar equation.

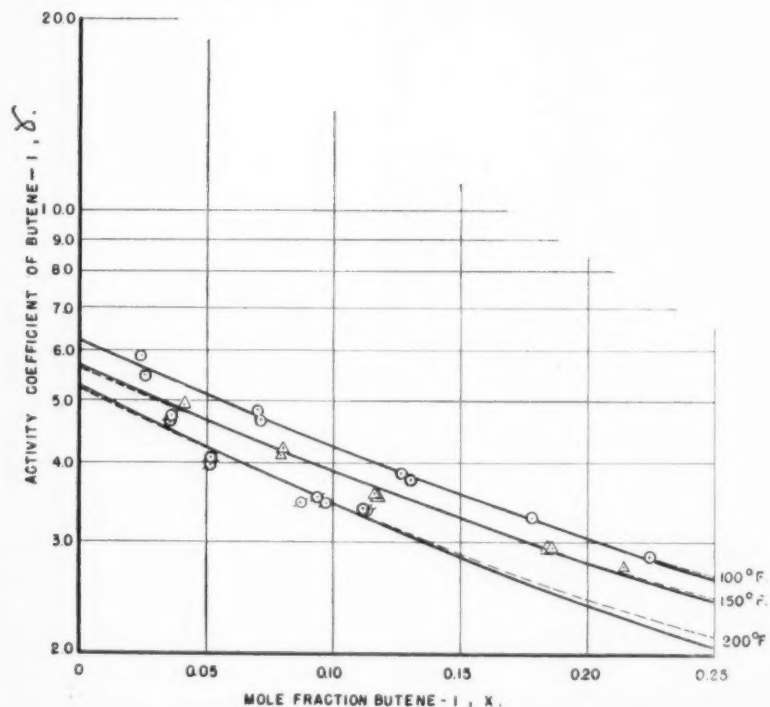


Figure 4—Activity coefficient values for butene-1 in acetone-water solvent containing 11.0 Wt. % water (C. Hydrocarbon-Free) showing effect of varying temperature. Solid curves are predicted by binary Margules equation. Dotted curves are predicted by van Laar equation.

Karl Fischer reagent.

Analysis for hydrocarbon

The closed sample bomb was placed in position, and carbon dioxide was passed through the apparatus to remove all air. The carbon dioxide was absorbed in the 25 wt. % solution of potassium hydroxide contained in the gas collection buret, and any impurity was collected in the buret. The flow of carbon dioxide was continued until successive metered volumes of carbon dioxide gave the same volume of impurity. The maximum amount of impurity was of the order of 0.1 ml. per litre of carbon dioxide.

After expelling the collected gas from the buret, the bomb was opened slowly, and the released hydrocarbon vapor passed through the hydroxylamine hydrochloride solution into the buret. A metered volume of carbon dioxide was passed through the apparatus to remove all hydrocarbon and acetone from the bomb and to strip any dissolved hydrocarbon from the hydroxylamine solution. Once more the flow of carbon dioxide was continued until successive volumes of gas gave the same volume of impurity. The collected gas was transferred to the measuring buret containing fresh potassium hydroxide solution, where its volume was measured and the temperature noted. Solubility of hydrocarbon in potassium hydroxide solution was negligible⁽¹⁾. The volume was corrected for the amount of impurity in the carbon dioxide; normally the value of the correction was less than 1 ml.

The weight of hydrocarbon was calculated from Equation 1.

$$m = \frac{pVM}{CRT} \dots \dots \dots (1)$$

The partial pressure of the measured volume of hydrocarbon was obtained by subtracting the water vapor pressure of the potassium hydroxide solution⁽¹⁾ from the corrected barometric pressure. Compressibility factors for n-butane and butene-1 were determined experimentally by using known weights of pure hydrocarbon as samples. Good agreement was obtained with the values determined by previous workers⁽¹⁾. For isobutane and cis-butene-2 the literature values were used^(1,4). Compressibility factors are given in Table 1.

In the case of hydrocarbon mixtures, two methods were used to determine the ratio of components in the mixture. For Runs 20-32 the gas sample collected in the buret was analyzed by infra-red absorption, and

weighted compressibility factors and molecular weights were used in the gas law equation. For runs 74-80, 84, 119 and 124, butene-1 was absorbed in a solution of mercuric nitrate catalyzed by silver nitrate ⁽²⁾, the residual volume of n-butane was measured and the volume of butene-1 obtained by subtraction.

Analysis for acetone

Acetone reacts almost quantitatively with hydroxylamine hydrochloride in aqueous solution releasing hydrochloric acid, which may be titrated with standard sodium hydroxide solution. The size of the sample was chosen to give a reasonable volume of hydrocarbon gas (at least 30 ml.), so the amount of acetone present varied over a wide range. Normally a 2% hydroxylamine hydrochloride solution was used. The volume of hydroxylamine hydrochloride solution in the bubbler varied from 250 ml. to 1000 ml. depending on the quantity of acetone present. At least four times the theoretical amount of hydrochloride required to react with the acetone was used in order to ensure that the reaction was as complete as possible.

After all the sample had been passed through the solution and the hydrocarbon gas had been collected in the buret, the solution was titrated potentiometrically to pH 3.75 with standard sodium hydroxide solution. A similar blank solution was titrated to pH 3.75, and a correction was applied to the original titre.

In calculating the weight of acetone present a factor was used to allow for the fact that the reaction was not quite complete. In a series of nine tests using a known weight of acetone made up in sample bombs with hydrocarbon present, the factor was determined as 1.0284 with a standard deviation of 0.0050.

Analysis for water

The sample was dissolved in pyridine, and transferred to a titration vessel which was closed to exclude atmospheric moisture. The sample was titrated with Karl Fisher reagent using the "deap-stop" direct titration method ⁽⁷⁾. In nearly anhydrous media, acetone reacts with methanol in the Karl Fischer reagent to form a ketal with the release of water. To inhibit this reaction, the methanol content of the reagent was reduced to a low value, viz. 50 ml. methanol in a solution of 900 ml. pyridine, 133 gm. iodine, and 70 ml. sulphur dioxide, and the titration was carried out rapidly in dilute solution in pyridine. Allowance was made in the result for the small amount of water in the pyridine used to dilute the sample.

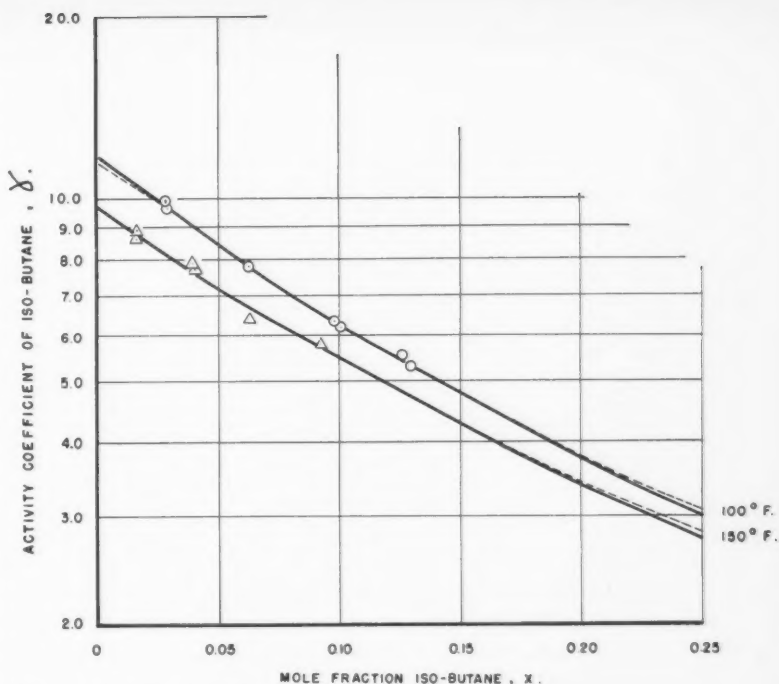


Figure 5—Activity coefficient values for isobutane in acetone-water solvent containing 11.0 Wt. % water (C₄ Hydrocarbon-Free) showing effect of varying temperature. Solid curves are predicted by binary Margules equation. Dotted curves are predicted by binary van Laar equation.

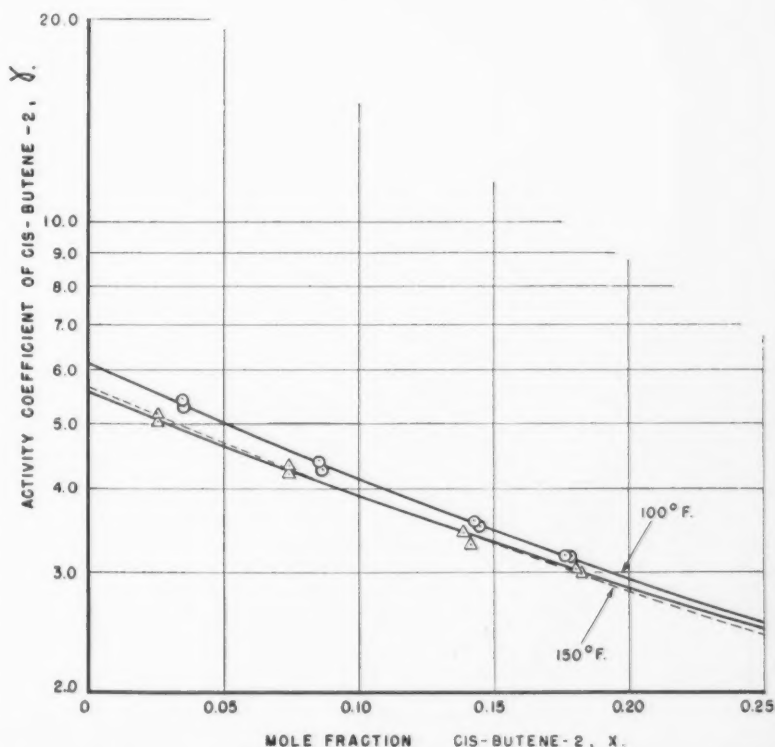


Figure 6—Activity coefficient values for cis-butene-2 in acetone-water solvent containing 11.0 Wt. % water (C₄ Hydrocarbon-Free) showing effect of varying temperature. Solid curves are predicted by binary Margules equation. Dotted curves are predicted by binary van Laar equation.

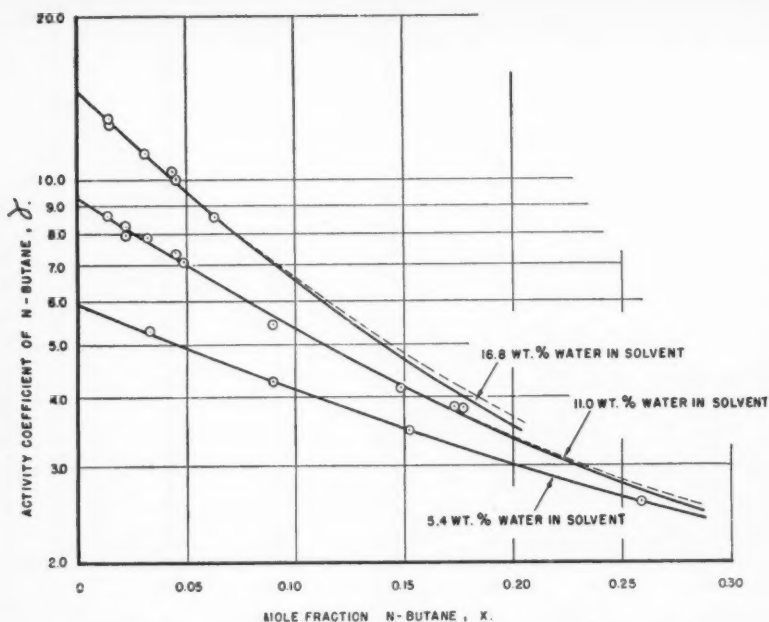


Figure 7—Activity coefficient values for n-butane at 150°F. In acetone-water solvent showing effect of varying solvent composition (C₁ Hydrocarbon-Free). Solid curves are predicted by binary Margules equation. Dotted curves are predicted by binary van Laar equation.

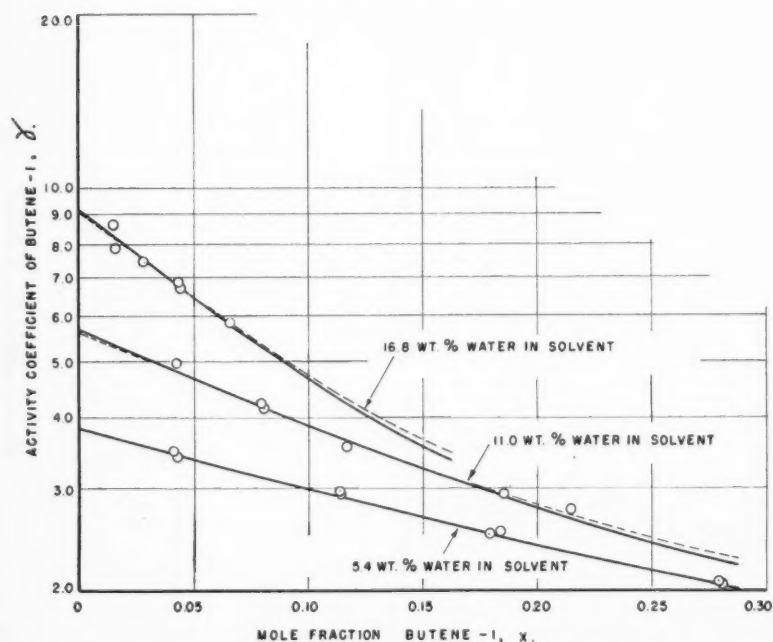


Figure 8—Activity coefficient values for butene-1 at 150°F. In acetone-water solvent showing effect of varying solvent composition (C₁ Hydrocarbon-Free). Solid curves are predicted by binary Margules equation. Dotted curves are predicted by binary van Laar equation.

Activity coefficients of pseudo-binary mixtures

Experimental results of pseudo-binary systems of hydrocarbon and solvent are given in Tables 2, 3, and 4. The activity coefficients of the hydro-

carbons in these tables were calculated by Equation 2:

$$\gamma_1 = \frac{z_1 P y_1}{P_1 x_1} \dots \dots \dots (2)$$

where

$$\log z_1 = \frac{(P_1 - P)(v_1 - B_1)}{2.303 RT} \dots \dots \dots (3)$$

The value z_1 is a correction factor which takes into account the non-ideality of the vapor and the effect of pressure on the liquid ⁽⁸⁾. Hydrocarbon vapor pressures were obtained from correlations by Griswold and Brooks ⁽⁹⁾. Values of liquid hydrocarbon specific volumes and virial coefficients were interpolated from tables given by Mertes and Colburn ⁽¹⁾, and Welty, Gerster, and Colburn ⁽⁴⁾.

The experimental equilibrium data are shown in Figures 3 to 8, inclusive, as the logarithm of the hydrocarbon activity coefficient plotted against the mole fraction of hydrocarbon in the liquid phase. Figures 3, 4, 5, and 6 show the effect of temperature on each hydrocarbon-solvent system, while Figures 7 and 8 show the effect of varying solvent composition at constant temperature for n-butane and butene-1, respectively. The solid curves through the experimental data indicated as circles and triangles were drawn using the binary Margules three-suffix equations ⁽⁶⁾. These may be written as:

$$\log \gamma_1 = x_2^2 [A_1 + 2(A_2 - A_1)x_1] \dots (4)$$

$$\text{limit } \log \gamma_1 \text{ as } x_1 \rightarrow 0 = A_1$$

$$\log \gamma_2 = x_1^2 [A_2 + 2(A_1 - A_2)x_2] \dots (5)$$

$$\text{limit } \log \gamma_2 \text{ as } x_2 \rightarrow 0 = A_2$$

The dotted curves through the experimental data were drawn using the binary van Laar two-suffix equations ⁽⁶⁾ which may be written as:

$$\log \gamma_1 = \frac{A_1 x_2^2}{\left[\frac{A_1}{A_2} x_1 + x_2 \right]^2} \dots \dots \dots (6)$$

$$\text{limit } \log \gamma_1 \text{ as } x_1 \rightarrow 0 = A_1$$

$$\log \gamma_2 = \frac{A_2 x_1^2}{\left[x_1 + \frac{A_2}{A_1} x_2 \right]^2} \dots \dots \dots (7)$$

$$\text{limit } \log \gamma_2 \text{ as } x_2 \rightarrow 0 = A_2$$

In equations 4 to 7 inclusive, the subscript 1 refers to the hydrocarbon component, and the subscript 2 refers to the solvent mixture, acetone-water.

In order to draw curves through the experimental points, values of the terminal activity coefficients, A_1 and A_2 , must be known for the Margules and van Laar equations. The procedure used to obtain values of A_1 and A_2 from the experimental activity coefficients was to apply the method of least squares to Equations 4 and 6.

TABLE 3
PSEUDO-BINARY VAPOR-LIQUID EQUILIBRIUM DATA FOR n-BUTANE, BUTENE-1, ISOBUTANE, AND CIS-BUTENE-2 IN
ACETONE-WATER SOLVENT CONTAINING 11.0 WT. % WATER (C₄ HYDROCARBON-FREE)

Run No.	Total Pressure Mm. Hg.	Vapor Analysis (Mole %)			Liquid Analysis (Mole %)			Correction Factor z	Activity Coefficient of Hydrocarbon
		Acetone	Water	Hydrocarbon	Acetone	Water	Hydrocarbon		
n-Butane, Temperature 99.7°F.									
8	740	40.4	3.6	56.0	70.6	27.8	1.62	1.083	10.54
	743	41.1	4.5	54.4	70.7	27.6	1.71	1.083	9.75
	743	41.1	4.6	54.3	70.9	27.3	1.79	1.083	9.29
11	1132	27.3	2.9	69.8	69.2	27.0	3.78	1.065	8.48
	1136	24.0	3.2	72.8	69.1	27.1	3.77	1.065	8.90
	1141	26.7	2.5	70.8	69.8	26.4	3.83	1.064	8.55
10	1499	19.3	3.2	77.5	67.1	26.6	6.30	1.049	7.36
7	1890	15.0	1.6	83.4	64.9	24.5	10.59	1.032	5.85
	1892	15.3	2.0	82.7	65.1	24.2	10.70	1.032	5.75
46	2124	12.9	2.3	84.8	61.0	24.7	14.32	1.021	4.89
	2113	13.5	2.1	84.4	61.1	24.9	13.94	1.022	4.98
n-Butane, Temperature 149.7°F.									
33	1474	51.4	8.5	40.1	70.8	27.8	1.42	1.138	8.71
81	1736	41.5	7.4	51.1	69.1	28.7	2.17	1.129	8.49
	1724	41.6	7.1	51.3	70.7	27.1	2.25	1.129	8.16
34	2109	35.7	6.1	58.2	69.0	27.8	3.19	1.115	7.89
82	2479	27.2	6.1	66.7	67.4	28.0	4.55	1.102	7.37
	2505	26.9	5.7	67.4	67.5	27.7	4.83	1.101	7.08
35	3288	20.0	4.4	75.6	66.4	24.7	8.96	1.073	5.48
36	4054	16.9	3.9	79.2	61.8	23.4	14.82	1.046	4.17
44	4330	14.9	3.5	81.6	58.8	23.5	17.66	1.037	3.82
	4336	15.9	3.5	80.6	58.6	24.1	17.28	1.037	3.86
n-Butane, Temperature 199.0°F.									
71	3553	48.4	11.5	40.1	69.5	27.8	2.68	1.185	6.31
	3555	45.4	10.6	44.0	69.6	27.8	2.63	1.185	7.02
70	4562	34.5	9.2	56.3	68.2	26.9	4.93	1.154	6.02
	4566	35.3	8.6	56.1	67.8	27.0	5.21	1.154	5.69
69	5078	31.0	8.2	60.7	67.0	26.4	6.61	1.138	5.32
	5084	30.7	7.3	62.0	66.6	26.8	6.58	1.138	5.46
68	5430	28.7	7.3	64.0	66.1	25.9	7.94	1.128	4.94
67	5832	26.7	6.6	66.7	66.0	25.0	9.04	1.116	4.81
	5831	27.6	6.4	66.0	65.2	25.9	8.94	1.116	4.81
Butene-1, Temperature 99.7°F.									
12	751	40.0	4.9	55.0	70.0	27.6	2.44	1.096	5.87
	751	39.3	5.5	55.2	69.8	27.6	2.62	1.096	5.48
16	1293	19.5	3.1	77.3	66.8	26.2	7.02	1.074	4.83
	1288	20.8	3.1	76.1	67.2	25.7	7.17	1.074	4.64
14	1766	15.0	2.1	82.9	62.8	24.5	12.76	1.055	3.82
	1771	15.1	1.9	83.0	62.9	24.1	13.04	1.055	3.76
18	2068	11.6	2.4	86.0	59.2	22.9	17.84	1.043	3.28
24	2244	10.1	2.0	87.9	54.3	23.2	22.47	1.036	2.87
Butene-1, Temperature 149.7°F.									
54	2041	36.2	6.5	57.3	67.9	27.9	4.16	1.140	4.97
72	2768	26.3	5.2	68.6	65.1	27.0	7.93	1.116	4.14
	2761	24.5	5.3	70.2	65.3	26.7	7.99	1.116	4.20
38	3278	20.4	5.3	74.3	63.9	24.4	11.70	1.096	3.54
	3278	20.2	5.1	74.7	63.7	24.6	11.72	1.096	3.55
39	4067	16.2	4.0	79.8	59.1	22.4	18.45	1.073	2.93
	4065	15.6	4.0	80.7	59.0	22.4	18.57	1.073	2.94
43	4343	14.1	3.6	82.3	56.0	22.6	21.42	1.065	2.76
Butene-1, Temperature 199.0°F.									
65	3544	45.3	10.7	44.0	69.3	27.2	3.52	1.218	4.61
	3547	43.8	10.4	45.8	69.0	27.4	3.55	1.218	4.76
57	4082	41.0	10.2	48.8	68.1	26.8	5.15	1.202	3.97
	4082	39.8	10.1	50.1	67.4	27.5	5.13	1.202	4.09
55	5098	32.7	7.9	59.4	66.5	24.8	8.72	1.173	3.48
66	5412	30.7	7.3	62.0	64.5	25.8	9.73	1.164	3.43
	5404	32.0	7.0	61.0	64.6	26.0	9.37	1.164	3.50
64	5762	26.3	7.3	66.4	63.0	25.8	11.18	1.155	3.38
	5752	26.0	7.1	67.0	63.5	25.1	11.37	1.155	3.35

TABLE 3 (Continued)

PSEUDO-BINARY VAPOR-LIQUID EQUILIBRIUM DATA FOR n-BUTANE, BUTENE-1, ISOBUTANE, AND CIS-BUTENE-2 IN ACETONE-WATER SOLVENT CONTAINING 11.0 WT. % WATER (C₄ HYDROCARBON-FREE)

Run No.	Total Pressure Mm. Hg.	Vapor Analysis (Mole %)			Liquid Analysis (Mole %)			Correction Factor z	Activity Coefficient of Hydrocarbon
		Acetone	Water	Hydrocarbon	Acetone	Water	Hydrocarbon		
Isobutane, Temperature 99.7°F.									
62	1257	24.1	2.9	73.0	69.9	27.2	2.83	1.101	9.64
	1259	22.1	2.9	75.0	69.5	27.6	2.86	1.101	9.81
61	2031	15.4	1.7	82.9	67.0	26.8	6.22	1.069	7.82
	2028	14.4	1.9	83.7	66.8	26.9	6.27	1.069	7.81
60	2527	11.6	1.4	87.0	64.7	25.5	9.83	1.048	6.33
	2523	11.0	1.8	87.2	64.2	25.7	10.06	1.049	6.19
59	2797	9.0	1.8	89.3	61.7	25.6	12.69	1.038	5.51
	2780	10.2	2.0	87.8	62.2	24.9	12.94	1.038	5.28
Isobutane, Temperature 149.7°F.									
87	1793	44.7	7.7	47.6	70.0	28.4	1.59	1.184	8.62
	1796	42.9	7.9	49.2	69.7	28.7	1.62	1.184	8.76
86	2767	23.4	5.6	71.0	68.3	27.7	3.96	1.150	7.74
	2764	23.8	5.6	70.6	68.4	27.7	3.90	1.150	7.81
88	3481	20.0	4.2	75.8	66.8	26.9	6.31	1.126	6.39
85	4288	14.2	3.2	82.6	64.9	25.9	9.18	1.098	5.75
cis-Butene-2, Temperature 99.7°F.									
95	744	39.6	5.1	55.3	67.8	28.7	3.51	1.066	5.33
	744	39.4	4.9	55.7	67.8	28.7	3.48	1.066	5.42
94	1155	23.9	3.5	72.6	64.9	26.6	8.56	1.049	4.39
	1152	24.3	3.5	72.2	65.1	26.2	8.66	1.049	4.30
96	1471	17.8	2.8	79.4	61.3	24.2	14.52	1.036	3.55
	1476	18.0	3.0	79.0	61.0	24.7	14.34	1.036	3.59
118	1611	17.5	3.2	79.3	58.4	23.9	17.68	1.030	3.17
	1611	17.0	2.9	80.1	58.0	24.1	17.93	1.030	3.16
cis-Butene-2, Temperature 150.0°F.									
117*	1506	50.9	9.3	39.8	70.1	27.3	2.57	1.116	5.17
	1506	51.6	8.9	39.5	68.9	28.5	2.60	1.116	5.06
91	2273	29.7	6.0	64.3	65.5	27.1	7.40	1.089	4.29
	2265	27.8	6.2	66.0	66.2	26.3	7.47	1.089	4.35
92	3004	20.4	4.5	75.1	61.5	24.6	13.92	1.064	3.44
	2986	21.3	5.0	73.7	61.6	24.2	14.16	1.065	3.30
98	3285	16.8	4.5	78.7	59.7	22.1	18.25	1.055	2.99
	3285	17.5	3.5	79.0	59.8	22.1	18.08	1.055	3.03

*The temperature for Run 117 was 150.4°F.

The terminal activity coefficients are tabulated in Table 5.

A pseudo-component treatment may be used when the ratio $x_{\text{acetone}}/x_{\text{water}}$ (K) remains constant. The analytical results in Tables 2 to 4 show some variation in the value of K. The resulting variation in hydrocarbon activity coefficients is small, and the values of the terminal activity coefficients are essentially those for a solvent with the average value of K. An alternative treatment⁽⁴⁾, in which hydrocarbon concentrations were estimated for an exact value of K, gave values up to 3% different for A₁ and 6% different for A₂ in the worst case. The consistency of results, as shown in Figures 3 to 8 inclusive, indicates that the C₄ hydrocarbon-acetone-water pseudo-binary systems can be reliably interpreted by the Margules and van Laar equations. Further evidence will show that treat-

ment of acetone-water as one component in a pseudo-ternary system with two hydrocarbons can also be interpreted by Margules and van Laar equations.

Calculation of enthalpy values

For design and optimum operation of extractive distillation towers knowledge is required of heats of solution for calculation of enthalpies and fluid rates within the tower. Since the experimental data on activity coefficients appear consistent, reliable values of heats of solution may be derived using Equation 8.

$$\frac{d \log \gamma_1}{d(1/T)} = \frac{L_1}{2.303R} \quad (8)$$

The function on the left side of Equation 8 is the slope of a curve formed by plotting the logarithm of the activity coefficient for a given hydrocarbon of composition x_1 against

the reciprocal of the absolute temperature. When $x_1 = 0$, this involves plotting the terminal activity coefficient A₁ against 1/T. The A₁ values of Table 5 appear to be linear functions of 1/T, from which it follows that the heat of solution for the four hydrocarbons in the solvent is essentially independent of temperature in the range of 100° to 200°F.

While A₁ can be calculated accurately by applying experimental results to Equations 4 and 6, the determination of A₂ is much less accurate, particularly at high temperatures where the range of hydrocarbon concentrations was limited. Values of A₂ were plotted against 1/T. For n-butane, isobutane and butene-1 straight lines were drawn through the points at 99.7° and 149.7°F., while for cis-butene-2 a line parallel to that for butene-1 was drawn through the point at 99.7°F. Smoothed Margules

TABLE 4
PSEUDO-BINARY VAPOR-LIQUID EQUILIBRIUM DATA FOR n-BUTANE AND BUTENE-1 IN ACETONE-WATER SOLVENT
CONTAINING 16.8 WT. % WATER (C₄ HYDROCARBON-FREE)

Run No.	Total Pressure Mm. Hg.	Vapor Analysis (Mole %)			Liquid Analysis (Mole %)			Correction Factor z	Activity Coefficient of Hydrocarbon
		Acetone	Water	Hydrocarbon	Acetone	Water	Hydrocarbon		
		n-Butane, Temperature 150.3°F.							
103	1772	42.3	8.4	49.3	59.7	38.8	1.43	1.128	12.58
	1772	41.3	8.5	50.2	59.7	38.9	1.41	1.128	12.99
106	2535	26.7	5.9	67.4	59.2	37.7	3.08	1.101	11.14
	2535	26.9	5.9	67.2	59.4	37.5	3.06	1.101	11.19
104	3037	19.3	5.0	75.7	58.3	37.3	4.37	1.083	10.40
	3036	19.2	5.0	75.8	57.4	38.0	4.53	1.083	10.04
101	3466	17.7	3.4	78.9	56.4	37.4	6.21	1.068	8.59
	3466	17.4	3.1	79.5	56.4	37.4	6.26	1.068	8.59
		Butene-1, Temperature 150.4°F.							
110	1507	41.5	9.5	48.9	59.7	38.8	1.51	1.160	8.70
	1507	43.3	8.8	47.9	59.6	38.8	1.63	1.160	7.88
115	2021	34.7	7.2	58.1	58.3	38.9	2.76	1.142	7.46
	2021	33.6	7.4	59.0	58.8	38.4	2.79	1.142	7.50
112	2519	25.1	6.9	68.0	57.9	37.8	4.34	1.125	6.83
	2519	26.1	5.7	68.1	58.1	37.5	4.41	1.125	6.73
109	3028	19.6	5.6	74.8	56.9	36.5	6.59	1.109	5.86

TABLE 5
TERMINAL ACTIVITY COEFFICIENTS OF PSEUDO-BINARY SYSTEMS

-Binary System	Average Water Conc. of Solvent, wt. %	Temp. °F.	Terminal Activity Coefficients			
			Margules		van Laar	
			A ₁	A ₂	A ₁	A ₂
n-Butane-Solvent	10.8	99.7	1.038	0.677	1.039	0.755
	5.4	150.3	0.775	0.709	0.773	0.718
	11.0	149.7	0.978	0.603	0.978	0.692
	16.8	150.3	1.163	0.400	1.166	0.676
	10.9	199.0	0.890	0.492	0.891	0.603
Isobutane-Solvent	11.0	99.7	1.070	0.642	1.072	0.746
	11.1	149.7	0.986	0.598	0.987	0.696
Butene-1-Solvent	10.9	99.7	0.796	0.695	0.793	0.715
	5.4	150.4	0.585	0.623	0.585	0.626
	10.9	149.7	0.756	0.610	0.749	0.645
	16.8	150.4	0.956	0.428	0.967	0.557
	11.0	199.0	0.725	0.398	0.721	0.500
cis-Butene-2-Solvent	11.2	99.7	0.791	0.650	0.791	0.667
	10.9	150.0	0.747	0.671	0.755	0.646

TABLE 6
SMOOTHED MARGULES PSEUDO-BINARY TERMINAL ACTIVITY COEFFICIENTS IN
SOLVENT CONTAINING 11.0 WT. % WATER (C₄ HYDROCARBON-FREE)

Temp., °F.	n-Butane		Isobutane		Butene-1		cis-Butene-2	
	A ₁	A ₂	A ₁	A ₂	A ₁	A ₂	A ₁	A ₂
99.7	1.047	0.677	1.070	0.642	0.796	0.695	0.791	0.650
149.7	0.964	0.603	0.986	0.598	0.756	0.610	0.747	0.565
199.0	0.895	0.542	0.916	0.561	0.722	0.538	0.710	0.493

values of A₁ and A₂ are presented in Table 6. The linear relationships of A₁ and A₂ with 1/T was chosen to simplify interpolation of values at intermediate temperatures. Such a relationship is consistent with data on C₄ hydrocarbon-furfural systems (1,4), and there is no reason to believe a more complicated relationship exists in the present system. Nevertheless, caution should be applied when using values of the constants at 200°F.

The binary Margules equation, Equation 4, with smoothed values of A₁ and A₂ from Table 6 was used to compute activity coefficients at various hydrocarbon concentrations. These values plotted against 1/T gave straight lines for each hydrocarbon concentration. The slopes of the lines were determined, and by means of Equation 8 the differential heats of solution of the liquid hydrocarbons in the acetone-water solvent were calculated. These are presented in Figure 9. The curves in Figure 9 were integrated graphically to obtain integral heats of solution, which are presented in Table 7. The sign is positive since these heats of solution represent the heat absorbed during solution of liquid hydrocarbon in the solvent.

Similar results for heats of solution would be obtained using Equation 6 and smoothed values of the van Laar constants, A₁ and A₂. As seen in Table 5 the A₁ values are practically identical with the Margules values. The van Laar A₂ values are higher but essentially parallel to the Margules values when plotted against 1/T.

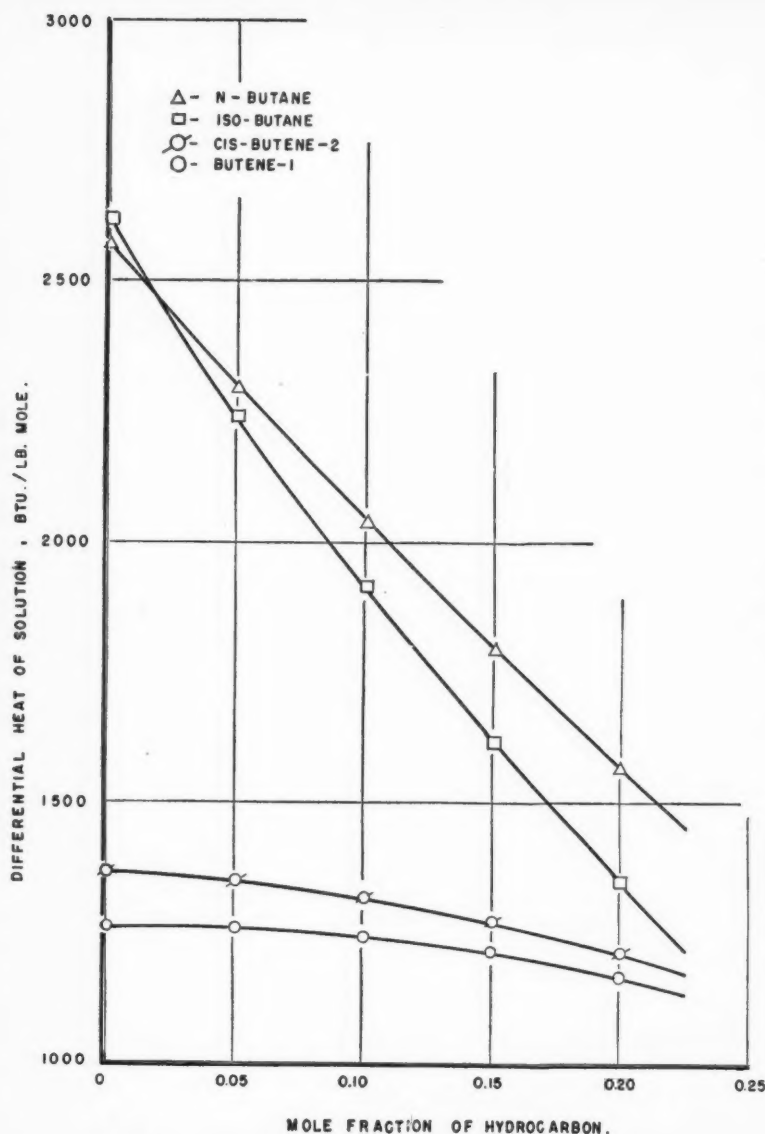


Figure 9—Differential heats of solution of liquid C₄ hydrocarbons in acetone-water solvent containing 11.0 Wt. % water (C₄ Hydrocarbon-Free) in temperature range of 100° to 200°F.

TABLE 7
INTEGRAL HEATS OF SOLUTION OF LIQUID C₄ HYDROCARBONS IN ACETONE-WATER SOLVENT CONTAINING 11.0 Wt. % WATER (C₄ HYDROCARBON-FREE) IN THE TEMPERATURE RANGE OF 100° TO 200°F.

Composition Mole % C ₄ Hydrocarbon	Integral Heats of Solution, Btu./Lb. Mole of Hydrocarbon Dissolved			
	n-Butane	Isobutane	Butene-1	cis-Butene-2
0	2570	2610	1260	1370
5	2440	2430	1260	1360
10	2300	2250	1260	1350
15	2170	2090	1250	1330
20	2050	1940	1240	1310

Since the values of the differential heats of solution are obtained from slopes of $\log \gamma_1$ versus $1/T$, the results will be the same using both Margules and van Laar constants. Easier manipulations with the Margules equation was the reason for its use in these calculations.

The saturated liquid enthalpy of a mixture is the sum of the enthalpies of the pure liquid components and the integral heat of solution of the liquid components when mixed together, and will be expressed at Btu. per pound of solution. A reference state was arbitrarily chosen as the saturated liquid at 0°F. Enthalpies of the pure liquid hydrocarbons were obtained from data published by Maxwell⁽¹⁰⁾, while enthalpies of the pure liquid mixture of acetone and water were obtained from Shell Development Company⁽¹¹⁾. These enthalpies were combined with the integral heats of solution to give saturated liquid enthalpy-concentration curves as shown in Figure 10 for the n-butane-acetone-water system.

For multicomponent liquid or vapor mixtures, such as several C₄ hydrocarbons dissolved in acetone-water, enthalpies are conveniently obtained from the partial enthalpies of the components. The enthalpy is obtained by adding the products of weight fraction and partial enthalpy of all the components as indicated by Equation 9.

$$h = \sum w_i \bar{h}_i \dots \dots \dots (9)$$

Partial liquid enthalpies are determined from saturated liquid enthalpy-concentration curves such as shown in Figure 10 by the method of intercepts⁽¹²⁾. A tangent, for example A B C, is drawn to a curve at a given n-butane concentration, say 20 wt. %. Values of partial enthalpies are read at both extremities of the diagram. At C, the value is the partial enthalpy of n-butane at the given concentration of 20 wt. % and a temperature of 150°F. At A, the value is the partial enthalpy of the solvent at 150°F. containing 20 wt. % n-butane. Values such as C yield partial liquid enthalpy-concentration curves for the four hydrocarbons studied. These curves are presented in Figure 11. Values such as A are found to be almost identical for all four hydrocarbon-solvent systems at given hydrocarbon concentrations and temperatures. These values are averaged and presented in Figure 12 as partial liquid enthalpy-concentration curves for acetone-water solvent containing any C₄ hydrocarbon.

The partial enthalpies of vapor

Figure 10—Saturated liquid enthalpy-concentration curves for the n-butane-acetone-water system. Solvent contains 11.0 Wt. % water (C_4 Hydrocarbon-Free).

phase mixtures of C_4 hydrocarbon-acetone-water are the same as the enthalpies of the pure components at any given temperature and solvent composition. This result follows from the assumption that the heat of mixing of a C_4 hydrocarbon and solvent in the vapor phase is negligible.

Activity coefficients of pseudo-ternary systems

The pseudo-ternary system of n-butane-butene-1-acetone-water was investigated at 100° and 150°F., at a water concentration of 11.0 wt. % (C_4 hydrocarbon-free). Values of activity coefficients for n-butane and butene-1 were computed by Equations 2 and 3. Results are given in Table 8.

An analysis of theoretical equations which describe ternary vapor-liquid equilibrium data has been made by Wohl^(6,13). The ternary Margules three-suffix equations, for example Equation 10 for component 1, and the ternary van Laar two-suffix equation, for example Equation 11 for component 1, were used in the present investigation. Similar equations may be written for the other components by the cyclic rearrangement of subscripts, that is, substituting 2 for 1, 3 for 2, and 1 for 3.

$$\log \gamma_1 = x_2^2 [A_{1-2} + 2x_1 (A_{2-1} - A_{1-2})] + x_3^2 [A_{1-3} + 2x_1 (A_{3-1} - A_{1-3})] + x_2 x_3 [A_{2-1} + A_{1-3} - A_{3-2} + 2x_1 (A_{3-1} - A_{1-3}) + 2x_3 (A_{3-2} - A_{2-3}) - C_{123} (1 - 2x_1)] \quad (10)$$

(see Equation 11 on page 30)

For the pseudo-ternary system studied, the subscripts 1, 2, and 3 refer to n-butane, butene-1, and acetone-water solvent, respectively. The terminal activity coefficients, A_{1-2} and A_{2-1} , for the n-butane-butene-1 system were assumed to be zero, assuming that a binary system of two hydrocarbons is ideal⁽²⁾. In the van Laar equation, where these constants appear as a quotient, the value may be computed in terms of the other four binary constants of the ternary system⁽⁶⁾. Equation 12 expresses the relationship.

$$\frac{A_{2-1}}{A_{1-2}} = \frac{A_{3-1} A_{2-3}}{A_{1-3} A_{3-2}} \quad (12)$$

Figure 11—Partial liquid enthalpy of C_4 hydrocarbons in acetone-water solvent containing 11.0 Wt. % (C_4 Hydrocarbon-Free).

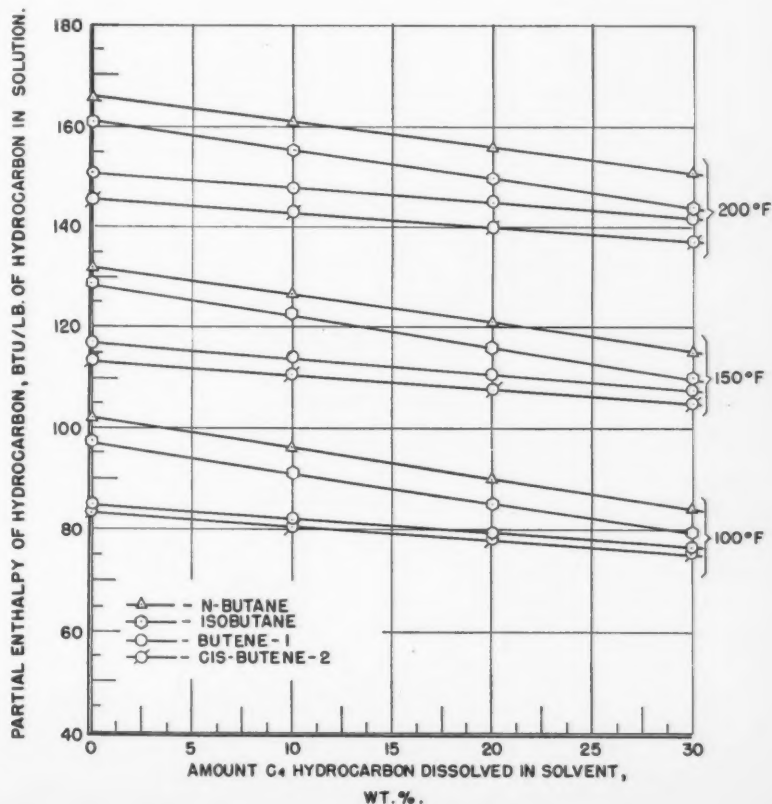
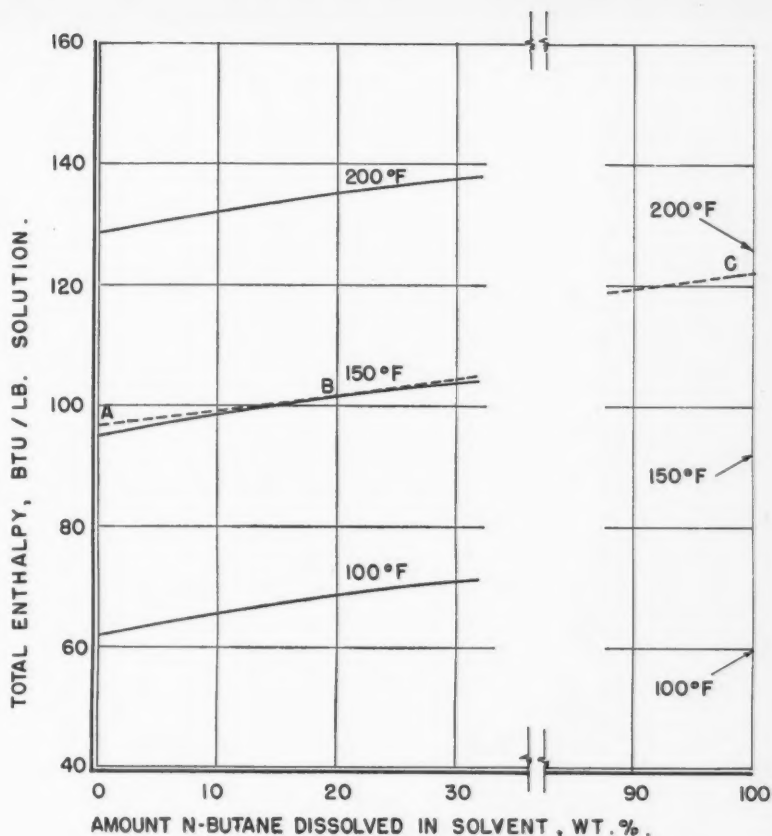


TABLE 8
PSEUDO-TERNARY VAPOR-LIQUID EQUILIBRIUM DATA FOR THE SYSTEM n-BUTANE-BUTENE-1-ACETONE-WATER
SOLVENT CONTAINING 11.0 Wt. % WATER (C₄ HYDROCARBON-FREE)

Run No.	Total Pressure Mm. Hg.	Vapor Analysis (Mole %)				Liquid Analysis (Mole %)				Correction Factor α_1	Activity Coefficient of n-Butane	Correction Factor α_2	Activity Coefficient of Butene-1
		Acetone	Water	n-Butane	Butene-1	Acetone	Water	n-Butane	Butene-1				
Temperature = 99.7°F.													
25	745	39.0	5.4	19.6	36.0	70.7	27.1	0.61	1.61	1.083	9.85	1.097	5.77
29	1015	25.7	5.4	16.5	52.3	68.3	27.4	0.81	3.55	1.070	8.44	1.085	5.13
30	1420	18.5	2.4	18.7	60.4	66.6	25.6	1.46	6.36	1.052	7.29	1.069	4.56
26	1427	18.8	4.1	29.9	47.2	65.9	26.8	2.28	4.97	1.052	7.50	1.069	4.57
21	1446	20.3	3.7	55.5	20.5	66.9	26.5	4.39	2.22	1.051	7.31	1.068	4.51
	1456	17.8	3.3	57.6	21.3	66.7	26.6	4.46	2.25	1.051	7.52	1.068	4.65
31	1840	14.7	2.5	22.7	60.1	63.3	23.7	3.03	9.95	1.034	5.42	1.052	3.69
	1845	14.7	2.5	22.7	60.1	63.6	23.4	3.03	9.95	1.034	5.44	1.052	3.70
22	1922	13.7	2.7	62.0	21.6	63.4	25.2	7.90	3.48	1.030	5.91	1.049	3.95
32	2130	12.0	2.1	24.3	61.4	60.2	21.1	4.29	14.39	1.021	4.72	1.040	2.99
	2122	12.6	2.2	24.3	60.9	59.7	22.0	4.21	14.12	1.022	4.76	1.041	3.01
28	2179	11.9	2.2	48.5	37.4	59.9	22.1	9.35	8.60	1.019	4.39	1.039	3.11
23	2188	10.9	2.1	63.4	23.6	59.7	21.5	12.97	5.89	1.019	4.15	1.038	2.87
Temperature = 149.7°F.													
75	2007	36.3	7.2	17.4	39.1	68.3	28.1	0.94	2.67	1.119	7.64	1.141	5.20
	2001	39.5	6.8	16.9	36.8	68.7	27.8	0.86	2.61	1.119	8.10	1.141	4.99
	1999	39.5	6.8	16.5	37.2	68.7	27.7	0.89	2.66	1.119	7.61	1.142	4.95
84	2009	36.7	7.4	38.8	17.1	69.8	26.9	2.08	1.19	1.119	7.71	1.141	5.10
	2012	37.4	7.1	38.5	17.1	70.0	26.7	2.05	1.21	1.119	7.77	1.141	5.02
124*	2755	25.1	5.9	22.5	46.6	67.4	25.7	1.84	5.11	1.093	6.70	1.118	4.31
	2762	24.5	5.0	22.5	48.0	67.5	25.6	1.81	5.13	1.093	6.83	1.118	4.43
	2765	25.2	5.3	22.3	47.2	67.7	25.3	1.89	5.12	1.093	6.51	1.118	4.37
119*	2782	24.9	5.1	43.7	26.3	66.4	27.3	3.48	2.81	1.092	6.96	1.117	4.47
74	3515	17.8	3.9	23.4	54.9	62.1	26.3	3.05	8.51	1.065	5.28	1.091	3.83
	3525	20.2	3.5	23.3	53.0	62.3	26.0	3.06	8.59	1.064	5.26	1.091	3.68
	3501	19.8	3.7	22.7	53.8	62.1	26.4	2.90	8.58	1.065	5.38	1.092	3.71
79	3547	19.7	3.2	52.8	24.3	63.3	26.0	6.82	3.87	1.064	5.38	1.090	3.76
80	4041	14.9	3.1	54.3	27.7	60.4	24.3	9.37	5.96	1.047	4.51	1.074	3.12
	4041	16.8	2.4	54.1	26.7	60.2	24.3	9.63	5.85	1.047	4.37	1.074	3.07
76	4068	17.9	3.0	25.7	53.4	59.6	24.1	4.62	11.68	1.046	4.35	1.073	3.09
	4073	14.7	3.0	27.3	55.0	59.8	23.9	4.68	11.63	1.046	4.57	1.073	3.20
	4078	14.9	3.0	26.3	55.8	59.5	23.9	4.85	11.78	1.046	4.25	1.073	3.21

*The temperature for Runs 119 and 124 was 150.4°F.

TABLE 9
SAMPLE CALCULATION OF VAPOR PHASE COMPOSITION BY THE RELATIVE VOLATILITY METHOD

Component	Liquid Phase Composition x_i , Mole Fraction	Amount of Component Relative to Butene-1, %	Volatility of Component Relative to Butene-1 at 150.4°F. α	αx	Calculated Equilibrium Vapor Phase Composition, y_i , Mole Fraction	Experimental Equilibrium Vapor Phase Composition, y_i , Mole Fraction
Butene-1	0.0195	100.0	1.000	0.0195	0.136	0.136
cis-Butene-2	0.0331	62.9	0.778	0.0258	0.180	0.185
n-Butane	0.0174	47.1	1.275	0.0222	0.155	0.151
Isobutane	0.0258	57.0	1.695	0.0437	0.305	0.305
Solvent	0.9042	97.9	0.0353	0.0319	0.223	0.223
				Sum = 0.1431		

Equation 11

$$\log \gamma_1 = \frac{\left[x_2^2 A_{1-2} \left(\frac{A_{2-1}}{A_{1-2}} \right)^2 + x_3^2 A_{1-3} \left(\frac{A_{3-1}}{A_{1-3}} \right)^2 + x_2 x_3 \left(\frac{A_{2-1}}{A_{1-2}} \right) \left(\frac{A_{3-1}}{A_{1-3}} \right) \left(A_{1-2} + A_{1-3} - A_{3-2} \frac{A_{1-3}}{A_{3-1}} \right) \right]}{\left(x_1 + x_2 \frac{A_{2-1}}{A_{1-2}} + x_3 \frac{A_{3-1}}{A_{1-3}} \right)^2} \quad (11)$$

At a first approximation the ternary constant, C_{123} , in the Margules equation was assumed to be zero. As will be seen later, this assumption was justified.

In Figures 13, 14, 15 and 16 the experimental values of hydrocarbon activity coefficients, indicated by circles, are shown as functions of composition. The abscissa is mole

fraction of hydrocarbon component, while the parameter $\frac{100 x_3}{x_2 + x_3}$ or $\frac{100 x_3}{x_1 + x_3}$ represents the relative amount of the other two components. Values of activity coefficients predicted by Equations 10 and 11 are shown as solid and dotted curves, respectively. Smoothed values of the terminal activity coefficients were used. Good agreement was obtained between experimental activity coefficients and those predicted by the ternary equations, as shown in Figures 13 to 16, inclusive. Hence, a value of $C_{123} = 0$ appears to be justified.

It is not surprising to see both the van Laar and Margules ternary equations describe equally well the present system at 100° and 150°F. In systems like the present or the C_4 hydrocarbon-furfural system (1,3,4) which are slightly dissimilar as indicated by the

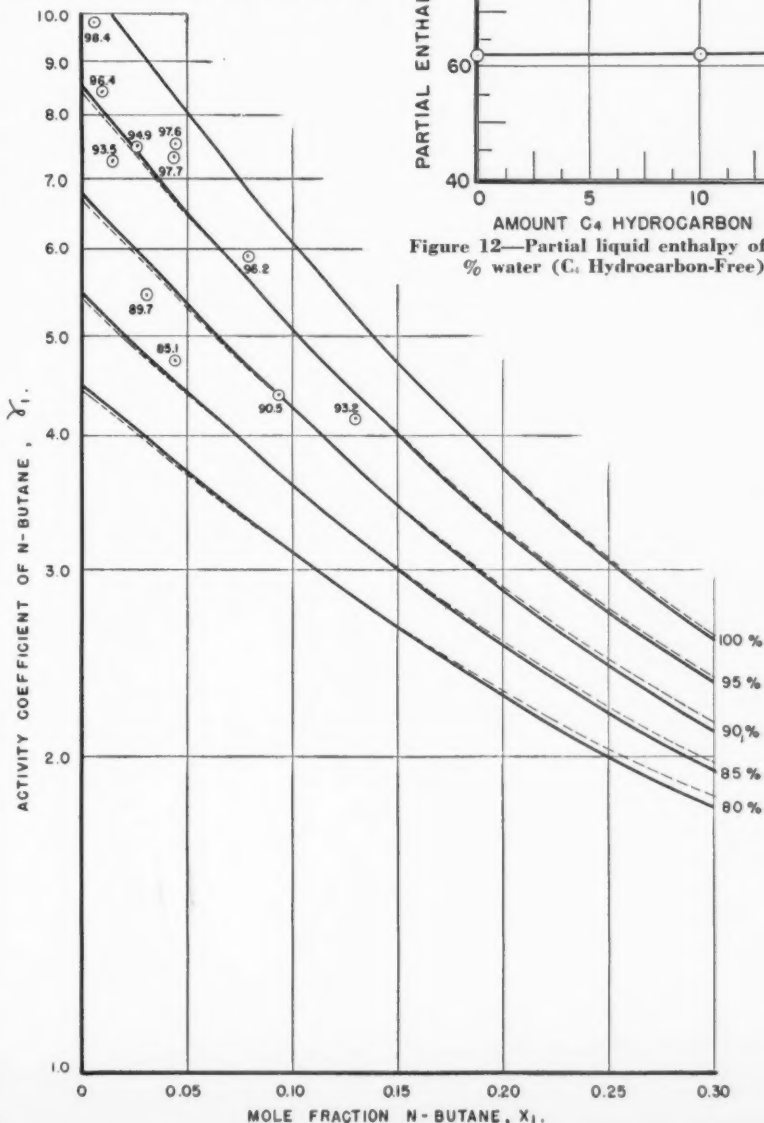


Figure 12—Partial liquid enthalpy of acetone-water solvent containing 11.0 Wt. % water (C_4 Hydrocarbon-Free) in solution with any C_4 hydrocarbon.

ratio of A_2 to A_1 being near 1 both equations give similar results (6). Thus, calculations involving the ternary equations justified using the Margules equations because they were easier to work with. Since the ternary equations were not checked experimentally at 200°F, caution should be exercised when using the terminal activity coefficients at this temperature.

Relative volatility values

In distillation applications relative volatility is of prime importance. The dependence of relative volatility on other variables is often expressed in terms of activity coefficients as defined by Equation 13.

$$\alpha_{1-2} = \frac{\gamma_1 P_{122}}{\gamma_2 P_{221}} \dots \dots \dots (13)$$

Figure 13—Activity coefficients of n-butane in mixtures with butene-1 and acetone-water solvent at 100°F. Solvent contains 11.0 Wt. % water (C_4 Hydrocarbon-Free). Solid curves are predicted by ternary Margules equation. Dotted curves are predicted by ternary van Laar equation. Values of parameter are $100 x_3 / (x_2 + x_3)$.

Figure 15 — Activity coefficients of butene-1 in mixtures with n-butane and acetone-water solvent at 100°F. Solvent contains 11.0 Wt. % water (C. Hydrocarbon-Free). Solid curves are predicted by ternary Margules equation. Dotted curves are predicted by ternary van Laar equation. Values of parameter are $100 x_3/(x_1 + x_2)$.

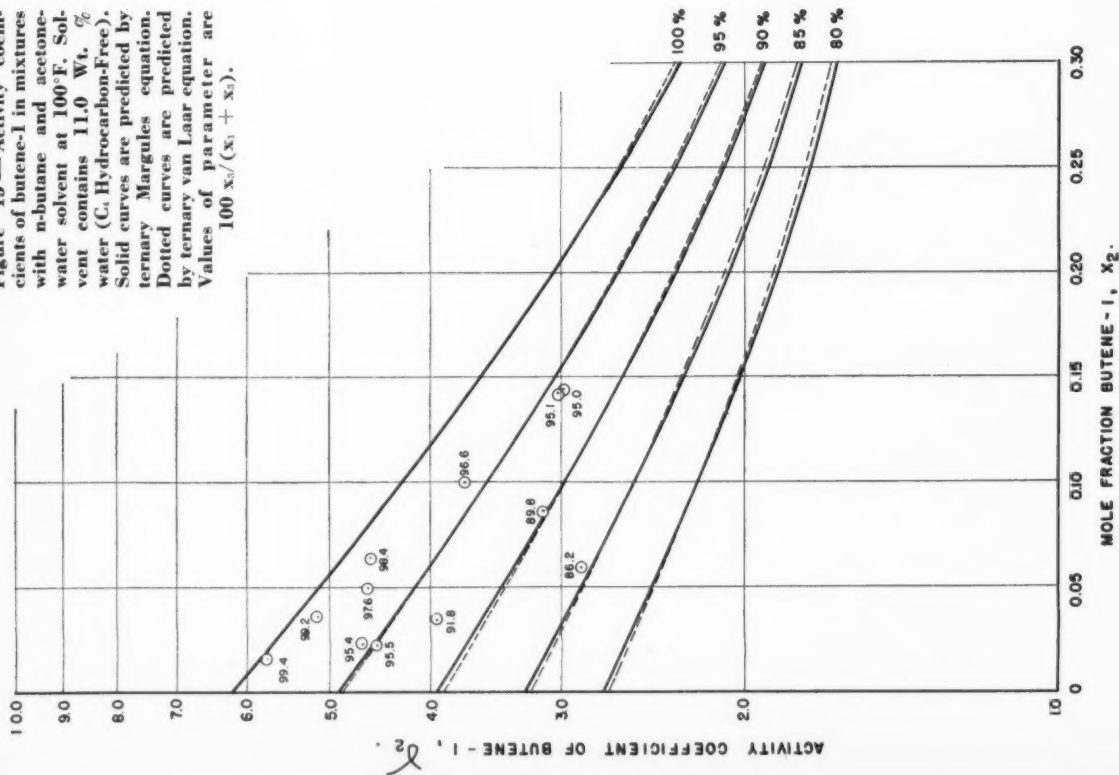
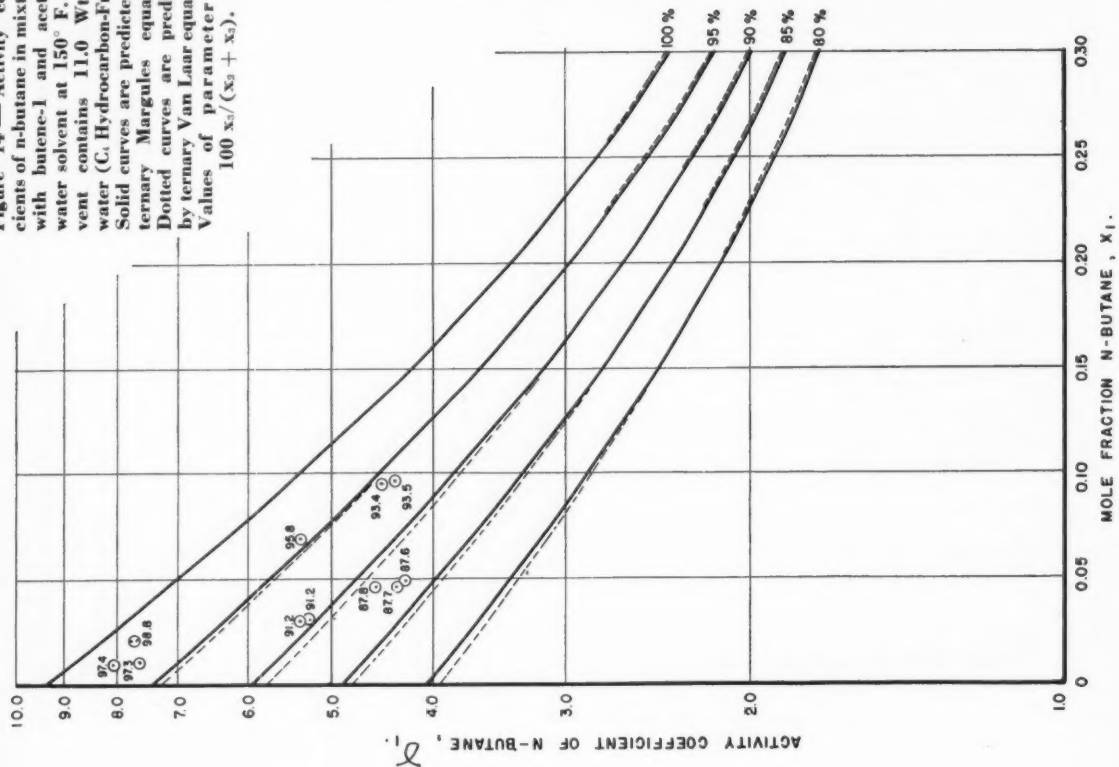


Figure 14 — Activity coefficients of n-butane in mixtures with butene-1 and acetone-water solvent at 150°F. Solvent contains 11.0 Wt. % water (C. Hydrocarbon-Free). Solid curves are predicted by ternary Margules equation. Dotted curves are predicted by ternary van Laar equation. Values of parameter are $100 x_3/(x_1 + x_2)$.



The ratio γ_1/γ_2 may be calculated from the ternary Margules or van Laar equations. The former equations yield the simpler expression, given by Equation 14, assuming that A_{1-2} , A_{2-1} , and C_{123} are each zero.

$$\log \frac{\gamma_1}{\gamma_2} = x_3 [(1 - 2x_1) A_{1-3} - x_3 A_{2-3} + 2x_1 A_{3-1} - (1 - x_3) A_{3-2}] \quad (14)$$

Values of vapor pressures were obtained from Griswold and Brooks⁽⁹⁾, while the correction factors z_1 , z_2 , were calculated by Equation 3. Smoothed values of the terminal activity coefficients were used in Equation 14.

Volatilities of n-butane isobutane, and cis-butene-2 relative to butene-1 present in solvent containing 11.0 wt. % water (C_4 hydrocarbon-free), calculated by Equations 13 and 14, are shown in Figure 17, 18 and 19 as functions of temperature and composition. Figure 20 shows the volatility of the solvent mixture containing 11.0 wt. % water (C_4 hydrocarbon-free) relative to butene-1 as a function of temperature and composition. In Figures 17, 18 and 19 the relative volatility is seen to decrease with increasing temperature and with increasing total hydrocarbon concentration in the liquid phase.

In a multicomponent extractive distillation calculation the composition of vapor phase in equilibrium with a liquid phase is conveniently determined by the relative volatility method⁽¹⁴⁾. Equation 15 is used in the method.

$$y_n = \frac{a_n x_n}{\sum a_n x_n} \quad (15)$$

It is desirable to have the volatilities relative to one of the components; butene-1 was chosen in this investigation.

Table 9 provides a sample calculation of the vapor-phase composition by the above method when the liquid phase composition is known. The liquid phase composition was obtained from a run at 150.4°F. with a multicomponent C_4 hydrocarbon and solvent mixture containing 11.0 wt. % water (C_4 hydrocarbon-free). The experimental vapor phase composition is also shown to compare with the calculated composition. The agreement is satisfactory and indicates that the relative volatility data of Figures 17 to 20 inclusive, may be used in calculations provided some caution is exercised in the 200°F. range where the bulk of the smoothing has been done.

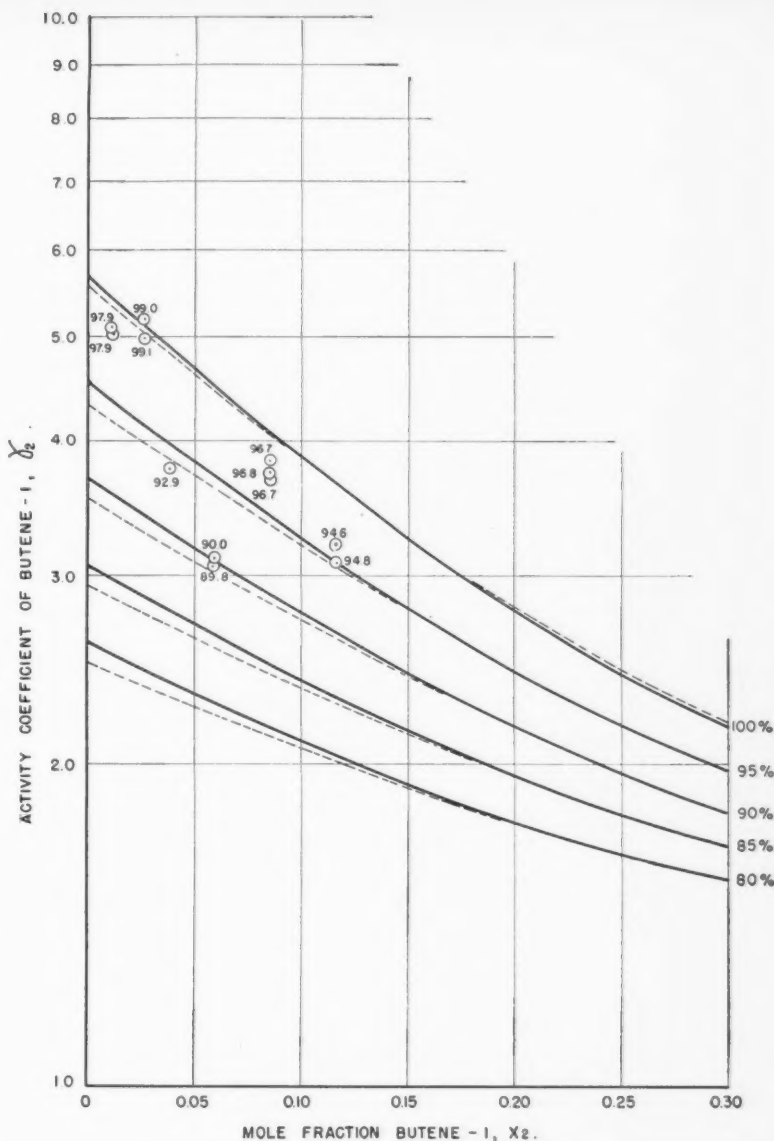


Figure 16—Activity coefficients of butene-1 in mixtures with n-butane and acetone-water solvent at 150°F. Solvent contains 11.0 Wt. % water (C_4 Hydrocarbon-Free). Solid curves are predicted by ternary Margules equation. Dotted curves are predicted by ternary van Laar equation. Values of parameter are $100 x_3/(x_1 + x_3)$.

Conclusions

Vapor-liquid equilibrium data for C_4 hydrocarbons-acetone-water systems have been measured. The consistency of the experimental data interpreted as activity coefficients confirm the reliability of the flow-type apparatus and the analytical methods. Correlation of the experimental pseudo-binary and pseudo-ternary data by use of binary and ternary Margules three-suffix and van Laar two-suffix equations was satisfactory in the range of composition

and temperature studied. The solvent, acetone-water of constant composition, can be treated as one component.

Treatment of the vapor-liquid equilibrium data with Margules three-suffix equations to yield enthalpy and relative volatility data was found to be adequate. The enthalpy and relative volatility data are expressed as functions of temperature and composition. Such data can be used for calculation of rates of flow and compositions of vapor and liquid in extractive distillation towers.

Acknowledgement

Acknowledgement is extended to J. A. Gerster of the University of Delaware for consultation and advice throughout this project; to D. B. Robinson of the University of Alberta for assistance in some phases of the calculations, and to Shell Development Company for permission to publish some of their data on enthalpy of acetone-water mixtures.

The authors appreciate the permission of Polymer Corporation Limited to publish this paper.

Nomenclature

- A_1 = terminal activity coefficient of hydrocarbon in binary equations, limit $\log \gamma_1$, as $x_1 \rightarrow 0$.
 A_2 = terminal activity coefficient of solvent in binary equations limit $\log \gamma_2$ as $x_2 \rightarrow 0$.
 A_{1-2} etc. = terminal activity coefficient in ternary equations, limit $\log \gamma_1$ as $x_1 \rightarrow 0$ and $x_2 \rightarrow 1$.
 B = second virial coefficient in the equation of state, ml./gm.mole.
 C = compressibility factor.
 C_{123} = ternary constant in Margules three-suffix equation for ter-

- nary system of components 1, 2, and 3.
 d = differential operator.
 h = total enthalpy of liquid, Btu./lb. of solution.
 \bar{h} = partial enthalpy of component in solution, Btu./lb. of component.
 K = ratio of mole fraction acetone/water in liquid phase.
 L = differential molal heat of solution of liquid C_4 hydrocarbon in acetone-water solvent, Btu./lb. mole of hydrocarbon.
 M = molecular weight.
 m = weight of hydrocarbon, gm.
 P = total pressure of system, mm. Hg.
 P_1 = vapor pressure of pure component, mm. Hg.
 p = partial pressure of component, mm. Hg.
 R = gas law constant, 62,365 (ml.) (mm. Hg.) ($^{\circ}K$.) (gm. mole) or 1.987 Btu./($^{\circ}R$.) (lb. mole).
 T = absolute temperature, $^{\circ}R$. or $^{\circ}K$.
 V = volume of hydrocarbon gas, ml.
 v = liquid specific volume, ml./gm. mole.

- w = weight fraction of component.
 x = mole fraction of component in liquid phase.
 y = mole fraction of component in vapor phase.
 z = gas law deviation and liquid pressure factor of component.
 α_{1-2} = relative volatility of component 1 to component 2.
 γ = activity coefficient in liquid phase.
 Σ = summation sign.

Subscripts

- 1 = component 1, any C_4 hydrocarbon in binary equations or n-butane in ternary equations.
 2 = component 2, solvent in binary equations or butene-1 in ternary equations.
 3 = component 3, solvent in ternary equations.
 i = components 1 to i .
 n = any component.

References

- (1) Mertes, T. S., and Colburn, A. P., Ind. Eng. Chem. 39, 787, (1947).
- (2) Gerster, J. A., Mertes, T. S., and Colburn, A. P., Ind. Eng. Chem. 39, 797, (1947).
- (3) Jordan, D., Gerster, J. A., Colburn, A. P., and Wohl, K., Chem. Eng. Prog. 46, 601, (1950).
- (4) Welty, F., Gerster, J. A., and Colburn, A. P., Ind. Eng. Chem. 43, 162, (1951).

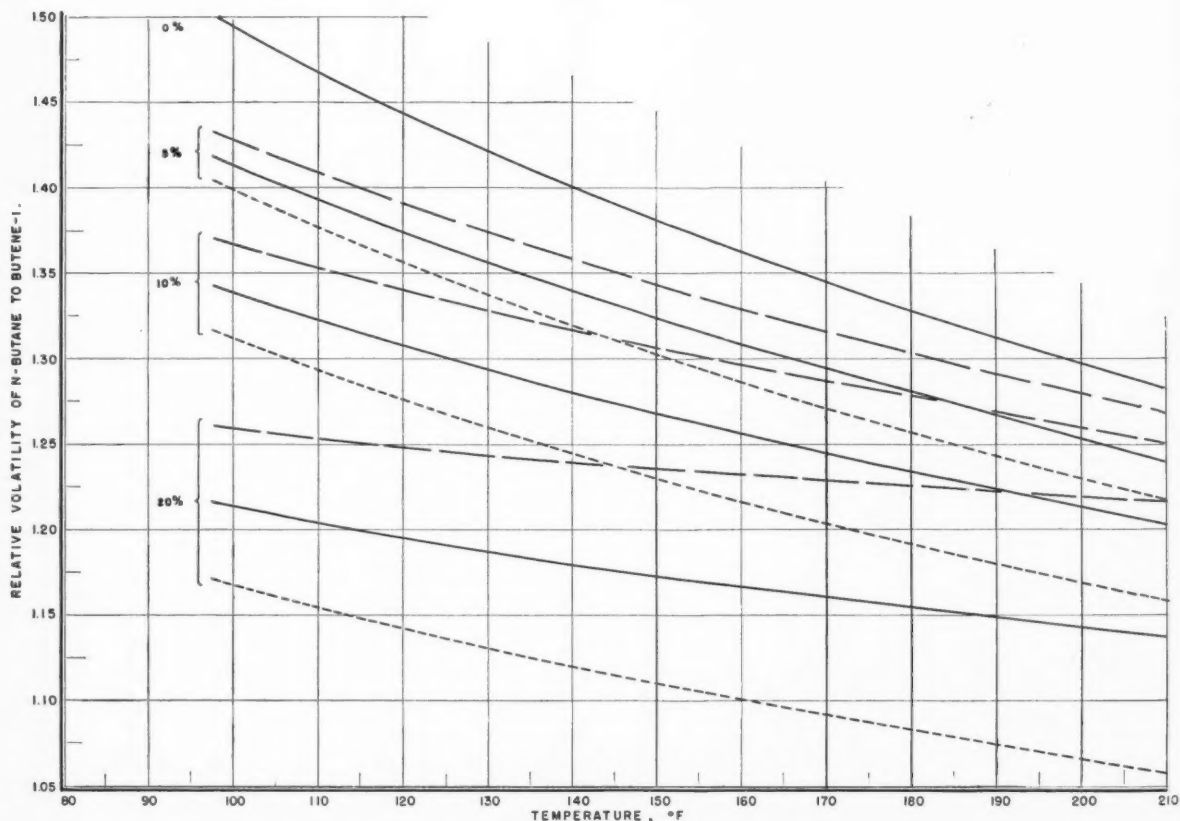


Figure 17—Relative volatility of n-butane to butene-1 in acetone-water solvent as a function of temperature and composition. Solvent contains 11.0 Wt. % water (C_4 Hydrocarbon-Free). Parameter is total hydrocarbon dissolved, Mole %, in the liquid phase. Dashed, solid, and dotted curves are for 0, 50, and 100 Mole % n-butane, respectively, on a solvent-free basis. Curves are predicted by Margules ternary equations.

Figure 18—Relative volatility of isobutane to butene-1 in acetone-water solvent as a function of temperature and composition. Solvent contains 11.0 Wt. % water (C_1 Hydrocarbon-Free). Parameter is total hydrocarbon dissolved, mole % in the liquid phase. Dashed, solid and dotted curves are for 0, 50, and 100 mole % by isobutane, respectively, on a solvent-free basis. Curves are predicted by Margules ternary equations.

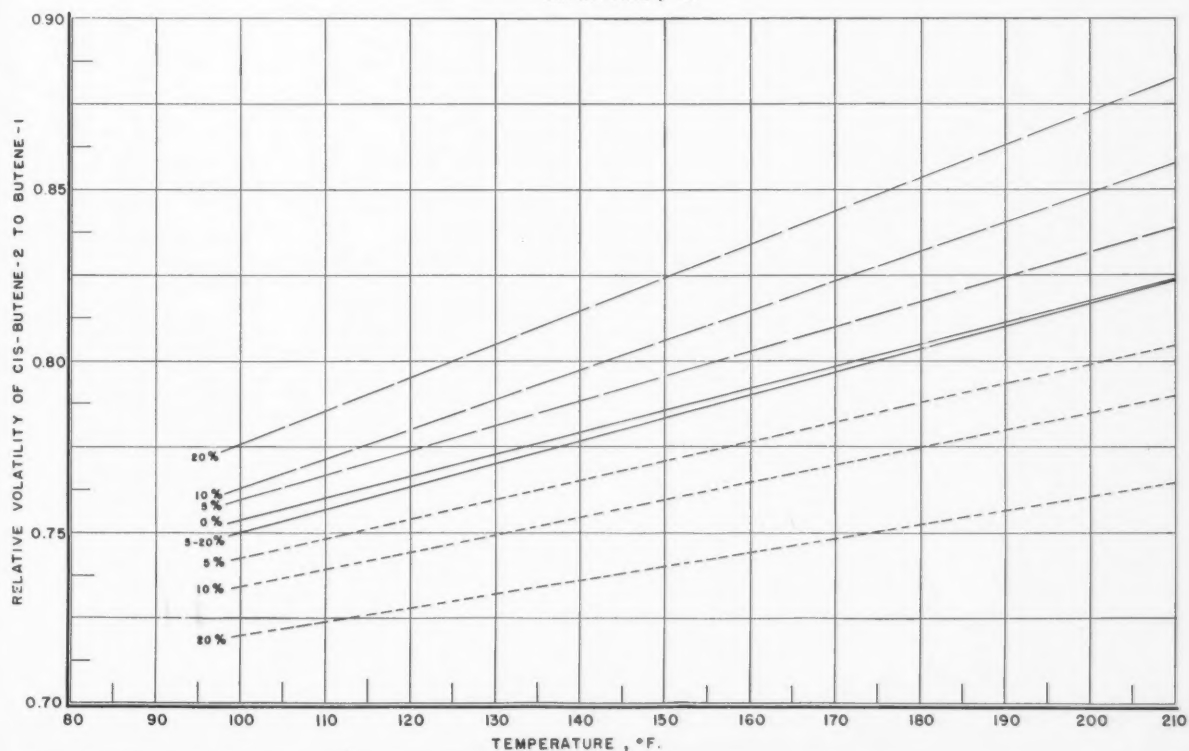
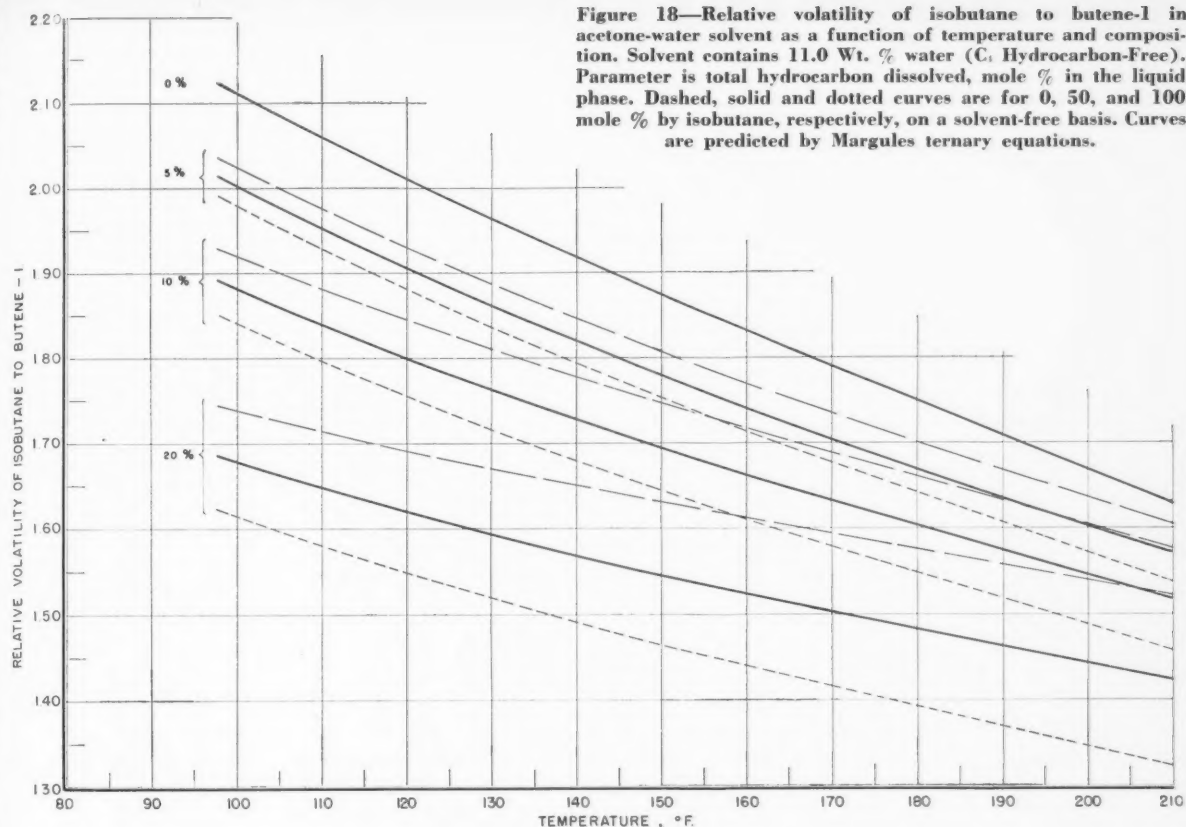


Figure 19—Relative volatility of cis-butene-2 to butene-1, in acetone-water solvent as a function of temperature and composition. Solvent contains 11.0 Wt. % water (C_1 Hydrocarbon-Free). Parameter is total hydrocarbon dissolved, mole %, in the liquid phase, dashed, solid, and dotted curves are for 0, 50, and 100 mole % cis-butene-2, respectively, on a solvent-free basis. Curves are predicted by Margules ternary equations.

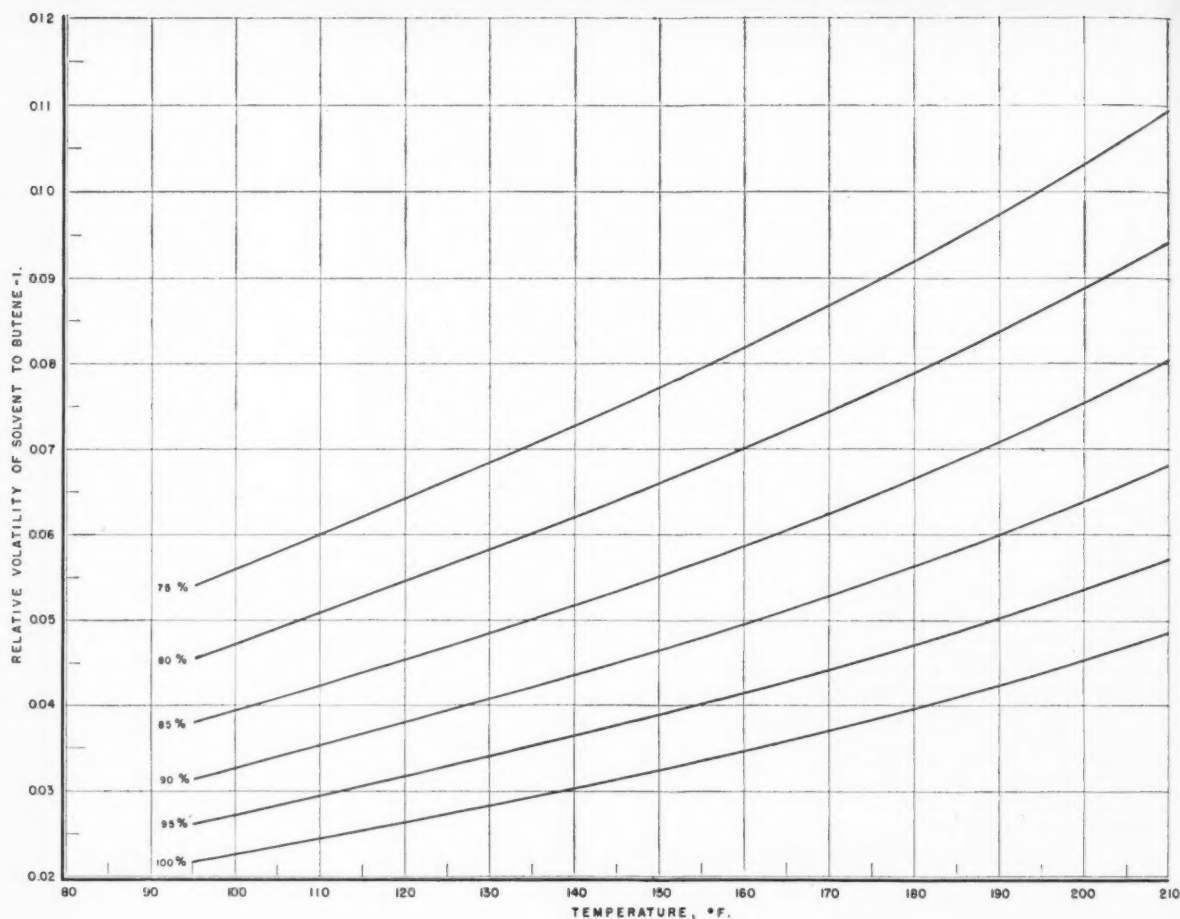


Figure 20—Relative volatility of acetone-water solvent to butene-1 as a function of temperature and composition. Solvent contains 11.0 Wt. % water (C₁ Hydrocarbon-Free). Parameter is mole % solvent in liquid phase.

- (5) Carlson, H. C., and Colburn, A. P., *Ind. Eng. Chem.* 34, 581, (1942).
- (6) Wohl, K., *Trans. Am. Inst. Chem. Engrs.* 42, 215, (1946).
- (7) Mitchell, J. and Smith, D. M., "Aquame-try", Interscience Publishers Inc., (1948).
- (8) Benedict, M., Johnson, C. A., Solomon, E., and Rubin, L. C., *Trans. Am. Inst. Chem. Engrs.* 41, 371, (1945).
- (9) Griswold, J., and Brooks, W. B., *Pet. Ref.* 26, 819, (1947).
- (10) Maxwell, J. B., "Data Book on Hydrocarbons", D. Van Nostrand Co., Inc., New York, (1950).
- (11) Shell Development Co. personal communication, (1942).
- (12) Glasstone, S., "Textbook of Physical Chemistry", 2nd ed., p. 239, D. Van Nostrand Co., Inc., New York, (1946).
- (13) Wohl, K., *Chem. Eng. Prog.* 49, 218, (1953).
- (14) Robinson, C. S., and Gilliland, E. R., "Elements of Fractional Distillation", 4th ed., p. 232, McGraw-Hill Book Co., Inc., New York, 1950.

★ ★ ★

The Leaching of Manganese from Pyrolusite Ore by Pyrite¹

G. THOMAS² and B. J. P. WHALLEY³

A new method of leaching low-grade manganese ore (< 5% Mn) utilizing pyrite as a reagent was developed. By heating an aerated slurry of ore and pyrite and by recycling the leach liquor at controlled acidity to attack fresh ore, a manganous sulphate solution free of iron was obtained which when heated to about 175°C., yielded manganous sulphate monohydrate. During the leaching process, iron in the liquor was alternately oxidized by the pyrolusite and reduced by the pyrite. In an alternative leaching procedure, the heating of an aqueous slurry of pyrite in an autoclave first under oxygen pressure and then in the absence of oxygen produced an acidic ferrous sulphate solution suitable for the subsequent leaching of pyrolusite ore at ambient temperatures.

IN conjunction with a major iron mining operation in Ontario, a large annual tonnage of manganiferous low-grade iron ore is brought to the surface as waste material. The average composition of this material is 50% silica, 40% iron oxides, 6% clay and accessory minerals and 4% manganese oxides, principally pyrolusite, MnO_2 . If the manganese could be recovered from this waste material, the amount available would almost satisfy Canada's annual manganese requirement of 30,000 tons. During a Mines Branch investigation of this material, a new process for leaching manganese was developed. This paper describes the development and chemistry of the leaching process.

There is an abundant literature on processes for the recovery of manganese from relatively high-grade pyrolusite ore. Of the many processes, the most interesting approach for the recovery of manganese from this low-grade material appeared to be that based on the use of pickle liquor from the steel industry. Hoak and Coull (1)

have shown that pickle liquor, which contains free sulphuric acid and ferrous sulphate, would give a 98% extraction from ores containing 15 to 25% manganese. There are many literature references (2-5) stating that sulphuric acid and ferrous sulphate are formed, in the presence of water, by the air oxidation of the relatively cheap and abundant mineral pyrite, FeS_2 . It seemed reasonable therefore to determine if manganese could be leached from an aerated slurry of pyrolusite ore using pyrite as the leaching agent.

Experimental leaching of manganese dioxide

The initial experimental work to test the feasibility of leaching pyrolusite ore by pyrite was done using pure manganese dioxide. When a slurry of pyrite (80% minus 200 mesh) and manganese dioxide in water was treated at 175°C. and under 100 psig oxygen pressure for two hours in an autoclave, very little manganese was dissolved. Although

manganese dioxide is insoluble in dilute sulphuric acid, the addition of this acid was found to accelerate the dissolution of manganese dioxide by pyrite. For example, when 1% v/v H_2SO_4 was substituted for water in the above experiment, the manganese was dissolved completely in two hours.

Additional experiments were done to determine the effect of lower temperatures on the dissolution of manganese dioxide. The experimental conditions and results for these experiments, given in Figure 1, curve 1, show that the dissolution of manganese by pyrite in 1% v/v H_2SO_4 was complete after two hours at 110°C. Analysis of the leach liquors from these experiments showed that high manganese:iron ratios of from 8:1 to 42:1 were obtained.

A pachuca was used for many of the subsequent experiments. It consisted of a glass cylinder fitted with a sintered glass disc in its conical base for air dispersion. In an experiment using the pachuca, air at atmospheric pressure was bubbled through a slurry of 2 gm manganese dioxide and 2 gm pyrite in 500 ml 2% v/v H_2SO_4 at 90°C. Under these leaching conditions with the open vessel, the MnO_2 was completely dissolved in six hours.

Experimental leaching of pyrolusite ore

To determine if pyrite could be used to leach manganese from the low-grade pyrolusite ore, samples of ore containing 3.7% Mn were treated at various temperatures in an autoclave for two hours with 1% v/v H_2SO_4 and 100 psig oxygen pressure. The results of these experiments are shown in Figure 1, curve 2. A com-

¹Manuscript received December 9, 1957.

²Senior Scientific Officers, Extractive Metallurgy Section, Mines Branch, Ottawa, Ont. Contribution from the Mineral Dressing and Process Metallurgy Division, Mines Branch, Department of Mines and Technical Surveys, Ottawa, Ont.

Published with permission of the Director of the Mines Branch.

This article is based in part on papers that were presented at the Symposium on Mineral Beneficiation and Extractive Metallurgical Techniques, Jamshedpur, India, February 1957 and at the 7th Annual Conference of the Chemical Engineering Division, The Chemical Institute of Canada, Kingston, March, 1957.

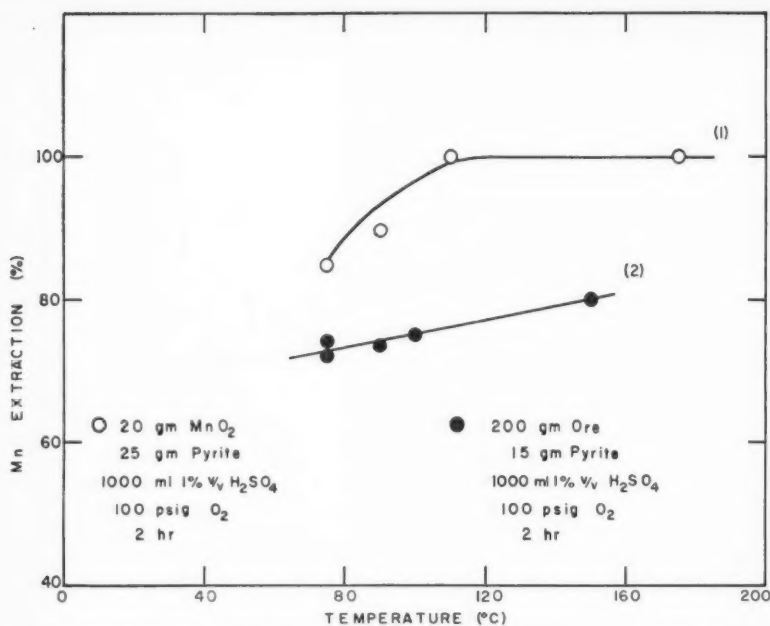


Figure 1—Effect of temperature on the extraction of manganese from ore and from MnO₂ in the presence of pyrite.

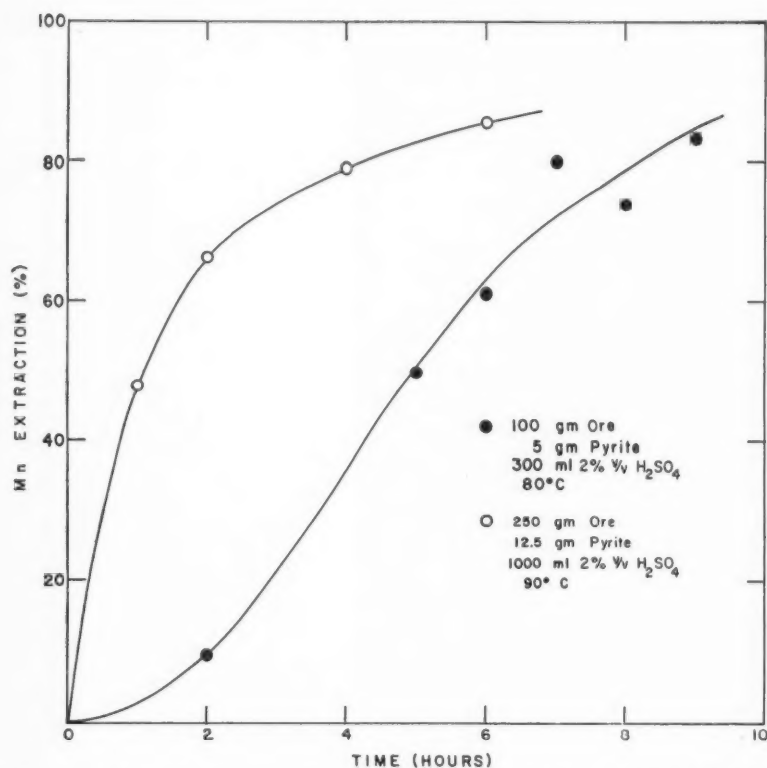


Figure 2—Rate of extraction of manganese from ore in the presence of pyrite.

parison of these results with those for the leaching of manganese from pure MnO₂, curve 1, shows that the leaching of manganese from the ore was somewhat slower but nevertheless promising.

Additional experiments on the leaching of pyrolusite ore were then done in an open vessel. The leaching experiments were done with pyrite and 2% v/v H₂SO₄ in a pachuca at temperatures of 80°C. and

with acid to ore ratios of 3:1 and 4:1 with results as shown in Figure 2*. By the combined use of the higher temperature and the higher acid to ore ratio, a more rapid extraction of manganese was obtained. After several hours, the percentage extraction of manganese was approximately the same in both experiments. The two experiments show that with an adequate amount of acid and with suitable reaction conditions of time and temperature, open vessels can be used for leaching operations.

Having produced manganous sulphate liquors by single-stage leaching, it was necessary to determine if recycling would build up the concentration of manganese in the liquor. An aerated slurry of 200 gm 4.3% Mn ore and 10 gm pyrite in 800 ml 2% v/v H₂SO₄ (pH 0.4) was heated in a pachuca at 90°C. for four hours. After separating the leach liquor from the ore, some water was added to the liquor to compensate for that which adhered to the ore. The pH of the liquor was restored from approximately 1.0 to its original value of 0.4 with about 25 gm conc. H₂SO₄ and the liquor was recycled with fresh ore and pyrite to the pachuca. The process was repeated for 11 cycles with the acidity of the leach liquor adjusted only for the first six cycles.

Figure 3 shows that during the first six cycles, when H₂SO₄ additions were made, there was a build up in the manganous sulphate concentration of the leach liquor to about 100 gm MnSO₄/l. Although the average manganese extraction was 65%, in certain cycles the extraction was as high as 90%. Subsequent to the sixth cycle, the manganese concentration of the liquor increased slightly and then decreased. The decrease was probably due to a combination of the lower manganese extraction during the last few cycles and the dilution involved at each cycle in restoring the volume of the liquor to its initial value. During the cyclic leaching experiments, about two moles of sulphuric acid were required for every mole of manganese that was leached.

After six cycles, the leach liquor contained 3 gm Fe⁺⁺⁺/l and 7 gm Fe⁺⁺/l. An important fact noted during later cycles was that when the pH increased to above approximately 1.5, the iron was precipitated by hydrolysis; after cycle 8, no iron was detected in the leach liquor. Hence, the cyclic leaching of manganese from the low-grade pyrolusite ore produced a strong manganous sulphate solution that was free of iron.

*In all graphs where pressures are not indicated, the experiments were done at atmospheric pressure in a pachuca.

Evaporation of the recycled leach liquor gave a hydrated manganous sulphate. The main impurities were Al, Ca, Mg, and Si, and these comprised less than 4% by weight of the manganous sulphate. Manganous sulphate monohydrate, the solubility of which decreases at high temperatures, was recovered by heating the recycled leach liquor to about 175°C. in a closed tube, using a thermal precipitation method developed at the Mines Branch.*

Study of the leaching reactions

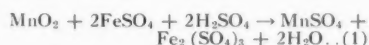
To elucidate the chemistry of the leaching process, a number of experiments were done with ore or pure MnO_2 using a glass pachuca and a reaction temperature of 90°C.

The effect of pyrite in the leaching process

To demonstrate that the leaching of manganese involved more than a simple acid leach, the following experiment was done. An aerated slurry of ore in 2% v/v H_2SO_4 was heated for two hours in the absence of pyrite. The extraction of manganese was about 7%. (Possibly this represents the percentage of the manganese that is present in the divalent state in the ore). As soon as pyrite was added, the percentage extraction of manganese from the pyrolusite ore was greatly increased as shown in Figure 4.**

Reactions of ferrous sulphate in the leaching process

Since ferrous sulphate is probably the main leaching reagent in the process, a study was made of its relevant reactions and their comparative rates. The reaction by which manganese dioxide is dissolved by an acidic ferrous sulphate solution is usually written as (6)



The rate of this reaction was very rapid at 90°C. as shown by Figure 5, with the dissolution of the manganese dioxide being complete in about one minute. In agreement with Equation 1, the curves of Figure 5 show a change in pH and in ferrous ion concentration during the dissolution of the manganese.

Although the reaction of ferrous sulphate with manganese dioxide is fast, the formation of ferrous sulphate

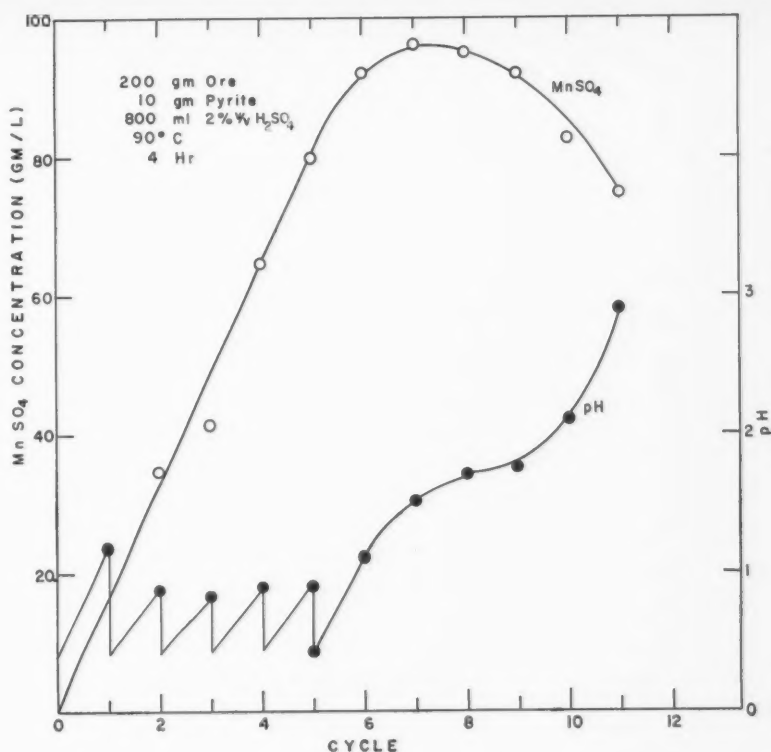


Figure 3—Cyclic extraction of manganese from ore in the presence of pyrite.

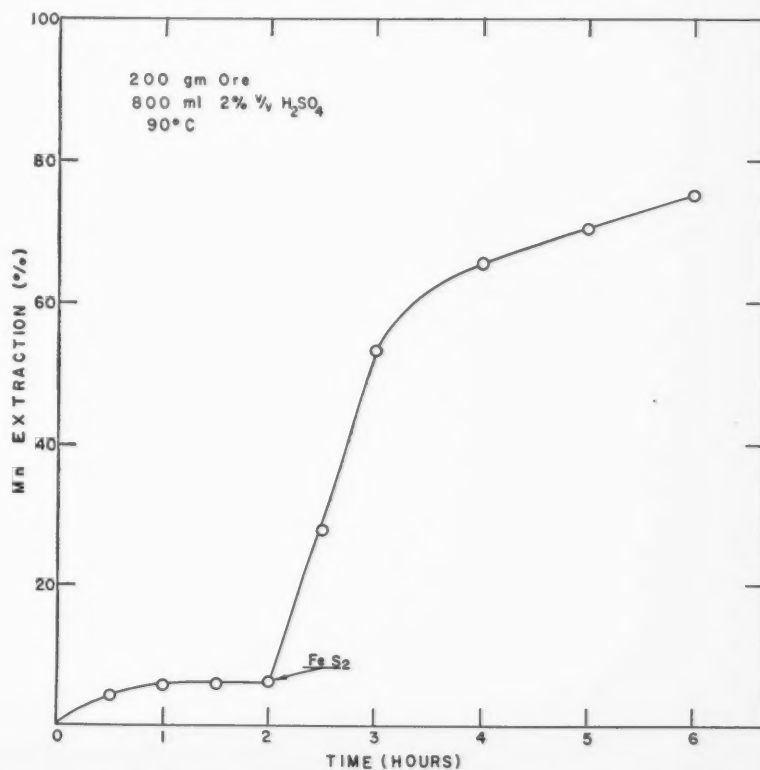


Figure 4—Effect of addition of pyrite on extraction of manganese from ore.

*In preparation for publication.

**When pyrrhotite, Fe_7S_8 , was substituted for pyrite, no significant change was observed in the leaching reaction rate. See also recent paper by Bjorling(11) on the autoclave leaching of manganese ore by pyrrhotite.

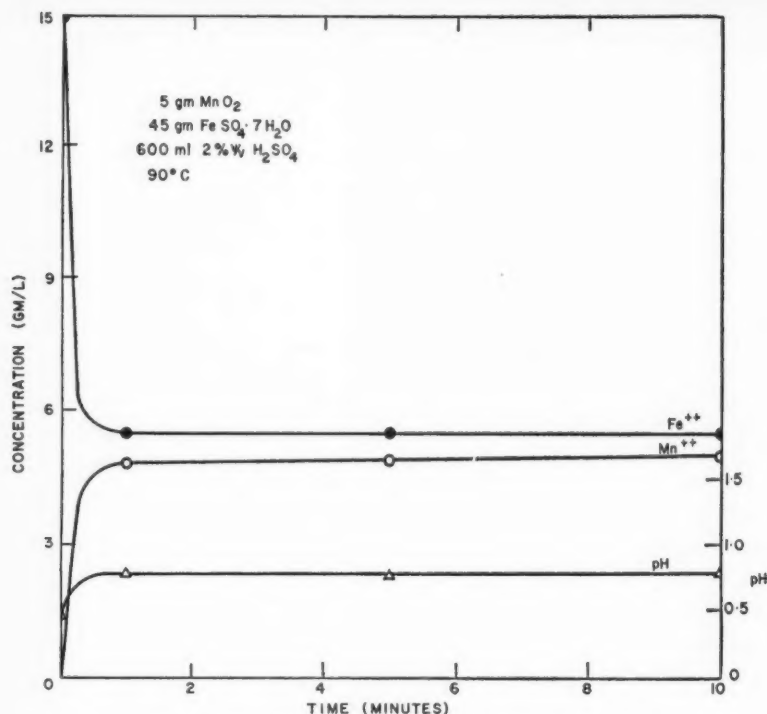


Figure 5—Rate of reduction of MnO₂ by ferrous sulphate.

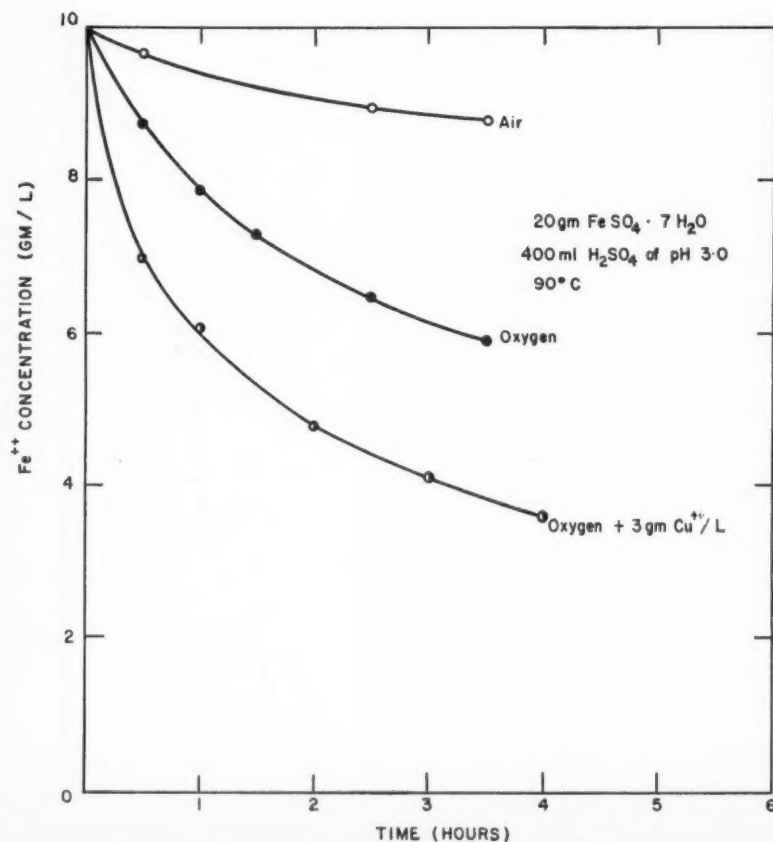
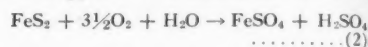


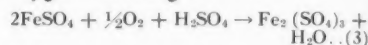
Figure 6—Rate of oxidation of ferrous sulphate by air and by oxygen.

from pyrite⁽⁵⁾ is known to be slow.



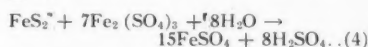
For example, only 5% of the pyrite was oxidized in four hours when a slurry of minus 200 mesh pyrite in dilute H₂SO₄ of pH 1.0 at 90°C. was aerated with oxygen. No significant change in the reaction rate was observed when an H₂SO₄ solution of pH 0.4 was used.

The ferrous sulphate formed by reaction 2 may be oxidized^(4,5) by oxygen according to



The removal of ferrous ion by this reaction might be expected to interfere with the leaching of pyrolusite by reaction 1. However, Figure 6 shows that even when copper sulphate is present as a catalyst, the oxidation of ferrous sulphate by air or oxygen is relatively slow. Hence the air oxidation of ferrous ion in acidic solution is not likely to impede the leaching operations.

Although equations 2 and 3 indicate that ferric sulphate could be formed when pyrite is oxidized, no ferric ion was detected when acidic slurries of pyrite at 90°C. were aerated at atmospheric pressure. Any ferric ion that was formed must have been reduced again by the residual pyrite, possibly by a reaction such as⁽²⁾



The rate of reduction of a ferric sulphate solution by minus 200 mesh pyrite is shown graphically by Figure 7. Although this is a slow reaction, it might be, for liquors containing ferric sulphate, the main source of ferrous ion for leaching pyrolusite ore.

The effect of acid concentration and of ferric sulphate addition on the leaching process

In the first experiment, a slurry of MnO₂ and pyrite in an H₂SO₄ solution of pH 0.4 at 90°C. was aerated with oxygen. Figure 8 shows that the manganese was dissolved at a uniform rate; after four hours approximately 80% of the manganese had reacted with the pyrite to form manganous and ferric ions. The initial rise in the pH of the solution was probably due to the impurity siderite, FeCO₃, that was present in the pyrite and the subsequent progressive rise in the pH was likely due to the dissolution of the manganese dioxide.

When dilute H₂SO₄ of pH 1.0 was substituted for acid of pH 0.4 in the above experiment, the results shown

in Figure 9 were obtained. With the dilute acid of this experiment, most of the acid was soon used up and the remaining was insufficient to keep ferric ion in solution. The curves show that for pH values above approximately 1.7, the rate of dissolution of manganese was very slow.

The effect of adding ferric sulphate to an acidic aerated slurry of MnO_2 and pyrite, as shown by a comparison of Figure 8 with Figure 10, was to increase the rate of dissolution of the MnO_2 . Evidently the ferric sulphate was reduced by the pyrite to form ferrous sulphate which reacted rapidly with the MnO_2 . The ferric ion continued to be reduced by the pyrite after all the MnO_2 had dissolved.

Autoclave-produced acidic ferrous sulphate solutions

Since the leaching of pyrolusite ore by pyrite consumes acid, an alternative procedure was investigated. The objective was to adapt the oxidation of an aqueous slurry of pyrite in an autoclave (7-10) for the production of an acidic ferrous sulphate solution. Hoak and Coull (1) have shown previously that pyrolusite ore can be leached rapidly at ambient temperatures with acidic solutions of ferrous sulphate.

In one experiment, a slurry of pyrite in 2% v/v H_2SO_4 was heated in an autoclave at a temperature of 110°C . and under an oxygen pressure of 300 psig. The acid was added to decrease the precipitation of ferric ion by hydrolysis in the initial stages of the reaction. About 60% of the pyrite was oxidized in five hours with nearly 70% of the pyritic sulphur being changed to sulphate sulphur and 30% being recovered as elemental sulphur. This autoclave treatment produced an acidic liquor containing predominantly ferric sulphate. To obtain a ferrous sulphate liquor, the same experiment was repeated but the oxygen was released after three hours and replaced by nitrogen.

Figure 11 shows that the treatment of pyrite in an autoclave produced quickly a liquor containing both ferrous and ferric sulphate. When a high oxygen pressure was present, the iron was changed mainly to the ferric state. When the oxygen was replaced by nitrogen, the reduction of the ferric ion by pyrite produced an acidic liquor containing approximately 200 gm $\text{FeSO}_4/1$, 60 gm $\text{Fe}_2(\text{SO}_4)_3/1$ and 70 gm $\text{H}_2\text{SO}_4/1$. This autoclave liquor is similar in composition to pickle liquor which has been reported (1) to be suitable for leaching pyrolusite ore at room temperature. The autoclave process appears to be a con-

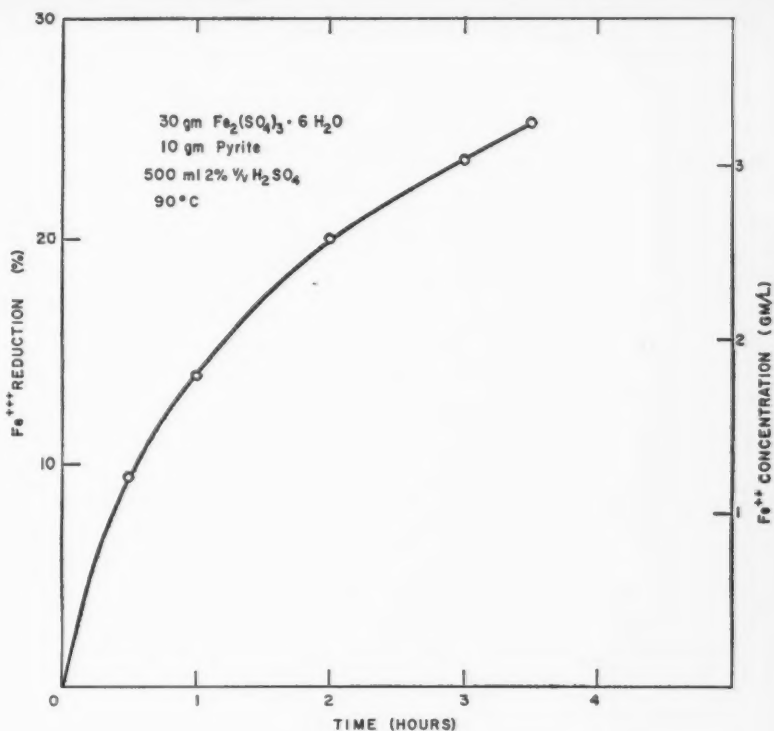


Figure 7—Rate of reduction of ferric sulphate by pyrite.

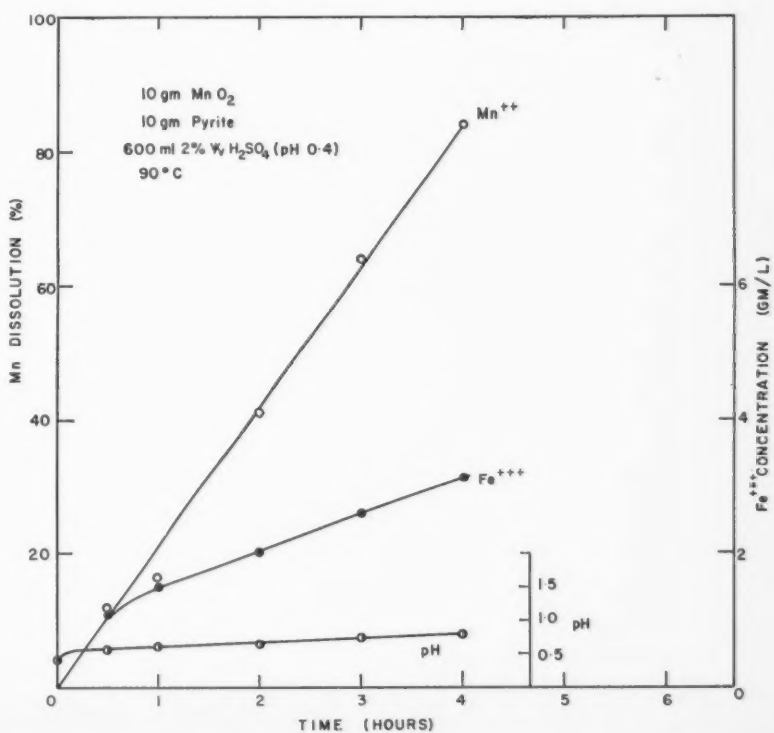


Figure 8—Rate of dissolution of MnO_2 in 2% v/v H_2SO_4 in the presence of pyrite.

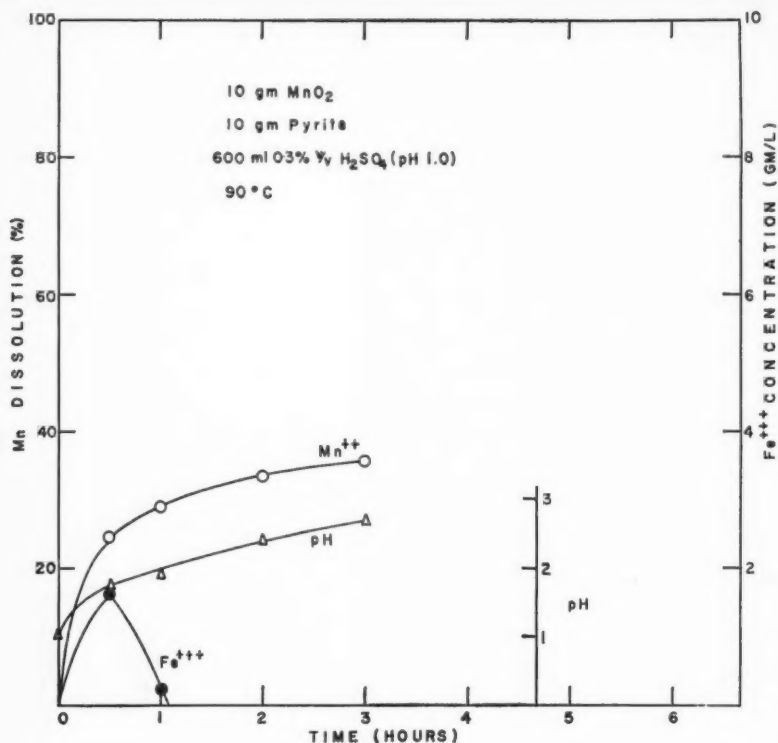


Figure 9—Rate of dissolution of MnO_2 in 0.3% v/v H_2SO_4 in the presence of pyrite.

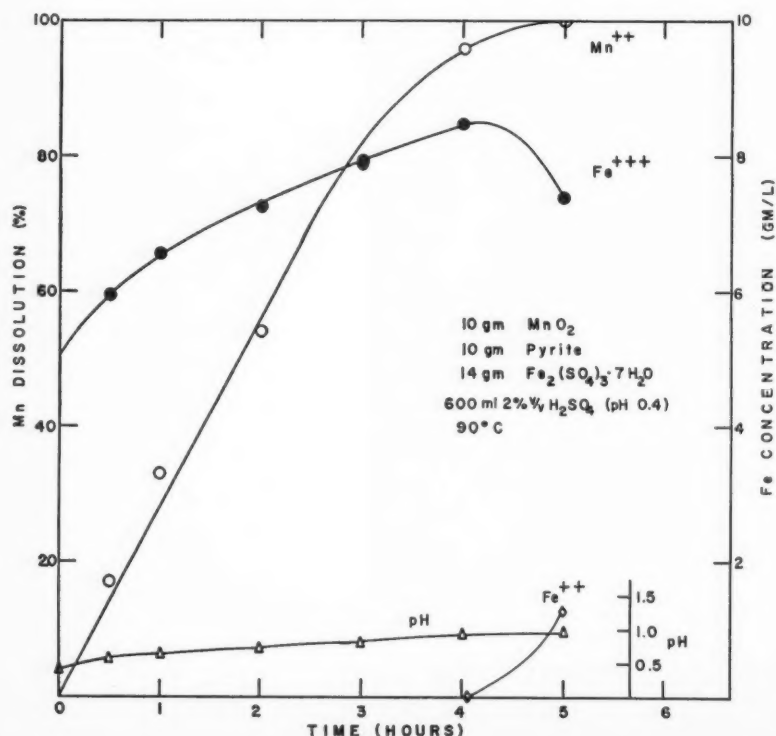


Figure 10—Rate of dissolution of MnO_2 in 2% v/v H_2SO_4 in the presence of pyrite and ferric sulphate.

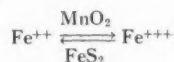
venient method of producing an acidic ferrous sulphate liquor for leaching purposes.

Summary and Conclusions

Manganese was extracted from a pyrolusite ore (4% Mn) by heating an aerated aqueous slurry of ore and pyrite. A rapid extraction of manganese was obtained by leaching the ore in an autoclave at high oxygen pressures and high temperatures. It was found that satisfactory extraction could be obtained, at a slower rate, by using open vessels and relatively low temperatures. A temperature of 90°C . was used for most of the experimental work since adequate extractions could be obtained in a relatively short time, e.g. manganese extractions of up to 90% were obtained within four hours. For commercial operations, prolonged leaching periods at lower temperatures might be more economical.

Recycling the leach liquor at controlled acidity to leach additional ore gave a concentrated solution containing about 100 gm MnSO_4 /l. Approximately two moles of sulphuric acid were required to dissolve one mole of pyrolusite from the ore. Evaporation of the recycled solution gave an iron-free hydrated manganous sulphate of which the main impurities, Al, Ca, Mg and Si, comprised less than 4% by weight of the product. Manganous sulphate was recovered using substantially less heat when evaporation was replaced by heating the recycled solution to about 175°C . to precipitate manganous sulphate monohydrate.

Although many chemical reactions are undoubtedly involved, the leaching of pyrolusite ore by this process is essentially the reduction of MnO_2 by ferrous ion to acid-solution divalent manganese. The ferrous ion is obtained from the reaction of pyrite with air or with ferric ion. During the dissolution of manganese, the iron is alternately oxidized by the pyrolusite and reduced by the pyrite, as shown by



i.e. the ferrous ion is continuously regenerated during the leaching process.

By heating an aqueous slurry of pyrite at 110°C . in an autoclave, first under oxygen pressure and then in the absence of oxygen, a concentrated acidic solution of ferrous sulphate (200 gm FeSO_4 /l) was obtained. Hoak and Coull⁽¹⁾ found that solutions of similar composition were

suitable for leaching pyrolusite ore at room temperature. Hence, for large-scale leaching operations with the low-grade ore used in this investigation, two leaching procedures might be feasible. In the one process, the leaching would be done by heating aerated slurries of ore, pyrite, acid and water in pachucas. In the alternative process, pyrite and water, in amounts small in comparison with that of the ore, would be treated in autoclaves to produce acidic solutions of ferrous sulphate for the subsequent leaching of ore at ambient temperatures.

References

- (1) Hoak, R. D., and Coull, J., *J. Chem. Eng. Prog.* 46, 158, (1950).
- (2) Fennell, J. H., *Mining Mag.* 37, 207, (1927).
- (3) Nelson, H. W., Snow, R. D., and Keyes, D. B., *Ind. Eng. Chem.* 25, 1355, (1933).
- (4) Hodge, W. W., *ibid* 29, 1048, (1937).
- (5) Taylor, J. H., and Whelan, P. F., *Trans. Inst. Mining Met.* 52, 35, (1942).
- (6) Kolthoff, I. M., and Sandell, E. G., "Textbook of Quantitative Inorganic Analysis", Macmillan and Co., New York, 1936.
- (7) Bergholm, A., *Jernkontorets Ann.* 139, 531, (1955).
- (8) Halpern, J., and Forward, F. A., *Bull. Inst. Mining Met.* 603, 181, (1957).
- (9) Gray, P. M. J., *Revs. Pure Appl. Chem.* 5, 194, (1955).
- (10) Warren, I. H., *Australian J. Appl. Sci.* 7, 346, (1956).
- (11) Bjorling, G. *International Mineral Dressing Congress*, VII:5, Stockholm, September 1957.

★ ★ ★

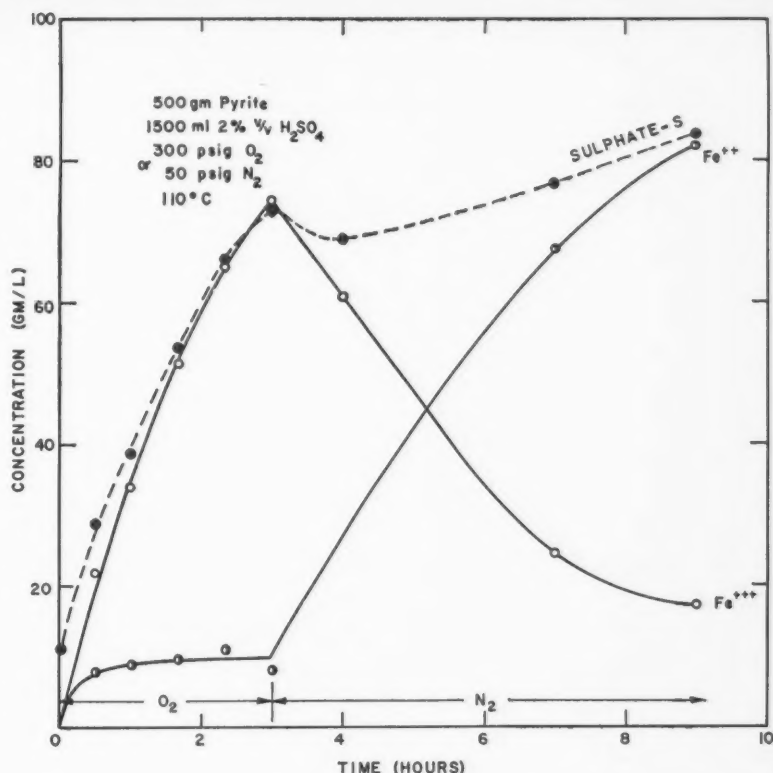


Figure 11—Production of an acidic ferrous sulphate solution by heating pyrite in an autoclave.

Be
Ba
Ba
Ba
Br
Br
Ca
Ca
Ch
Cr
Do
Du
Ec
El
Ep
Ev
Ew
Ga
Gil
Go
Go
Gu
He
He
Ho
Th

INDEX OF AUTHORS THE CANADIAN JOURNAL OF CHEMICAL ENGINEERING — 1957

Baddour, R. F., Goldstein, D. J., and Gilliland, E. R., "Counter Diffusion of Ions in Water".....	June	10
Bailey, J. A., and Robinson, D. B., "The Carbon Dioxide-Hydrogen Sulphide-Methane System. Part I — Phase Behaviour at 100°F.".....	Dec.	151
Bancroft, A. R., and Rae, H. K., "Wetted-Wall Packing — A New Distillation Column Packing".....	Aug.	77
Bata, G. L., "Recent Developments in the Extrusion of Plastics".....	Dec.	159
Bralda, L., and Johnson, A. I., "The Velocity of Fall of Circulating and Oscillating Liquid Drops through Quiescent Liquid Phases".....	Dec.	165
Bryant, Jr., H. S., and Sherwood, T. K., "Mass Transfer Through Compressible Turbulent Boundary Layers".....	Aug.	51
Cavers, S. D., Van Cleave, A. B., Crawford, L. W., and Gunn, Brad, "Beneficiation of Low Grade Saskatchewan Uranium Ores IV".....	Oct.	99
Cavers, S. D., and Ewanchyna, J. E., "Circulation and End Effects in a Liquid Extraction Spray Column".....	Oct.	113
Chiang, P., Evans, D. J. I., and Kunda, W., "Studies on Flocculants for Settling, Thickening and Filtration in the Sherritt Gordon Process".....	June	25
Crawford, L. W., Gunn, Brad, Cavers, S. D., and Van Cleave, A. B., "Beneficiation of Low Grade Saskatchewan Uranium Ores IV".....	Oct.	99
Dougherty, P. F., and Henderson, G. R., "Underground Storage Created in Salt Beds at Sun's Sarnia Refinery".....	Aug.	91
Dunn, J. S. C., Govier, G. W., and Radford, B. A., "The Upwards Vertical Flow of Air-Water Mixtures. I. Effect of Air and Water Rates on Flow Pattern, Holdup and Pressure Drop".....	Aug.	58
Eckenfelder, W. Wesley, "Principles of Aeration as Applied to Waste Treatment".....	Dec.	173
Elkin, H. F., and Henderson, G. R., "Waste Treatment at Sun Oil's Sarnia Refinery".....	Oct.	129
Epstein, N., Galloway, L. R., and Komarnicky, W., "Effect of Packing Configuration on Mass and Heat Transfer in Beds of Stacked Spheres".....	Dec.	139
Evans, D. J. I., Kunda, W., and Chiang, P., "Studies on Flocculants for Settling, Thickening and Filtration in the Sherritt Gordon Process".....	June	25
Ewanchyna, J. E., and Cavers, S. D., "Circulation and End Effects in a Liquid Extraction Spray Column".....	Oct.	113
Galloway, L. R., Komarnicky, W., and Epstein, N., "Effect of Packing Configuration on Mass and Heat Transfer in Beds of Stacked Spheres".....	Dec.	139
Gilliland, E. R., Baddour, R. F., and Goldstein, D. J., "Counter Diffusion of Ions in Water".....	June	10
Goldstein, D. J., Gilliland, E. R., and Baddour, R. F., "Counter Diffusion of Ions in Water".....	June	10
Govier, G. W., Radford, B. A., and Dunn, J. S. C., "The Upwards Vertical Flow of Air-Water Mixtures. I. Effect of Air and Water Rates on Flow Pattern, Holdup and Pressure Drop".....	Aug.	58
Gunn, Brad, Cavers, S. D., Van Cleave, A. B., and Crawford, L. W., "Beneficiation of Low Grade Saskatchewan Uranium Ores IV".....	Oct.	99
Henderson, G. R., and Dougherty, P. F., "Underground Storage Created in Salt Beds at Sun's Sarnia Refinery".....	Aug.	91
Henderson, G. R., and Elkin, H. F., "Waste Treatment at Sun Oil's Sarnia Refinery".....	Oct.	129
Hodgins, J. W., Hoffman, T. W., and Pei, D. C., "The Effect of Sonic Energy on Mass Transfer in Solid-Gas Contacting Operations".....	June	18
Hoffman, T. W., Pei, D. C., and Hodgins, J. W., "The Effect of Sonic Energy on Mass Transfer in Solid-Gas Contacting Operations".....	June	18
Jacob, A., and Osberg, G. L., "The Effect of Gas Thermal Conductivity on Local Heat Transfer in a Fluidized Bed".....	June	5
Johnson, A. I., and Bralda, L., "The Velocity of Fall of Circulating and Oscillating Liquid Drops through Quiescent Liquid Phases".....	Dec.	165
King, R. O., Sandler, S., and Strom, R., "The Decomposition, Oxidation, Ignition and Detonation of Fuel Vapors and Gases. Part 31 — The Effect of Flow Configuration in an Annular Reactor of Vycor Glass on the Oxidation of Pentane".....	June	33
Komarnicky, W., Epstein, N., and Galloway, L. R., "Effect of Packing Configuration on Mass and Heat Transfer in Beds of Stacked Spheres".....	Dec.	139
Kunda, W., Chiang, P., and Evans, D. J. I., "Studies on Flocculants for Settling, Thickening and Filtration in the Sherritt Gordon Process".....	June	25
Kure, A. R., "Ethyl Alcohol From Sulphite Waste Liquor".....	Aug.	86
Leva, Max, "Correlations of the Dense-Phase Fluidized State and Their Applications".....	Aug.	71
Minard, G. W., and Winning, M. D., "Flooding Phenomena in Packed Gas Absorption Columns".....	June	39
Osberg, G. L., and Jacob, A., "Effect of Gas Thermal Conductivity on Local Heat Transfer in a Fluidized Bed".....	June	5
Pei, D. C., Hodgins, J. W., and Hoffman, T. W., "The Effect of Sonic Energy on Mass Transfer in Solid-Gas Contacting Operations".....	June	18
Radford, B. A., Dunn, J. S. C., and Govier, G. W., "The Upwards Vertical Flow of Air-Water Mixtures. I. Effect of Air and Water Rates in Flow Pattern, Holdup and Pressure Drop".....	Aug.	58
Rae, H. K., and Bancroft, A. R., "Wetted-Wall Packing — A New Distillation Column Packing".....	Aug.	77
Roberts, J. E., and Robinson, J. N., "A Mathematical Study of Crystal Growth in a Cascade of Agitators".....	Oct.	105
Robinson, D. B., and Bailey, J. A., "The Carbon Dioxide-Hydrogen Sulphide-Methane System. Part I — Phase Behaviour at 100°F.".....	Dec.	151
Robinson, J. N., and Roberts, J. E., "A Mathematical Study of Crystal Growth in a Cascade of Agitators".....	Oct.	105
Sandler, S., Strom, R., and King, R. O., "The Decomposition, Oxidation, Ignition and Detonation of Fuel Vapors and Gases. Part 31 — The Effect of Flow Configuration in an Annular Reactor of Vycor Glass on the Oxidation of Pentane".....	June	33
Sherwood, T. K., and Bryant, Jr., H. S., "Mass Transfer Through Compressible Turbulent Boundary Layers".....	Aug.	51
Strom, R., King, R. O., and Sandler, S., "The Decomposition, Oxidation, Ignition and Detonation of Fuel Vapors and Gases. Part 31 — The Effect of Flow Configuration in an Annular Reactor of Vycor Glass on the Oxidation of Pentane".....	June	33
Van Cleave, A. B., Crawford, L. W., Gunn, Brad, and Cavers, S. D., "Beneficiation of Low Grade Saskatchewan Uranium Ores IV".....	Oct.	99
Winning, M. D., and Minard, G. W., "Flooding Phenomena in Packed Gas Absorption Columns".....	June	39

INDEX OF ARTICLES THE CANADIAN JOURNAL OF CHEMICAL ENGINEERING — 1957

Absorption Columns, Flooding Phenomena in Packed Gas	June	39	Heat Transfer in a Fluidized Bed, Effect of Gas Thermal Conductivity on Local	June	5
Aeration as Applied to Waste Treatment, Principles of	Dec.	173	Heat Transfer in Beds of Stacked Spheres, Effect of Packing Configuration on Mass and	Dec.	139
Air-Water Mixtures. I. Effect of Air and Water Rates on Flow Pattern, Holdup and Pressure Drop, The Upwards Vertical Flow of	Aug.	58	Holdup and Pressure Drop, The Upwards Vertical Flow of Air-Water Mixtures. I. Effect of Air and Water Rates on Flow Pattern	Aug.	58
Agitators, A Mathematical Study of Crystal Growth in a Cascade of	Oct.	105	Hydrogen Sulphide-Methane System, Part I — Phase Behaviour at 100°F., The Carbon Dioxide	Dec.	151
Ammonia Pressure Leaching — "Studies on Flocculants for Settling, Thickening and Filtration in the Sherritt Gordon Process"	June	25	Ions in Water, Counter Diffusion of	June	10
Carbon Dioxide-Hydrogen Sulphide-Methane System. Part I — Phase Behaviour at 100°F., The	Dec.	151	Liquid Extraction Spray Column, Circulation and End Effects in an	Oct.	113
Column, Circulation and End Effects in a Liquid Extraction Spray	Oct.	113	Mass and Heat Transfer in Beds of Stacked Spheres, Effect of Packing Configuration on	Dec.	139
Column Packing, Wetted-Wall Packing — A New Distillation	Aug.	77	Mass Transfer in Solid-Gas Contacting Operations, The Effect of Sonic Energy on	June	18
Columns, Flooding Phenomena in Packed Gas Absorption	June	39	Mass Transfer Through Compressible Turbulent Boundary Layers	Aug.	51
Crystal Growth in a Cascade of Agitators, A Mathematical Study of	Oct.	105	Methane System, Part I — Phase Behaviour at 100°F., The Carbon Dioxide-Hydrogen Sulphide	Dec.	151
Dense-Phase Fluidized State and their Applications, Correlations of the	Aug.	71	Oxidation of Pentane, The Decomposition, Oxidation, Ignition and Detonation of Fuel Vapors and Gases. Part 31 — The Effect of Flow Configuration in an Annular Reactor of Vycor Glass on the	June	33
Diffusion of Ions in Water, Counter	June	10	Packing Configuration on Mass and Heat Transfer in Beds of Stacked Spheres, Effect of	Dec.	139
Distillation Column Packing, Wetted-Wall Packing — A New	Aug.	77	Packing — A New Distillation Column Packing, Wetted Wall	Aug.	77
Drops Through Quiescent Liquid Phases, The Velocity of Fall of Circulating and Oscillating Liquid	Dec.	165	Pentane, The Decomposition, Oxidation, Ignition and Detonation of Fuel Vapors and Gases. Part 31 — The Effect of Flow Configuration in an Annular Reactor of Vycor Glass on the Oxidation of	June	33
Ethyl Alcohol from Sulphite Waste Liquor	Aug.	86	Plastics, Recent Developments in the Extrusion of	Dec.	159
Flooding Phenomena in Packed Gas Absorption Columns	June	39	Phases, The Velocity of Fall of Circulating and Oscillating Liquid Drops Through Quiescent Liquid	Dec.	165
Flow Configuration in an Annular Reactor of Vycor Glass on the Oxidation of Pentane, The Decomposition, Oxidation, Ignition and Detonation of Fuel Vapors and Gases. Part 31 — The Effect of	June	33	Pressure Drop, The Upwards Vertical Flow of Air-Water Mixtures. I. Effect of Air and Water Rates on Flow Pattern, Holdup and	Aug.	58
Flow of Air-Water Mixtures. I. Effect of Air and Water Rates on Flow Pattern, Holdup and Pressure Drop, The Upwards	Aug.	58	Salt Beds at Sun's Sarnia Refinery, Underground Storage Created in	Aug.	91
Flow Pattern, Holdup and Pressure Drop, The Upwards Vertical Flow of Air-Water Mixtures. I. Effect of Air-Water Rates on	Aug.	58	Sherritt Gordon Process, Studies on Flocculants for Settling, Thickening and Filtration in the	June	25
Flocculants for Settling, Thickening and Filtration in the Sherritt Gordon Process, Studies on	June	25	Solid-Gas Contacting Operations, The Effect of Sonic Energy on Mass Transfer in	June	18
Fluidized Bed, Effect of Gas Thermal Conductivity on Local Heat Transfer in a	June	5	Sonic Energy on Mass Transfer in Solid-Gas Contacting Operations, The Effect of	June	18
Fluidized State and their Applications, Correlations of the Dense-Phase	Aug.	71	Spheres, Effect of Packing Configuration on Mass and Heat Transfer in Beds of Stacked	Dec.	139
Fuel Vapors and Gases. Part 31 — The Effect of Flow Configuration in an Annular Reactor of Vycor Glass on the Oxidation of Pentane, The Decomposition, Oxidation, Ignition and Detonation of	June	33	Spray Column, Circulation and End Effects in a Liquid Extraction	Oct.	113
Gas Absorption Columns, Flooding Phenomena in Packed	June	39	Stacked Spheres, Effect of Packing Configuration on Mass and Heat Transfer in Beds of	Dec.	139
Gas Thermal Conductivity on Local Heat Transfer in a Fluidized Bed, Effect of	June	5	Storage Created in Salt Beds at Sun's Sarnia Refinery, Underground	Aug.	91
Gases. Part 31 — The Effect of Flow Configuration in an Annular Reactor of Vycor Glass on the Oxidation of Pentane, The Decomposition, Oxidation, Ignition and Detonation of Fuel Vapors and	June	33	Sulphite Waste Liquor, Ethyl Alcohol from	Aug.	86
			Uranium Ores, IV, Beneficiation of Low Grade Saskatchewan	Oct.	99
			Waste Treatment at Sun Oil's Sarnia Refinery	Oct.	129
			Waste Treatment, Principles of Aeration as Applied to	Dec.	173

5
139
58
51
10
13
39
18
51
51
33
49
7
3
9
5
8
1
5
8
8
9
3
9
1
6
9
9
3
8